ISBN 978-82-326-4262-5 (printed version)
ISBN 978-82-326-4263-2 (electronic version)
ISSN 1503-8181

Doctoral Thesis

Miodrag Spasić

Doctoral theses at NTNU, 2019:333

NTNU
Norwegian University of
Science and Technology

Doctoral theses at NTNU, 2019:333

Miodrag Spasić

NTNU
Norwegian University of
Science and Technology
Faculty of Information Technology
and Electrical Engineering
Department of Engineering Cybernetics

NTNU
Norwegian University of
Science and Technology

Doctoral theses at NTNU, 2019:333

Miodrag Spasić

Model Predictive Control based on Sliding Mode Control

Miodrag Spasić

Model Predictive Control based on Sliding Mode Control

Thesis for the degree of Philosophiae Doctor

Trondheim, September 2019

Norwegian University of Science and Technology
Faculty of Information Technology
and Electrical Engineering
Department of Engineering Cybernetics

NTNU
Norwegian University of
Science and Technology

NTNU
Norwegian University of Science and Technology

Thesis for the degree of Philosophiae Doctor

Faculty of Information Technology
and Electrical Engineering
Department of Engineering Cybernetics

ISBN 978-82-326-4262-5 (printed version)
ISBN 978-82-326-4263-2 (electronic version)
ISSN 1503-8181

ITK-report: 2019-11-W

Doctoral theses at NTNU, 2019:333

Printed by Skipnes Kommunikasjon as

Norwegian University of Science and Technology
Faculty of Information Technology
and Electrical Engineering

University of Niš
Faculty of Electronic Engineering

Miodrag D. Spasić

Model predictive control based on sliding mode control

Thesis for the degree of Philosophiae Doctor

Norwegian University of Science and Technology
Faculty of Information Technology and
Electrical Engineering
Department of Engineering Cybernetics

Thesis for the degree of Doctor of Science

University of Niš
Faculty of Electronic Engineering
Department of Control Systems

This thesis is the result of the project "Norwegian, Bosnian, and Serbian cooperation platform for university and industry ICT R&D – NORBAS".

Trondheim, September 2019

Norveški univerzitet za nauku i tehnologiju
Fakultet informacionih tehnologija i elektrotehnike

Univerzitet u Nišu
Elektronski fakultet

Miodrag D. Spasić

Model prediktivno upravljanje zasnovano na kliznim režimima

Doktorska disertacija

Norveški univerzitet za nauku i tehnologiju
Fakultet informacionih tehnologija i elektrotehnike
Departman za kibernetiku

Doktoska disertacija

Univerzitet u Nišu
Elektronski fakultet
Katedra za automatiku

Ova disertacija je rezultat projekta "Norwegian, Bosnian, and Serbian cooperation platform for university and industry ICT R&D – NORBAS".

Trondhajm, septembar 2019

To Sanjče, Mace, Cace and Dace for their immense love and support.

Thesis data

Supervisors:
Professor Morten Hovd, Norwegian University of Science and Technology (NTNU),
Faculty of Information Technology and Electrical Engineering,
Department of Engineering Cybernetics

Professor Dragan Antić, University of Niš,
Faculty of Electronic Engineering,
Department of Control Systems

Title:
Model predictive control based on sliding mode control

Abstract:
Design of a controller that is capable to control the process in order to obtain desired overall system performance is a standard problem in all industries. Use of computers and microprocessors have resulted in increased interest in research and design of the control in discrete-time. The main goal is to obtain optimal control moves in presence of disturbances despite inaccuracies in the model of the system. This implies the need for a robust controller as well as a control algorithm that is not time consuming to compute. The research described in this thesis addresses the combination of the strengths of two different control methodologies to design an optimal and robust controller with insignificant online calculation conditions subject to defined objectives.

The first approach presents the combination of generalized predictive and sliding mode control (SMC) techniques in order to improve the system robustness to parameter variation. The proposed control algorithm belongs to the group of chattering-free sliding mode control laws, and it provides the minimum value of the cost function in the presence of parameter perturbations. Digital simulation results are given to verify the sliding mode based generalized predictive controller.

The next approach presents Tube Model Predictive Control (TMPC) with a SMC as an auxiliary controller. It is shown how to calculate the tube widths under SMC

control, and thus how much the constraints of the nominal MPC have to be tightened in order to achieve robust stability and constraint fulfilment. Digital simulations and real-time experiments are performed for demonstrating theoretical framework.

Improved TMPC with a SMC as an auxiliary controller is studied and presented in the sequel. To ensure the reduced size of the optimization problem, while allowing for large prediction horizons, orthogonal functions are used for the design of the nominal Model Predictive Control (MPC). The MPC component is parameterized using Laguerre functions in discrete-time. This control algorithm is also verified using real-time experiments.

Finally, Predictive Sliding Mode Control (PSMC) that uses Laguerre functions in the design of a control input signal is investigated. Two types of PSMC algorithms are considered: one originating from the digital equivalent control method approach, and another containing an additional sliding mode control component that provides the robustness and determines the system dynamics in reaching mode. A one-step-delayed disturbance estimator is introduced to account for system nonlinearities and unknown disturbances, as well as to ensure better system steady-state accuracy. The proposed algorithms are demonstrated by conducting several real-time experiments. Robustness of the closed loop, affected by tuning parameter values, is demonstrated as well.

Scientific Field:
Electrical Engineering and Computer Science
Scientific Discipline:
Automation
Keywords:
sliding mode control, model predictive control, chattering suppression, tube model predictive control, predictive sliding mode control, orthogonal functions, Laguerre network, DC servo system
UDC:
(681.5.015+681.5.01):681.513.3+519
CERIF Classification:
T125

Podaci o doktorskoj disertaciji

Mentori:
Prof. dr Morten Hovd, Norveški univerzitet za nauku i tehnologiju (NTNU),
Fakultet informacionih tehnologija i elektrotehnike,
Katedra za kibernetiku

Prof. dr Dragan Antić, Univezitet u Nišu,
Elektronski fakultet,
Katedra za automatiku

Naslov:
Model prediktivno upravljanje zasnovano na kliznim režimima

Rezime:
Projektovanje regulatora koji služi za upravljanje procesom u cilju postizanja željenih performansi celokupnog sistema je standardni problem u svim granama industrije. Razvoj računara i mikroprocesora je u značajnoj meri uticao na povećanje interesovanja za istraživanje u oblasti projektovanje regulatora u diskretnom domenu. Glavni cilj je dobijanje optimalnog upravljanja u prisustvu poremećaja bez obzira na tačnost modela procesa. To podrazumeva robustnost regulatora kao i to da algoritam upravljanja ne koristi previše procesorskog vremena za izračunavanje. Istraživanje koje je opisano u ovoj tezi prikazuje kombinaciju dobrih osobina dveju metodologija u cilju projektovanja optimalnog i robusnog upravljanja sa beznačajnim uslovima *online* izračunavanja pri unapred definisanim ograničenjima.

Prvi prilaz pokazuje kombinaciju generalizovanog prediktvnog upravljanja i upravljanja sa kliznim režimima u ciju poboljšanja robustnosti pri promeni parametara sistema. Predloženi algoritam upravljanja pripada grupi zakona upravljanja sa kliznim režimima koji smanjuju četering i obezbeđuju minimalnu vrednost kriterijumske funkcije pri parametarskoj perturbaciji. Rezultati digitalne simulacije su dati u cilju provere upravljanja generalizovanog prediktivnog upravljanja zasnovanog na kliznim režimima.

Sledeći pristup prikazuje *Tube* model prediktivno upravljanje (TMPU) sa regula-

torom zasnovanim na kliznim režimima kao pomoćnim regulatorom. Pokazano je kako se računa širina 'cevi' (eng. *Tube*) pri upravljanju sa kliznim režimima, i za koliko treba smanjiti ograničenja za nominalni model prediktivni regulator (MPR) kako bi se postigla robustnost i stabilnost sistema pri ograničenjima. Digitalna simulacija i eksperimenti u realnom vremenu su izvršeni kako bi se potvrdili teoretski dobijeni rezultati.

Poboljšan TMPU sa regulatorom sa kliznim režimima je proučavan i prikazan u nastavku. U cilju smanjenja optimizacionog problema, a da se pri tom kosristi dovoljno veliki horizont predikcije, za projektovanje nominalnog MPRa korišćene su ortogonalne funkcije u diskretnom domenu. MPR je projektovan pomoću diskretnih Lagerovih funkcija. Ovaj upravljačkoi algoritma je takođe proveren pomoću eksperimenata u realnom vremenu.

Na kraju je proučavano prediktivno upravljanje sa kliznim režimima (PUKR) koje koristi Lagerove funkcije za projektovanje upravljačkog signala. Razmatrana su dva tipa PUKR algoritma: jedan koji je zasnovan na metodi ekvivalentnog upravljanja i drugi koji sadrži dodatnu komponentu upravljanja sa kliznim režimima, koja obezbeđuje robustnost sistema i koja određuje dinamiku sistema u fazi dosezanja. Estimator poremećaja je uveden kako bi se estimirale nelinearnosti sistema i poremećaj, kao i za obezbeđenje boljeg odziva sistema u ustaljenom stanju. Predloženi algoritam je demonstriran pomoću nekoliko eksperimenata u realnom vremenu. Takođe, pokazana je i robustnost sistema na promenu parametara.

Naučna oblast:
Elektrotehnika i računarstvo
Naučna disciplina:
Automatika
Ključne reči:
upravljanje kliznim režimima, model prediktivno upravljanje, smanjenje četeringa, *tube* prediktivno upravljanje, prediktivno upravljanje kliznim režimima, ortogonalne funkcije, Lagerova mreža, DC servo sistem
UDK:
(681.5.015+681.5.01):681.513.3+519
CERIF klasifikacija:
T125

Preface

This dissertation is submitted in partial fulfilment of the requirements for the degree of *philosophiae doctor* (Ph.D.) at the Norwegian University of Science and Technology (NTNU), and for the degree *doctor of science* at the University of Niš (UNiš). My main supervisor has been Professor Morten Hovd at the Department of Engineering Cybernetics at NTNU, while my co-supervisor has been Professor Dragan Antić from the Department of Control Systems at UNiš, Faculty of Electronic Engineering.

The studies have been carried out at NTNU and UNiš in the period from December 2012 to July 2019.

This work has been funded by the Norwegian Ministry for Foreign Affairs through the HERD program under the project “Norwegian, Bosnian, and Serbian cooperation platform for university and industry ICT R&D – NORBAS".

Acknowledgements

I would like to thank my main supervisor Prof. Morten Hovd for enormous patience and support during my work on the thesis. His guidelines and very quick answering on my questions were very encouraging when it was most needed to me. He has supported my ideas and given valuable suggestions which have resulted in this thesis. I would also appreciate my co-supervisor Prof. Dragan Antić for his help during my PhD studies. Without his professional support, this work will not be completed. Many thanks go to Prof. Darko Mitić. His knowledge together with long discussions within the area of control systems was very useful.

Special thank goes to NORBAS project coordinator, Tore Jørgensen, for his encouragement and generous speeches during all formal and informal meetings within NORBAS project. Also I would like to thank NORBAS team members and administrative officers from NTNU and UNI for practical arrangements of my work.

For very pleasant stay in Norway, I would to thank my friends and colleagues Mladen Veletić and Dijana Vuković.

Last but not least, I would like to thank the guys from Department of Control Systems at UNI. Their friendship and social gathering were very supportive. And will be in the future.

Miodrag Spasić
July 2019, Niš

Contents

List of Figures

Abbreviations

ACK	Acknowledgement
ACS	Automatic Control System
CARIMA	Controlled Auto-Regressive and Integrated Moving-Average
DC	Direct Current
DMC	Dynamic Matrix Control
DSMC	discrete-time Sliding Mode Control
FIR	Finite Impulse Response
GMVC	Generalized Minimum Variance Control
GPC	Generalized Predictive Control
IRM	Impulse Response Model
LP	Linear Program
LQ	linear quadratic
MIMO	multiple-input multiple-output
MOAS	maximal output admissible set
MPC	Model Predictive Control
MPCBLF	Model Predictive Control based on Laguerre Functions
MPHC	Model Predictive Heuristic Control
mRPI	Minimal Robustly Positive Invariant
MVC	Minimum Variance Control
nMP	non-Minimum Phase
PSMC	Predictive Sliding Mode Control
QDMC	Quadratic Dynamic Matrix Control
QP	Quadratic Programming
qSM	quasi-Sliding Mode

qSMC	quasi Sliding Mode Control
RHC	Receding Horizon Control
RPI	Robust Positively Invariant
SISO	single-input single-output
SM	Sliding Mode
SMC	Sliding Mode Control
SMCS	Sliding Mode Control System
SMGPC	Sliding Mode based GPC
SRM	Step Response Model
TF	Transfer Function
TMPC	Tube Model Predictive Control
VSC	Variable Structure Control
VSCS	Variable Structure Control Systems
VSS	Variable Structure System

Chapter 1

Introduction

1.1 Motivation

The primary objective of this chapter is to provide a compact overview of some aspects of the control approaches used as a starting point for the research in the area of control systems leading to this thesis.

The idea was to examine how two different control methodologies can be combined to obtain a robust control method which would give the desired performance to the closed-loop system in the presence of the disturbances and uncertainties. One of these control methodologies is MPC that has the capability to cope with constraints on the input, output or states of the controlled system. The computational efficiency of a nominal (error-free) MPC problem is acceptable, and the design for the online implementation is straightforward, but as is noted in [1], optimal or close-to-optimal approaches to robust MPC generally have prohibitive online calculation requirements. More practical approaches are therefore a compromise between performance and online calculation requirements.

To overcome this issue, some second control method can be combined with MPC. One of the control methods known for its robustness to parameter variations and external disturbances is Sliding Mode Control (SMC). Due to its order reduction property[1], and negligible online calculation requirements, SMC is a good candidate for combining with MPC to develop a control approach inheriting the strengths of both.

For a better understanding of the work described in this thesis, the next sections give the structure and contribution of the thesis, following the basic concepts of MPC, SMC and related elements defined in Chapter 2.

[1] See section 2.3 for details

1.2 Structure and Contributions of the Thesis

Chapter 2 presents background theory on dynamic system models, together with key elements of the MPC and SMC control methodologies that are used as starting points for this research.

Chapter 3 presents a novel control design algorithm for improving robustness of the system using techniques inspired by a particular subclass of discrete-time SMC algorithms. The design is based on an input/output model, combining Generalized Minimum Variance Control (GMVC) and discrete-time SMC techniques. Developments in the field of predictive control makes it natural to use of Generalized Predictive Control (GPC) instead of GMVC [2], resulting in better system performance. Similar to the case with GMVC, GPC replaces the equivalent control in the traditional discrete-time SMC design based on state-space models. This combination of SMC and GPC is analyzed and the results are published in [3]:

- D. Mitić, M. Spasić, M. Hovd, D. Antić, "An Approach to Design of Sliding Mode based Generalized Predictive Control," *Proceedings of IEEE 8th International Symposium on Applied Computational Intelligence and Informatics (SACI) 2013*, pp. 347–351, May 2013.

This paper proposes the modification of the SMC component by implementing the chattering free SMC algorithm, which results in improvement of the system robustness.

Chapter 4 presents a Tube Model Predictive Control (TMPC) method that uses SMC as an auxiliary controller. In this chapter, it is chosen to use a nominal TMPC as in the original TMPC formulation, in order to highlight the robustness improvement from the auxiliary controller. The work in this area is published in [4]:

- M. Spasić, M. Hovd, D. Mitić, D. Antić, "Tube Model Predictive Control with an Auxiliary Sliding Mode Controller," *Modeling, Identification and Control*, vol. 37, pp. 181–193, November 2016.

In addition to describing the implementation of two proposed types of SMC auxiliary controllers within a TMPC framework, the paper also presents how to calculate, for each constraint, how far in the direction of constraint the true system can be driven by the model uncertainty. This gives a direct measure of how much each constraint will need to be tightened for the two proposed of SMC auxiliary controllers.

Chapter 5 extends the examination of the TMPC approach. The results presented herein are the modified control methods, elaborated in previous chapter, where the nominal traditional MPC is replaced by one based on discrete-time Laguerre functions. Obtained results are published in [5]:

- M. Spasić, D. Mitić, M. Hovd, D. Antić, "Tube Model Predictive Control based

on Laguerre functions with an Auxiliary Sliding Mode Controller," *Proceedings of IEEE 15th International Symposium on Intelligent Systems and Informatics (SISY) 2017*, pp. 243–248, September 2017.

The main advantage of using Model Predictive Control based on Laguerre Functions (MPCBLF) lies in the design of the nominal MPC defined by only few parameters of the Laguerre functions obtained from the discrete-time Laguerre network. This allows reduction of number of parameters, smaller number of decision variables, thereby making the optimization problem smaller. It also provides possibility of faster online calculations for the nominal MPC for large prediction horizons.

Chapter 6 deals with Predictive Sliding Mode Control (PSMC) that uses Laguerre functions in the design of a control input signal. Two types of PSMC algorithms are considered: one originating from the discrete-time equivalent control method approach, and another containing an additional sliding mode control component that provides robustness and determines the system dynamics in reaching mode. In both cases, the Laguerre functions compose the control components that are the analogues to the discrete-time equivalent control of SMC. These results are published in [6]:

- M. Spasić, D. Mitić, M. Hovd, D. Antić, "Predictive Sliding Mode Control based on Laguerre functions," *Journal of Control Engineering and Applied Informatics*, vol. 21, no. 1, pp. 12–20, March 2019.

The improvement compared to the previously published approaches is obtained using Laguerre functions for the controller design, where the cost function is optimized with respect to the coefficients of the Laguerre functions. The system dynamics in reaching mode is fully determined and the system state attains the sliding mode in a finite number of steps. Improved system robustness and steady-state accuracy is achieved by introducing the one-step delayed disturbance estimator.

1.3 Papers not included in the Thesis

During the PhD work, the author has also contributed to the papers in addition to the publications that this thesis is based on. Some of them are listed below.

- M. Milovanović, D. Antić, M. Spasić, S. Nikolić, S. Perić and M. Milojković, "Improvement of DC Motor Velocity Estimation Using a Feedforward Neural Network," *Acta Polytechnica Hungarica*, vol. 12, no.6, pp. 107–126, 2015.
- M. Milovanović, D. Antic, M. Milojković, S. Nikolic, S. Perić, and M. Spasić, "Adaptive PID control based on orthogonal endocrine neural networks," *Neural Networks*, vol. 84, pp. 80–90, 2016.
- M. Milovanović, D. Antić, S. Nikolić, S. Perić and M. Milojković, and M. Spasić,

"Neural Network Based on Orthogonal Polynomials Applied in Magnetic Levitation System Control," *ELEKTRONIKA IR ELEKTROTECHNIKA*, vol. 23, no. 3, pp. 24–29, 2017.

- M. Milovanović, D. Antić, M. Milojković, S. Nikolić, M. Spasić, and S. Perić "Time Series Forecasting With Orthogonal Endocrine Neural Network Based on Postsynaptic Potentials," *Journal of Dynamic Systems, Measurement, and Control*, vol. 139, no. 4, pp. 041006-1–041006-9, 2017.
- N. Danković, D. Antić, S. Nikolić, S. Perić and M. Spasić, "Generalized Cascade Orthogonal Filters based on Symmetric Bilinear Transformation with Application to Modeling of Dynamic Systems," *Filomat*, vol. 32, no. 12, pp. 4275–4284, 2018.
- M. Spasić, D. Antić, N. Danković, S. Perić and S. Nikolić, "Digital Model Predictive Control of the Three Tank System based on Laguerre Functions," *FACTA UNIVERSITATIS Series: Automatic Control and Robotics*, vol. 17, no. 3, pp. 153–164, 2018.

Chapter 2

Background theory

2.1 Dynamic System Models

Any MPC method is based on a dynamic model of the system, that describes the process behavior over time. Most physical systems are more naturally described using continuous-time models. However, most controllers are implemented in computers, leading to discrete-time control action. This is invariably the case for controllers with substantial computational requirements, such as MPC. This leads to a need for dynamic system models also in discrete-time. This thesis is not concerned with the development of dynamic models *per se*. Therefore, the starting point for the presentation in this thesis is the definition of a linear time-invariant model of the system.

If the system is defined by a continuous-time linear model in the form of

$$\begin{aligned} \frac{dx(t)}{dt} &= A_c x(t) + B_c u(t) \\ y(t) &= C_c x(t) \\ x(0) &= x_0 \end{aligned} \tag{2.1}$$

in which $x(t) \in \mathbb{R}^{n_x}$ is the state, $u(t) \in \mathbb{R}^{n_u}$ is the input, $y(t) \in \mathbb{R}^{n_p}$ is the output, and $t \in \mathbb{R}$ is time, then the matrices $A_c \in \mathbb{R}^{n_x \times n_x}$, $B_c \in \mathbb{R}^{n_x \times n_u}$, and $C_c \in \mathbb{R}^{n_p \times n_x}$ represent the state transition, input and output matrices of the system represented by eq. (2.1), respectively. The initial condition is defined by the state $x(t)$ at time $t = t_0$. The solution of eq. (2.1) is

$$x(t) = e^{A_c t} x_0 + \int_0^t e^{-A_c \tau} B_c u(\tau) d\tau. \tag{2.2}$$

The dynamics described by the discrete-time model corresponds to the behaviour observed when sampling the states and outputs of the continuous-time model (2.1). The aim is to obtain the discrete-time representation of the system model (2.1) that describes its evolution in interval $kT \leq t \leq (k+1)T$, where $k \in \mathbb{I}_{\geq 0}$ is a non-negative

integer representing sample instant, which is interconnected to time by $t = kT$, where T is the sampling time.

The evolution of the discrete-time state x_k with time, starting from the initial condition x_0, as it is affected by the manipulated, discrete-time input u_k, can be obtained from eq. (2.1). Assuming a sampling time T and zero order hold, the value of the state x_k at $t = kT + T$ can be calculated by

$$x(kT+T) = e^{A_c T} x(kT) + \int_{kT}^{kT+T} e^{A_c(kT+T-\tau)} B_c u(\tau) d\tau \tag{2.3}$$

The discrete-time representation of eq. (2.3) is

$$x_{k+1} = A_d x_k + B_d u_k \tag{2.4}$$

where

$$A_d = e^{A_c T}, \tag{2.5}$$

$$B_d = \int_{kT}^{kT+T} e^{A_c(kT+T-\tau)} B_c u(\tau) d\tau. \tag{2.6}$$

In that way, the corresponding discrete-time state-space model of the system described in continuous time by eq. (2.1) has a form

$$\begin{aligned} x_{k+1} &= A_d x_k + B_d u_k \\ y_k &= C_d x_k \end{aligned} \tag{2.7}$$

where $C_c = C_d$. Throughout the thesis it is assumed that the model of the system is known, i.e., a discrete-time model of the system is available. The subscript d in eq. (2.7) will be omitted in the rest of the thesis for notational simplicity.

If the exact structure of a system is not known, it is possible to neglect the system states and to consider only inputs and outputs. There are many forms of discrete-time input-output system models that can be used, such as:

- Impulse Response Model (IRM), where the connection between the output and the input of the system is described by

$$y_k = \sum_{i=1}^{\infty} h_i u_{k-i}. \tag{2.8}$$

  The sampled output y_k is obtained when the process is excited by the unit input function h_i. If the sum in eq. (2.8) is finite, the model is then called a Finite Impulse Response (FIR) model, and is represented by

$$y_k = \sum_{i=1}^{N} h_i u_{k-i} = H(z^{-1}) u_k \tag{2.9}$$

where z^{-1} is a backward shift operator such that $u_k z^{-1} = u_{k-1}$, and $H(z^{-1})$ is written as

$$H(z^{-1}) = h_1 z^{-1} + h_2 z^{-2} + \cdots + h_N z^{-N}; \tag{2.10}$$

- Step Response Model (SRM) where, by exciting the system with the step input signal, the output is obtained by

$$y_k = y_0 + \sum_{i=1}^{N} g_i \Delta u_{k-i} = y_0 + G(z^{-1})\Delta u_k \tag{2.11}$$

with $\Delta = 1 - z^{-1}$, and

- Transfer Function (TF) model in the form:

$$A(z^{-1})y_k = B(z^{-1})u_k \tag{2.12}$$

with

$$\begin{aligned} A(z^{-1}) &= 1 + a_1 z^{-1} + a_2 z^{-2} + \cdots + a_{n_a} z^{-n_a} \\ B(z^{-1}) &= b_0 + b_1 z^{-1} + b_2 z^{-2} + \cdots + b_{n_b} z^{-n_b} \end{aligned} \tag{2.13}$$

where $A(z^{-1})$ and $B(z{-}1)$ are appropriate polynomials of the system's transfer function $G(z^{-1}) = B(z^{-1})/A(z^{-1})$, where n_a and n_b represents the order of $A(z^{-1})$ and $B(z^{-1})$, respectively.

In this thesis, for the design and demonstration of the control methods, only the discrete-time TF and state-space models are used.

2.2 Model Predictive Control (MPC)

MPC is a family of advanced control methods. Traditionally, MPC has been applied to systems with relatively slow dynamics, in particular those found in the chemical processing industries. However, more recently this control method has found application in a wide range of industries, owing both to more efficient optimisation formulations and the availability of computational power. The main idea is to use a dynamical model and an optimization formulation to optimize the predicted future plant behaviour, with future inputs as degrees of freedom in the optimization.

The characteristics of all MPC-based strategies are presented in Fig. 2.1.

The future outputs of the controlled system within the prediction horizon N_p are denoted as y_{k+j}, for $j = 1, \ldots, N_p$. They depend on the already known values of the output up to instant k or equivalently the value of the state at time k, and the future input signal u_{k+j} for $j = 0, \ldots, N_c$, that is going to be calculated and applied. N_c is the control horizon and it is less or equal to N_p. The future input signal u_{k+j} is obtained by

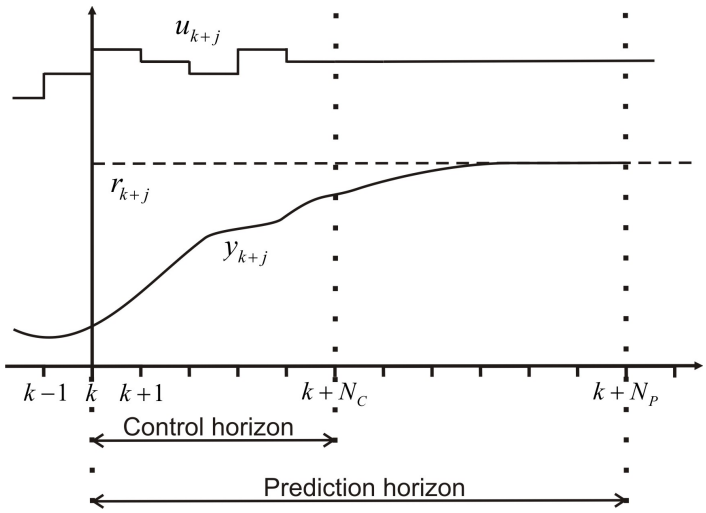

Figure 2.1: MPC-based strategy

minimization of some objective function J, with the goal of steering the process output as close as possible to the given reference trajectory r_{k+j}. The objective function J is usually a quadratic function of the deviation of the predicted output from the reference signal (or the states from the desired reference trajectory) and the deviation of the inputs from the desired input trajectory. From the set of calculated optimal control signals, whose size is given by N_c, only the first element of this set is applied to the process. The optimization is performed at every time instant with fixed control and prediction horizons. This concept is used all controllers in the MPC family and, is known as the *receding horizon method*.

Another feature that differentiates MPC from other optimal control methods is a possibility that input, output and state constraints can be accounted for when optimal control action is calculated. Such constraints typically arise from the technical limitations of the system, or its related safety requirements. The ability to take such considerations into account when calculating the optimal control action is a significant advantage for MPC. It means that the optimal control action is calculated with consideration of such previously defined bounds.

Despite the fact that the MPC family of controllers is very large, herein will be presented in detail only the MPC formulations used later in this thesis. The next section contains a short history of MPC, after which the basics of the MPC strategy and the methods applied in this thesis will be described.

2.2.1 A brief history of MPC

Although MPC is known as an optimal control strategy, at the very beginning of its development the close connection with traditional optimal control theory was not really recognized [7–9]. The first representatives of MPC familly were Model Predictive Heuristic Control (MPHC) and Dynamic Matrix Control (DMC). These approaches use a finite-impulse response and finite-step response models, respectively, to forecast the future system behaviour and calculate the future optimal control actions [10, 11]. The MPHC algorithm drives the predicted future output trajectory as closely as possible to a reference trajectory, defined as a first order path from the current output value to the desired set point. The speed of the desired closed-loop response is set by the time constant of the reference trajectory. This is important in practice because it provides a natural way to control the aggressiveness of the algorithm and increasing the time constant leads to a slower but more robust controller. The DMC approach relates changes in a process output to a weighted sum of past input changes, i.e. input moves. By using the step response model one can write predicted future output changes as a linear combination of future input moves. The matrix that ties these two together is the so-called dynamic matrix. One of the disadvantages of the DMC algorithm was a fact that only first N step response coefficients (where N is the number of time steps necessary to reach the steady-state) can be used for the process modelling. This disadvantage was also addressed in [12], where it is proposed to separate DMC into a predictor and an optimizer. A tuning strategy for unconstrained multivariable DMC is proposed in [13]. The authors noted that the prediction horizon N_p should be following the settling time of the process. Also, the control horizon N_c should be greater than or equal to the number of unstable modes of the system [14]. An on-line tuning strategy based on the use of sensitivity functions for the closed-loop response concerning the MPC tuning parameters is described in [15]. Both MPHC and DMC use Linear Program (LP) methods for solving the optimization problem.

The next MPC formulation, named Quadratic Dynamic Matrix Control (QDMC), is used for solving constrained, linear, open-loop optimal control problem employing Quadratic Programming (QP) [16]. The method is based on the online solution of a quadratic program to calculate the input required to keep the process variable close to its reference, and at the same time avoiding violation of defined constraints. The constraints are described by linear inequalities that capture the dynamic behaviour of the constrained variables.

The impulse/step response plant models, obtained by reasonably simple experiments, were very convenient for the approaches mentioned above, but the main issue is that a large number of parameters are needed. To get better models with fewer parameters,

researchers started to use TF models, based on physical models or system identification. In [17] the authors worked with the TF model of the plant and used Diophantine equations to compute future Minimum Variance Control (MVC) input. The optimization problem is solved by minimizing the error between the current output and the reference. Generalised MVC (GMVC) was developed from MVC by including a cost on the input and introducing modifications allowing it to handle non-Minimum Phase (nMP) zeros. Generalised Predictive Control (GPC) was then developed from GMVC [18–20]. The quadratic optimization is defined by a cost function which penalizes predicted output errors. There are different variations also of GPC, and the formulation used in this thesis will be described in detail later.

From a system theoretic point of view, simple impulse or step inputs used for system identification could be also an issue. This leads to the more common MPC formulation nowadays, which also results in a low number of model parameters - the state-space model based MPC. One of the first publications that presents the state-space model in the MPC design is [21]. Linear quadratic filtering theory is used for the output feedback realization. At the same time, the linear quadratic regulatory theory is used for the target tracking and embedding the integral action in the controller. Here, tuning of the controller for achieving nominal stability is eliminated by incorporating a nominal stabilizing constrained regulator [14]. Nominal stability of the controlled systems can be also achieved by adding a terminal cost and constraints or by introducing long horizons for the online calculation of the optimization problem [22].

Earlier MPC methods have been designed to control systems based on nominal models when uncertainty is not taken into account. Different types of uncertainties can be considered, like additive disturbance, model uncertainty, etc. This challenge produced a new generation of MPCs, so-called robust MPC. The main characteristic of a robust MPC is that the control objectives must be fulfilled by the controlled system for all realizations of the uncertainty. Several approaches have been proposed for achieving robustness with MPC. The simplest one is to rely on the inherent robustness of feedback, and hope that it provides adequate robustness for the closed-loop system. The second method of achieving robustness in the context of conventional MPC is the introduction of all possible realizations of the uncertainty in the MPC optimization problem, and minimization the objective function for the worst case uncertainty (min-max open-loop model predictive control). This generaly leads to very demanding optimization problems, which may be difficult to execute in real time. Other approaches combine the nominal performance and constraint handling capabilities of MPC with some other control algorithm whose main purpose is to provide robustness. As is noted in [1], optimal or close-to-optimal approaches to robust MPC generally have prohibitive online calculation requirements. More practical approaches are therefore a compromise between

performance and online calculation requirements.

In last 15 years differente MPC methodologies are developed. So-called Tube MPC (TMPC), where the MPC essentially controls the nominal plant, and an auxiliary controller keeps 'all possible' trajectories inside a 'tube' close to the nominal plant response. A thorough introduction to TMPC is given in [1]. The nominal trajectory is the center of the tube, while the tube represents the set of the possible states. To ensure robust constraint satisfaction, the state/output constraints of the nominal MPC have to be modified to account for the width of the tube, and the magnitudes of control inputs that are available to the nominal MPC also have to be reduced to account for the additional input component coming from the auxiliary controller. A modification of TMPC is proposed in [23], where the authors developed a solution for the robust MPC problem in the presence of bounded disturbances. The initial state is employed as a decision variable in the quadratic optimal control problem solved online. Some recent contributions in this area can be seen in [24–27].

Another contribution to the traditional MPC was introducing the orthonormal functions for design of the controllers. To generalize the traditional design, authors in [28] suggested introducing a set of discrete-time Laguerre functions into the design. They argue that this generalization helps with re-formulating the predictive control problem and simplifying the solutions, in addition to providing a set of new performance-tuning parameters that can be readily understood by engineers. Furthermore, a long control horizon can be realized through the exponential nature of the Laguerre functions, without having to solve a very large optimization problem. This method is used to replace the conventional MPC providing the reduced burden of online calculations. In this manner, in recent years, Model Predictive Control based on Laguerre Functions (MPCBLF) is used for different applications such as control of three-phase voltage source inverter [29], a real-time walking pattern generator [30] or control of dynamic positioning system of vessels [31].

The next three sections of this chapter present the basic formulations and elements of the used GPC, TMPC and TMPC based on orthonormal basis functions.

2.2.2 Generalized Predictive Control

GPC is a predictive control method that was proposed in 1987 [18, 19, 32]. The model of the plant used for the design of the controller is a TF model. GPC can deal with a wide range of plant control problems with a fair number of design variables, depending on prior knowledge of the plant and control objectives. It is already mentioned that GPC has been derived from GMVC. The design goal in GMVC is to define the control

that provides a minimum variance of the variable $\overline{g}$ defined by

$$\overline{g}_{k+1} = C(z^{-1})(y_{k+1} - r_{k+1}) + Q(z^{-1})u_k \tag{2.14}$$

whose minimum value ensures the good system tracking of the reference input r_k i.e. in the ideal case the zero value of the tracking error

$$e_k = y_k - r_k. \tag{2.15}$$

The polynomials $C(z^{-1})$ and $Q(z^{-1})$ are given by

$$C(z^{-1}) = c_0 + c_1 z^{-1} + ... + c_{n_c} z^{-n_c}, \tag{2.16}$$

$$Q(z^{-1}) = q_0 + q_1 z^{-1} + ... + q_{n_q} z^{-n_q}, \tag{2.17}$$

having the degrees n_c and n_q, respectively, and should be selected to assign the desired closed-loop systems dynamics. The variable $\hat{u}_k$ is obtained from the control input as

$$\hat{u}_k = C(z^{-1})u_k. \tag{2.18}$$

The predictions of the control signal is based on using a discrete-time model of the single-input single-output (SISO) plant given by

$$A(z^{-1})y_k = z^{-1}B(z^{-1})u_k \tag{2.19}$$

where u_k is the input and y_k is the output. $A(z^{-1})$ and $B(z^{-1})$ are model polynomials as defined in eq. (2.13).

To obtain a set of predicted control moves using this approach, a quadratic cost function, which measures the distance between the future output signals and given reference ones plus the control effort of the form

$$J = \overline{\mathbf{g}}^T \overline{\mathbf{g}} + \hat{\mathbf{u}}^T \lambda \hat{\mathbf{u}} \tag{2.20}$$

have to be minimized, where λ is a control weighting constant and

$$\overline{\mathbf{g}} = [\overline{g}_{k+1} \quad \cdots \quad \overline{g}_{k+N}]^T \tag{2.21}$$

$$\hat{\mathbf{u}} = [\Delta\hat{u}_k \quad \cdots \quad \Delta\hat{u}_{k+N-1}] \tag{2.22}$$

with N denoting the prediction horizon and $\Delta = 1 - z^{-1}$ denoting the difference operator. By minimizing the objective function in eq. (2.20), the computed future control increments drive the system output y_k close to the reference r_k.

To design GPC, let one consider the next two Diophantine equations

$$E_j(z^{-1})A(z^{-1})\Delta + z^{-1}F_j(z^{-1}) = 1, \tag{2.23}$$

$$E_j(z^{-1})B(z^{-1}) = G_j(z^{-1}) + z^{-1}H_j(z^{-1}) \tag{2.24}$$

whose solutions are the following polynomials:

$$E_j(z^{-1}) = {e_0}^j + {e_1}^j z^{-1} + ... + {e_{j-1}}^j z^{-(j-1)}, \quad (2.25)$$

$$F_j(z^{-1}) = {f_0}^j + {f_1}^j z^{-1} + ... + {f_{n_a}}^j z^{-n_a}, \quad (2.26)$$

$$G_j(z^{-1}) = g_0 + g_1 z^{-1} + ... + g_{j-1} z^{-(j-1)}, \quad (2.27)$$

$$H_j(z^{-1}) = {h_0}^j + {h_1}^j z^{-1} + ... + {h_{n_b-1}}^j z^{-(n_b-1)}, \quad (2.28)$$

for $j = 1, ..., N$. The first Diophantine equation (2.23) is used for obtaining the prediction output, whereas the second one (2.24) distinguishes future and past control values.

By multiplying the both sides of eq. (2.19) with $E_j(z^{-1})\Delta$ and by substituting eqs. (2.23) and (2.24) in the obtained result, the variable defined by eq. (2.14) can be rewritten as

$$\begin{aligned} \overline{g}_{k+j} &= C(z^{-1})[F_j(z^{-1})y_k + G_j(z^{-1})\Delta u_{k+j-1} + H_j(z^{-1})\Delta u_{k-1}] \\ &- C(z^{-1})r_{k+j} + Q(z^{-1})\Delta u_{k-1} \end{aligned} \quad (2.29)$$

for $j = 1, ..., N$, or in more compact form as

$$\overline{\mathbf{g}} = C(z^{-1})\mathbf{F}(z^{-1})y_k + \mathbf{G}\hat{\mathbf{u}} - C(z^{-1})\mathbf{r} + [C(z^{-1})\mathbf{H}(z^{-1}) + \mathbf{Q}(z^{-1})]\Delta u_{k-1} \quad (2.30)$$

where:

$$\mathbf{F}(z^{-1}) = [F_1(z^{-1}) \quad \cdots \quad]F_N(z^{-1})]^T, \quad (2.31)$$

$$\mathbf{Q}(z^{-1}) = Q(z^{-1})\hat{\mathbf{I}}, \quad \hat{\mathbf{I}} = [1 \quad \cdots \quad 1]^T, \quad (2.32)$$

$$\mathbf{H}(z^{-1}) = [H_1(z^{-1}) \quad \cdots \quad]H_N(z^{-1})]^T, \quad (2.33)$$

$$\hat{\mathbf{u}} = [\Delta\hat{u}_k \quad \cdots \Delta\hat{u}_{k+N-1}]^T, \quad (2.34)$$

$$\mathbf{r} = [r_{k+1} \quad \cdots r_{k+N}]^T, \quad (2.35)$$

$$\mathbf{G} = \begin{bmatrix} g_0 & 0 & 0 & \dots & 0 \\ g_1 & g_0 & 0 & \dots & 0 \\ \vdots & \vdots & \vdots & \vdots & \vdots \\ g_{N-1} & g_{N-2} & g_{N-3} & \cdots & g_0 \end{bmatrix}. \quad (2.36)$$

The next step is to minimize the cost function represented by eq. (2.20) with respect to the control $\hat{\mathbf{u}}$, taking into account eq. (2.30), which gives the following control vector

$$\begin{aligned} \hat{\mathbf{u}} = &- (\mathbf{G}^T\mathbf{G} + \lambda\mathbf{I})^{-1}\mathbf{G}^T\{C(z^{-1})\mathbf{F}(z^{-1})y_k - C(z^{-1})\mathbf{r} \\ &+ [C(z^{-1})\mathbf{H}(z^{-1}) + \mathbf{Q}(z^{-1})]\Delta u_{k-1}\}. \end{aligned} \quad (2.37)$$

GPC algorithm is now given by the first row of eq. (2.37):

$$\Delta\hat{u}_k = -\mathbf{m_1}\{C(z^{-1})\mathbf{F}(z^{-1})y_k - C(z^{-1})\mathbf{r} + [C(z^{-1})\mathbf{H}(z^{-1}) + \mathbf{Q}(z^{-1})]\Delta u_{k-1}\} \quad (2.38)$$

where

$$\mathbf{M} = (\mathbf{G}^T\mathbf{G} + \lambda\mathbf{I})^{-1}\mathbf{G}^T = [\mathbf{m}_1 \quad \mathbf{m}_2 \quad \cdots \quad \mathbf{m}_N]^T, \tag{2.39}$$

and can be represented by

$$\Delta u_k{}^{GPC} = -\Phi^{-1}(z^{-1})(\Upsilon(z^{-1})y_k - \Psi(z^{-1})r_{k+N}), \tag{2.40}$$

with

$$\Phi(z^{-1}) = C(z^{-1}) + \mathbf{m}_1 z^{-1}[C(z^{-1})\mathbf{H}(z^{-1}) + \mathbf{Q}(z^{-1})], \tag{2.41}$$

$$\Upsilon(z^{-1}) = \mathbf{m}_1 C(z^{-1})\mathbf{F}(z^{-1}), \tag{2.42}$$

$$\Psi(z^{-1})r_{k+N} = \mathbf{m}_1 C(z^{-1})\mathbf{r}. \tag{2.43}$$

Substituting eq. (2.40) in eq. (2.19) yields the closed-loop system transfer function described by

$$y_{k+1} = \frac{B(z^{-1})\Psi(z^{-1})}{\Phi(z^{-1})A(z^{-1})\Delta + B(z^{-1})\Upsilon(z^{-1})z^{-1}} r_{k+N}. \tag{2.44}$$

As one can see, by the proper choice of the polynomials $C(z^{-1})$ and $Q(z^{-1})$, the desired closed-loop dynamics can be obtained. Moreover, the polynomials $C(z^{-1})$ and $Q(z^{-1})$ can be calculated uniquely from

$$\Phi(z^{-1})A(z^{-1})\Delta + z^{-1}B(z^{-1})\Upsilon(z^{-1}) = P_{CL}(z^{-1}) \tag{2.45}$$

if $n_c = n_a + 1$ and $n_q = n_c + n_b - 1$, where $P_{CL}(z^{-1})$ is the polynomial obtained by assigning the desired closed-loop poles. Furthermore, the tracking error disappears if $\Upsilon(1) = \Psi(1)$ [33].

2.2.3 General MPC calculations

General algorithm for calculation of MPC is given by the next steps:

- Specify prediction and control horizons, N_p and N_c, respectively.
- Define an optimization problem using appropriate form of an objective function J.
- Define the set-point or the reference trajectory, $\mathbf{r}$.
- Measure (or estimate) the states x_k (or x_0 when $k = 0$).
- Make the predictions over the prediction horizon N_p.
- Calculate the predicted output trajectory $\mathbf{u}$ by minimizing the objective function over the control horizon N_c, and apply the first one to the plant.
- Repeat the last three steps at every next time instant.

Let one consider the linear, discrete-time system described by a state-space model described by eq. (2.7) and assume that the state x_k can be measured and is available to the controller at each sampling instant $k \geq 0$. For ease of the presentation it is assumed that SISO systems are used, but all following methods can be applied to multiple-input multiple-output (MIMO) systems as well.

For the unconstrained case, the predictive model of the system described by eq. (2.7) can be represented as

$$\mathbf{x} = \begin{bmatrix} A \\ A^2 \\ \vdots \\ A^{N_p} \end{bmatrix} x_k + \begin{bmatrix} B \\ AB \\ \vdots \\ \sum_{i=0}^{N_p} A^i B \end{bmatrix} u_{k-1} + \begin{bmatrix} B & \cdots & 0 \\ AB+B & \cdots & 0 \\ \vdots & \ddots & \vdots \\ \sum_{i=0}^{N_p-1} A^i B & \cdots & \sum_{i=0}^{N_p-N_c} A^i B \end{bmatrix} \mathbf{u} \tag{2.46}$$

where the predicted control trajectory is defined as

$$\mathbf{u} = [u_k \quad u_{k+1} \quad \cdots \quad u_{k+N_c}]^T, \tag{2.47}$$

and the predicted state trajectory is

$$\mathbf{x} = [x_{k+1} \quad x_{k+2} \quad \cdots \quad x_{k+N_p-1}]^T. \tag{2.48}$$

Using this concept, the vector of the future output of the system

$$\mathbf{y} = [y_{k+1} \quad y_{k+2} \quad \cdots \quad y_{k+N_p}]^T \tag{2.49}$$

can be calculated by

$$\mathbf{y} = \mathbf{F}x_k + \mathbf{\Psi}u_{k-1} + \mathbf{\Phi}\mathbf{u} \tag{2.50}$$

where

$$\mathbf{F} = \begin{bmatrix} CA \\ CA^2 \\ \vdots \\ CA^{N_p} \end{bmatrix}; \mathbf{\Psi} = \begin{bmatrix} CB \\ CAB \\ \vdots \\ \sum_{i=0}^{N_p} CA^i B \end{bmatrix}; \tag{2.51}$$

$$\mathbf{\Phi} = \begin{bmatrix} CB & \cdots & 0 \\ C(AB+B) & \cdots & 0 \\ \vdots & \ddots & \vdots \\ \sum_{i=0}^{N_p-1} CA^i B & \cdots & \sum_{i=0}^{N_p-N_c} CA^i B \end{bmatrix}. \tag{2.52}$$

The general form of the objective function, where the aim is that the system output follows the reference, and the control is penalized to reduce the big changes of the manipulated variable, can be chosen as

$$J = \sum_{j=0}^{N_p}(y_{k+j} - r_{k+j})^T Q(y_{k+j} - r_{k+j}) + \sum_{j=1}^{N_c}(u_{k+j} - u_{k+j-1})^T R(u_{k+j} - u_{k+j-1}), \quad (2.53)$$

where Q, R are positive definite matrices. If the vector of the future referent trajectory is described by

$$\mathbf{r} = [r(k+1) \quad r(k+2) \quad \cdots \quad r(k+N_p)]^T, \quad (2.54)$$

minimizing the cost function represented by eq. (2.53) gives the control action in a form of

$$\mathbf{u} = (\mathbf{\Phi}^T \bar{Q} \mathbf{\Phi} + \bar{R})^{-1} \mathbf{\Phi}^T (\mathbf{r} - \mathbf{F}x_k - \mathbf{\Psi}u_{k-1}), \quad (2.55)$$

where

$$\bar{Q} = \begin{bmatrix} Q & 0 & \cdots & 0 & 0 \\ 0 & Q & \ddots & \vdots & 0 \\ \vdots & \vdots & \ddots & Q & 0 \\ 0 & 0 & \cdots & 0 & S \end{bmatrix}; \quad \bar{R} = \begin{bmatrix} R & 0 & \cdots & 0 & 0 \\ 0 & R & \ddots & \vdots & 0 \\ \vdots & \vdots & \ddots & R & 0 \\ 0 & 0 & \cdots & 0 & R \end{bmatrix}. \quad (2.56)$$

The first element, for SISO, or the first n_u rows for MIMO systems, of the control $\mathbf{u}$ given by

$$u_k = \mathbf{m_1}(\mathbf{r} - \mathbf{F}x_k - \mathbf{\Psi}u_{k-1}) \quad (2.57)$$

is applied to the process, and $\mathbf{m_1}$ is the first row of the matrix $(\mathbf{\Phi}^T \bar{Q} \mathbf{\Phi} + \bar{R})^{-1} \mathbf{\Phi}^T$.

An incremental state-space model can be derived from eq. (2.7) as well. The design is based on the computation of the future control increments

$$\Delta u_{k+j}, \quad j = 1, N_c - 1,$$

which means that the model for the design of the controller is embedded with an integrator as in [28]. By defining $\Delta x_k = x_k - x_{k-1}$ and $\Delta u_k = u_k - u_{k-1}$, a new state variable vector can be formulated by

$${x_k}^{aug} = [\Delta x_k \quad y_k]^T. \quad (2.58)$$

The augmented model is now obtained in the form

$$\begin{aligned} {x_{k+1}}^{aug} &= A^{aug} {x_k}^{aug} + B^{aug} \Delta u_k \\ {y_k}^{aug} &= C^{aug} {x_k}^{aug} \end{aligned} \quad (2.59)$$

where

$$A^{aug} = \begin{bmatrix} A & \mathbf{0}^T \\ CA & 1 \end{bmatrix}; \quad B^{aug} = \begin{bmatrix} B \\ BC \end{bmatrix}; \quad C^{aug} = \begin{bmatrix} \mathbf{0} & 1 \end{bmatrix}. \quad (2.60)$$

Vector **0** is the vector with zeros of appropriate dimension. For the notation simplicity, A^{aug}, B^{aug}, C^{aug}, ${x_k}^{aug}$ and ${y_k}^{aug}$ will be denoted as A, B, C, x_k and y_k, respectively. The predicted control trajectory is defined by

$$\Delta\mathbf{u} = [\Delta u_k \quad \Delta u_{k+1} \quad \cdots \quad \Delta u_{k+N_c-1}] \tag{2.61}$$

then, the predicted, augmented state vector $\mathbf{x} = [x_{k+1} \quad x_{k+2} \quad \cdots \quad x_{k+N_p}]^T$ can be calculated using augmented system matrices described by eq. (2.60) as follows

$$\begin{aligned} x_{k+1} &= Ax_k + B\Delta u_k \\ x_{k+2} &= A^2x_k + AB\Delta u_k + B\Delta u_{k+1} \\ &\vdots \\ x_{k+N_p} &= A^{N_p}x_k + A^{N_p-1}B\Delta u_k + \cdots + A^{N_p-N_c-1}B\Delta u_{k+N_c-1}. \end{aligned} \tag{2.62}$$

Eqs. (2.62) can be rewritten in a form

$$\mathbf{x} = \tilde{F}x_k + \tilde{\Phi}\Delta\mathbf{u} \tag{2.63}$$

where

$$\tilde{F} = \begin{bmatrix} A \\ A^2 \\ \vdots \\ A^{N_p} \end{bmatrix}; \quad \tilde{\Phi} = \begin{bmatrix} B & 0 & 0 & \cdots & 0 \\ AB & B & 0 & \cdots & 0 \\ \vdots & \vdots & \vdots & \cdots & 0 \\ A^{N_p-1}B & A^{N_p-2}B & A^{N_p-3}B & \cdots & A^{N_p-N_c-1}B \end{bmatrix}. \tag{2.64}$$

The predicted output of the system can be calculated as well by

$$\mathbf{y} = C\mathbf{x} = \mathbf{F}x_k + \mathbf{\Phi}\Delta\mathbf{u}. \tag{2.65}$$

The cost function can be chosen as

$$J = (\mathbf{r} - \mathbf{y})^T\bar{Q}(\mathbf{r} - \mathbf{y}) + \Delta\mathbf{u}^T\bar{R}\Delta\mathbf{u} \tag{2.66}$$

where $\bar{Q}$ and $\bar{R}$ are defined by eq. (2.56) and $\mathbf{r}$ is a future set-point vector defined by eq. (2.54). Substituting eq. (2.65) into eq. (2.66) the cost function J has a following form

$$J = (\mathbf{r} - \mathbf{F}x_k)^T\bar{Q}(\mathbf{r} - \mathbf{F}x_k) - 2\Delta\mathbf{u}^T\mathbf{\Phi}^T\bar{Q}(\mathbf{r} - \mathbf{F}x_k) + \Delta\mathbf{u}^T(\mathbf{\Phi}^T\bar{Q}\mathbf{\Phi} + \bar{R})\Delta\mathbf{u} \tag{2.67}$$

and by its minimization, the optimal control increment sequence is calculated from

$$\Delta\mathbf{u} = (\mathbf{\Phi}^T\bar{Q}\mathbf{\Phi} + \bar{R})^{-1}\mathbf{\Phi}^T(\mathbf{r} - \mathbf{F}x_k), \tag{2.68}$$

and once again, only the first control increment Δu_k from eq. (2.68) is applied to the process in a form

$$u_k = u_{k-1} + \Delta u_k. \tag{2.69}$$

Constrained control problem for state-space models

The previous optimization problems are formulated without introducing the constraints in the calculations of the optimal control actions. When constraints are present, the optimization problem in MPC can be formulated as a QP problem in the standard form

$$\min_{\theta} \frac{1}{2}\theta^T H\theta + h^T\theta \tag{2.70}$$

subject to

$$L\theta \leq b \tag{2.71}$$

where the structure and size of the appropriate vectors and matrices depends on the used formulation. The matrix H is the Hessian matrix[1] that has to be positive definite. The linear part of the objective function is defined by the vector h whereas the matrix L and the vector b represent the linear constraints. Only the formulation for the state-space model with embedded integrator will be presented, but the similar approach is applicable to the other formulations presented in this thesis.

The constrained MPC problem can be defined by the following inequalities

$$\begin{aligned} \underline{u} \leq u_k \leq \bar{u} \\ \Delta\underline{u} \leq \Delta u_k \leq \Delta\bar{u} \\ \underline{y} \leq y_k \leq \bar{y} \end{aligned} \tag{2.72}$$

If the cost function for the predictive model described by eq. (2.63) is defined by eq. (2.66), penalizing the deviation of the predicted output $\mathbf{y}$ from the reference signal $\mathbf{r}$, and the predicted increment of the control signal $\Delta\mathbf{u}$, then the constraints defined by eq. (2.72) can be expressed in term of the parameter vector $\Delta\mathbf{u}$ as follows. The control signal constraints can be represented as

$$\underline{U} \leq L_1 u_{k-1} + L_2\Delta\mathbf{u} \leq \bar{U} \tag{2.73}$$

where $\underline{U} = [\underline{u} \quad \underline{u} \quad \cdots \quad \underline{u}]^T$, $\bar{U} = [\bar{u} \quad \bar{u} \quad \cdots \quad \bar{u}]^T$ are the vectors of size $Nc - 1$ and

$$L_1 = \begin{bmatrix} I \\ I \\ \vdots \\ I \end{bmatrix}; \quad L_2 = \begin{bmatrix} I & 0 & 0 & \cdots & 0 \\ I & I & 0 & \cdots & 0 \\ \vdots & \vdots & \vdots & \cdots & 0 \\ I & I & I & \cdots & I \end{bmatrix} \tag{2.74}$$

[1]The Hessian matrix defines the quadratic term in the objective function, and is a symmetric matrix. Positive definiteness means that all eigenvalues are positive - for a mono-variable optimization problem this implies that the coefficient for the quadratic term in the objective function is positive.

of appropriate dimensions. In a standard QP formulation the constraints described by eq. (2.73) are represented as

$$\begin{bmatrix} L_2 \\ -L_2 \end{bmatrix} \Delta\mathbf{u} \leq \begin{bmatrix} \bar{U} - L_1 u_{k-1} \\ -\underline{U} + L_1 u_{k-1} \end{bmatrix}. \tag{2.75}$$

The increment of control signal constraints can be rewritten as

$$\Delta\underline{U} \leq \Delta\mathbf{u} \leq \Delta\bar{U} \tag{2.76}$$

or in a standard QP form

$$\begin{bmatrix} I \\ -I \end{bmatrix} \Delta\mathbf{u} \leq \begin{bmatrix} \Delta\bar{U} \\ \Delta\underline{U} \end{bmatrix} \tag{2.77}$$

where $\Delta\underline{U} = [\Delta\underline{u} \quad \Delta\underline{u} \quad \cdots \quad \Delta\underline{u}]^T$, $\Delta\bar{U} = [\Delta\bar{u} \quad \Delta\bar{u} \quad \cdots \quad \Delta\bar{u}]^T$ are of the same dimensions as vector $\Delta\mathbf{u}$. The output constraints can be also be expressed in terms of the control increment signal $\Delta\mathbf{u}$, regarding the predictive output vector defined by eq. (2.65) by

$$\underline{Y} \leq \mathbf{F}x_k + \mathbf{\Phi}\Delta\mathbf{u} \leq \bar{Y}. \tag{2.78}$$

The form of standard QP problem formulation is then represented with

$$\begin{bmatrix} \mathbf{\Phi} \\ -\mathbf{\Phi} \end{bmatrix} \Delta\mathbf{u} \leq \begin{bmatrix} \bar{Y} - \mathbf{F}x_k \\ -\underline{Y} + \mathbf{F}x_k \end{bmatrix} \tag{2.79}$$

Finally, the constrained MPC problem as a standard QP formulation is defined by

$$H = \mathbf{\Phi}^T \bar{Q} \mathbf{\Phi} + \bar{R} \tag{2.80}$$

$$h^T = (\mathbf{r} - x_k \mathbf{F})^T \bar{Q} \mathbf{\Phi} \tag{2.81}$$

and the linear constraints matrices are

$$L = \begin{bmatrix} L_2 \\ -L_2 \\ I \\ -I \\ \mathbf{\Phi} \\ -\mathbf{\Phi} \end{bmatrix}; \quad b = \begin{bmatrix} \bar{U} - L_1 u_{k-1} \\ -\underline{U} + L_1 u_{k-1} \\ \Delta\bar{U} \\ \Delta\underline{U} \\ \bar{Y} - \mathbf{F}x_k \\ -\underline{Y} + \mathbf{F}x_k \end{bmatrix}. \tag{2.82}$$

2.2.4 MPC based on orthogonal basis functions

Another modification of the known MPC design procedures is orthogonal functions based representation of the input signal. The purpose of introducing orthogonal basis functions in the definition of the input signal is to be able to handle a long control horizon while having an optimization problem of modest size. The formulation used in this thesis uses Laguerre polynomials for the design of the MPC based on orthogonal basis functions. Reducing the degrees of freedom in the optimization reduces the computational load, caused by a very large number of parameters for on-line solving of the optimization problem, which provides the controller with the ability to handle both slow and fast(er) dynamics with a low number of decision variables. One of the Laguerre functions based realization is described in [28, 34].

The assumption, which justifies the use of Laguerre networks, is that the control increment performs like impulse response of a stable system. This means that it could be expressed by a Laguerre impulse response model. A good property of using this class of functions within the MPC framework is that there are only two tuning parameters which are independent of the sampling time T, and the closed-loop tuning is not much of an issue.

The method, presented in [28], shows the procedure for calculation of control increment Δu using a set of discrete-time Laguerre networks defined by

$$L_i(z) = \frac{\sqrt{(1-a)^2}}{1-az^{-1}}\Big[\frac{z^{-1}-a}{1-az^{-1}}\Big]^{i-1}, \tag{2.83}$$

where a represents the pole of the discrete-time Laguerre network, $0 \leq a < 1$, and $i = 1, \ldots, N$, where N denotes the number of Laguerre network terms.

The future control increment Δu_{k+j} is defined using the parameters of the discrete-time Laguerre function as follows

$$\Delta u_{k+j} = \sum_{i=1}^{N} c_i l_i(j); \quad j = 0, \cdots, N_p, \tag{2.84}$$

where c_i are the coefficients to be determined by the optimization problem and l_i is a function obtained using inverse z-transform of the discrete-time Laguerre network term L_i. The set of Laguerre functions described by eq. (2.83), can be represented by difference equation in a following form

$$L_{k+1} = \Omega L_k \tag{2.85}$$

where

$$L_k = \begin{bmatrix} l_1(k) & l_2(k) & \cdots & l_N(k) \end{bmatrix} \tag{2.86}$$

$$\Omega = \begin{bmatrix} a & 0 & \cdots & 0 \\ a^2-1 & a & \cdots & 0 \\ a(a^2-1) & a^2-1 & \cdots & 0 \\ \vdots & \vdots & \ddots & \vdots \\ a^{N-2}(a^2-1) & a^{N-3}(a^2-1) & \cdots & a \end{bmatrix} \tag{2.87}$$

with initial condition

$${L_0}^T = \sqrt{(1-a^2)}[1 \quad a \quad a^2 \quad \cdots \quad a^{N-1}]. \tag{2.88}$$

Eq. (2.84) now can be represented in a vector form

$$\Delta u_{k+j} = L_j^T \eta \tag{2.89}$$

where $\eta = [c_1 \quad c_2 \quad \cdots \quad c_N]$. Thus, computation of the optimal control input is obtained by minimization of the cost function in a form defined by eq. (2.66). Because the increment of the control action is parameterized in terms of η, the coefficient vector η is going to be calculated by solving the MPC optimization problem.

Using Laguerre functions, the future state at sample instant j can be calculated as

$$x_{k+j} = A^j x_k + \sum_{i=0}^{j-1} A^{j-i-1} B {L_i}^T \eta, \tag{2.90}$$

as well as the future output

$$y_{k+j} = CA^j x_k + \sum_{i=0}^{j-1} CA^{j-i-1} B {L_i}^T \eta. \tag{2.91}$$

It is obvious that obtaining the optimal control move is done by the optimization of the cost function over the coefficient vector of the Laguerre functions η. Hence, the new cost function is formulated as

$$J = \sum_{j=1}^{N_p} {x_{k+j}}^T Q x_{k+j} + \eta R \eta \tag{2.92}$$

where weighting matrices $Q \geq 0$ is chosen as $Q = C^T C$, and $R \geq 0$ have the dimensions equal to η. Substituting eq. (2.90) into eq. (2.92), and minimizing over η, the unconstrained optimal solution of Laguerre functions coefficients are computed as

$$\eta = -\left(\sum_{j=1}^{Np} \phi_i Q {\phi_i}^T + R \right)^{-1} \left(\sum_{j=1}^{N_p} \phi_i Q A^j \right) x_k, \tag{2.93}$$

where

$$\phi_i = \sum_{i=0}^{j-1} CA^{j-i-1}B{L_i}^T. \tag{2.94}$$

When η is calculated using eq. (2.93), control increment Δu_k is then obtained from eq. (2.89), and applied control action is computed by

$$u_k = u_{k-1} + \Delta u_k. \tag{2.95}$$

Constrained control problem for MPC based on Laguerre functions

If the cost function is represented by eq. (2.92), the future control increment constraints, in terms of Laguerre coefficients vector η, can be expressed as

$$\Delta\underline{U} \leq \begin{bmatrix} {L_{i1}}^T & {0_2}^T & \cdots & {0_m}^T \\ {0_1}^T & {L_{i2}}^T & \cdots & {0_m}^T \\ \vdots & \vdots & \ddots & \vdots \\ {0_1}^T & {0_2}^T & \cdots & {L_{im}}^T \end{bmatrix} \eta \leq \Delta\overline{U} \tag{2.96}$$

The constraints on the future control signal vector, defined using Laguerre coefficient vector η can be represented by

$$\underline{U} \leq \begin{bmatrix} \sum_{j=0}^{i-1} {L_{j1}}^T & {0_2}^T & \cdots & {0_m}^T \\ {0_1}^T & \sum_{j=0}^{i-1} {L_{j2}}^T & \cdots & {0_m}^T \\ \vdots & \vdots & \ddots & \vdots \\ {0_1}^T & {0_2}^T & \cdots & \sum_{j=0}^{i-1} {L_{jm}}^T \end{bmatrix} \eta \leq \overline{U} \tag{2.97}$$

Finally, the vector of future outputs in terms of η, using eq. (2.94) can be transformed as

$$y_{k+j} = CA^j x_k + \phi_i \eta. \tag{2.98}$$

and the constraints are defined as

$$\underline{Y} \leq \begin{bmatrix} CA \\ CA^2 \\ \vdots \\ CA^m \end{bmatrix} x_k + \begin{bmatrix} \phi_{i1} & 0 & \cdots & 0 \\ 0 & \phi_{i2} & \cdots & 0 \\ \vdots & \vdots & \ddots & \vdots \\ 0 & 0 & \cdots & \phi_{im} \end{bmatrix} \eta \leq \overline{Y} \tag{2.99}$$

If the matrices from eqs. (2.97), (2.96) and (2.99) are denoted as

$$M_1 = \begin{bmatrix} {L_{i1}}^T & {0_2}^T & \cdots & {0_m}^T \\ {0_1}^T & {L_{i2}}^T & \cdots & {0_m}^T \\ \vdots & \vdots & \ddots & \vdots \\ {0_1}^T & {0_2}^T & \cdots & {L_{im}}^T \end{bmatrix}, \quad M_2 = \begin{bmatrix} \sum_{j=0}^{i-1} {L_{j1}}^T & {0_2}^T & \cdots & {0_m}^T \\ {0_1}^T & \sum_{j=0}^{i-1} {L_{j2}}^T & \cdots & {0_m}^T \\ \vdots & \vdots & \ddots & \vdots \\ {0_1}^T & {0_2}^T & \cdots & \sum_{j=0}^{i-1} {L_{jm}}^T \end{bmatrix};$$

$$\tilde{\mathbf{\Phi}} = \begin{bmatrix} \phi_{i1} & 0 & \cdots & 0 \\ 0 & \phi_{i2} & \cdots & 0 \\ \vdots & \vdots & \ddots & \vdots \\ 0 & 0 & \cdots & \phi_{im} \end{bmatrix},$$

then the standard QP formulation for the MPC problem based on Laguerre functions as in eq. (2.70) subject to constraints defined by eq. (2.71) can be formulated as

$$H = \tilde{\mathbf{\Phi}}^T \bar{Q} \tilde{\mathbf{\Phi}} + \bar{R}, \tag{2.100}$$

$$h^T = \tilde{\mathbf{\Phi}}^T \bar{Q} A^j \tag{2.101}$$

subject to constraints

$$L = \begin{bmatrix} M_1 \\ -M_1 \\ M_2 \\ -M_2 \\ \tilde{\mathbf{\Phi}} \\ -\tilde{\mathbf{\Phi}} \end{bmatrix}; \quad b = \begin{bmatrix} \Delta\bar{U} \\ -\Delta\underline{U} \\ \bar{U} \\ -\underline{U} \\ \bar{Y} - \mathbf{F}x_k \\ -\underline{Y} + \mathbf{F}x_k \end{bmatrix}. \tag{2.102}$$

2.2.5 Stability of MPC

Stability of MPC is not always guaranteed, especially for reason of using constrained, finite-horizon optimal control principle. The typical way of establishing closed-loop stability is introducing terminal state x_{N_p} together with designing a 'hypothetical' state-feedback controller. This controller is usually discrete-time linear quadratic (LQ) controller K_{lq} with already defined Q and R weighting matrices that are used in the MPC formulation. It should be able to keep the state x_{N_p} within a set inside which all state and input constraints are inactive for all $i > N_p$. This set is called the maximal output admissible set (MOAS), denoted by $\mathcal{O}_\infty$, whose properties and the algorithm for its determination are presented in [35].

Design of the stabilizing state feedback controller K_{lq}, together with calculation of a stable weight on the terminal state, S, can be done by solving the Riccati equation. The obtained results are the terminal weight S calculated by

$$S = A^T SA + Q - A^T SB(R + B^T SB)^{-1} B^T SA \tag{2.103}$$

and the corresponding controller given by

$$K_{lq} = -(B^T SB + R)^{-1} B^T SA. \tag{2.104}$$

This controller, with the MOAS defined for it, will provide closed-loop stability and assure that constraints are not violated over the infinite horizon, is defined by

$$\Delta u_{k+N_p} = -K_{lq} x_{k+N_p} \tag{2.105}$$

Adding the terminal weight S to the objective function, and adding the MOAS as a terminal set will ensure stability of the MPC. Note that the terminal controller K_{lq} is never (explicitly) used, since the MPC is formulated to be equivalent to K_{lq} when no constraints are active.

2.2.6 Tube Model Predictive Control

A popular approach among such MPC formulations that trade off performance against online calculation requirements is the so-called Tube MPC [1, 23]. The applied control signal consist of two components: the auxiliary controller which is used to suppress disturbances and uncertainties, and a standard MPC which is applied on a nominal model of the system to be controlled.

Let one consider the plant to be controlled is described by

$$x_{k+1} = Ax_k + Bu_k + Ew_k \tag{2.106}$$

$$y_k = Cx_k \tag{2.107}$$

where the state x, the input u and the output y are defined as in eq. (2.7), and $w \in \mathbb{R}_w^n$ is a bounded disturbance. Constraints on the state and input trajectories are defined by

$$\begin{aligned} Fx &\leq f \\ \Gamma u &\leq \gamma \end{aligned} \tag{2.108}$$

or in a compact form

$$(x_k, u_k) \in \mathbb{Z} \tag{2.109}$$

It is assumed that sets $\mathbb{W}$ and $\mathbb{Z}$ are polyhedral, bounded, of full dimension and contain the origin in their interior. The nominal model of the plant defined by eq. (2.106) can be obtained by eliminating the disturbance. The nominal dynamics is given as

$$z_{k+1} = Az_k + Bv_k \tag{2.110}$$

where z and v are the nominal state and nominal input, respectively. If the vector of the future inputs is calculated for the nominal plant, then the predicted nominal state trajectory (starting from x) can be obtained by the recursion

$$z_{k+1} = Az_k + Bv_k; \quad z_0 = x. \tag{2.111}$$

If the real plant is disturbed, the true state will differ from the nominal state trajectory, causing a deviation, $e_k = x_k - z_k$. To cope with this issue, the auxiliary controller can be added. It will force the trajectory to lie as close as possible to the nominal one by choosing the control action expressed as

$$u_k = v_k + Ke_k. \tag{2.112}$$

Using eqs. (2.106), (2.110) and (2.112), the dynamics of the error signal is obtained as

$$e_{k+1} = A^K e_k + w_k; \quad A^K = A + BK. \tag{2.113}$$

The feedback control gain K is chosen such that A^K is Hurwitz, so the evolution of error is bounded and always is in a Robust Positively Invariant (RPI) set ϕ^K [23]. The set ϕ^K is called an RPI set for the system (2.113) if $A^K\phi^K \oplus \mathbb{W} \subseteq \phi^K$ [36, 37].

Regarding to this definition of the RPI set, the tube of trajectories can be represented as the set of possible trajectories of the disturbed system defined by eq. (2.106) and controlled by eq. (2.112). This set is defined by $x_k \in z_k \oplus \phi^K$ for any value of the disturbance w_k. Then, the trajectories and inputs satisfy

$$(x_k, v_k + K(x_k - z_k)) \in \mathbb{Z} \tag{2.114}$$

for any value of the disturbance $w_k \in \mathbb{R}^n_w$ as well. It means that using tighter constraints for the nominal system will provide robustly admissible evolution of the disturbed system [38].

The nominal optimal control problem is solved by the procedure described in section 2.2.3. The gain K, of the auxiliary controller, is very important because it affects the closed-loop system dynamics when the disturbance is present. There are different procedures for computation of the gain K, and some of them can be found in [38, 39].

The objective in this section has been to give an introduction to TMPC, and therefore the most basic formulation has been presented. However, various different forms of the auxiliary controller and its design are possible. This thesis proposes a new method for designing the auxiliary controller. The full details of this design are given in Chapter 4 for a traditional MPC, and in Chapter 5 for MPC based on Laguerre functions.

2.3 Sliding Mode Control (SMC)

As it is already mentioned, one of the main issues of modern control theory is a control in the presence of uncertainties. Uncertainty in the controlled system is usually caused by differences between the actual plant and its mathematical model dynamics used for the design of the controller. The most common differences are unknown plant parameters and external disturbances. Providing the desired closed-loop system performance in such a case is a very challenging problem, and it had led to huge research interest for finding robust control laws and methods that will solve this problem. SMC, as a particular kind of Variable Structure System (VSS), is one approach to robust controller design.

Dynamical systems, whose structure changes depending on the state in which the system is currently located, are called VSS. They can be considered as systems consisting of independent control structures and switching logic, whose control is formed as a discontinuous function of the state. Due to the use of switching control, the dynamic behaviour of the VSS is defined by the dynamics of its structures, which enables the combination of the useful properties of each of the structures at the expense of additional complexity of the controller. A VSS may even have new features that are not present in any one of its structures. For example, an asymptotically stable Variable Structure Control Systems (VSCS) can consist of structures that are not individually asymptotically stable.

SMC is based on definition of a properly designed function, named the switching function. When the value of this function becomes equal to zero, it defines the sliding manifold. The idea of SMC is to bring the system trajectory to the defined manifold, and to keep the trajectory on the manifold thereafter using the properly designed controller. The dynamics on the sliding manifold need to be stable. A brief history of development of this method, as well as the SMC design technique, will be described in the sequel.

2.3.1 A brief history of SMC

The history of Variable Structure Control (VSC) originated in early 60's, and Russian scientist Emelyanov was a pioneer in this area of automatic control systems [40]. From that time, the theory of VSC has been applied to many different types of automatic control for both SISO and MIMO systems. Until the 1980's, very few papers were published in the field of discrete-time VSC where the discrete-time implementation of the switching function and the hardware realisation of the continuous-time VSCS with the help of digital electronic circuits were considered. Around the same time, interest of researchers for this area of automatic control increased resulting in many published papers [41–45]. In [44], the term of zigzag motion was introduced, which later became

known as the *chattering phenomenon*. In discrete-time, VSC often forces the system state to stay within the vicinity of sliding manifold rather than exactly on it, resulting in so-called quasi-sliding mode (qSM) [45] or pseudo-sliding mode (pSM) in [46–48].

The necessary and sufficient conditions for the existence of qSM were analysed in [49–52], while discrete-time equivalent control[2], Lyapunov stability and discrete-time sliding mode were initially introduced and later elaborated and exploited in many papers [53–56]. In the 90's, discrete-time equivalent control, combined with triple relay control, was used to ensure the system moves in the predefined region [55]. Based on the so-called reaching law method for continuous-time systems, a new approach was developed for the design of discrete-time qSM control, which does not only define the dynamics of the system in the qSM but also defines a reaching phase [56]. The design of some adaptive methods within discrete-time SMC shows that an ideal sliding motion could be achieved if appropriate parameters are used [57]. The control algorithm considered in [58, 59] is inspired by the Gao's chattering-free reaching law method [56]. Chattering does not exist in the case of a nominal plant if the so-called continuous-time chattering free SMC with discrete-time signal processing is applied [60]. Another posibility for elimination of chattering is using higher-order SMC [61, 62]. Since discrete-time quasi Sliding Mode Control (qSMC) does not guarantee the invariance of the system to the effects of external disturbance, to increase robustness, it is necessary to introduce a disturbance estimator. The most commonly used type of estimator is the so-called one-step-delayed estimator [63–65], whose use leads to the increase in the system accuracy. VSCS are quite interesting because of their simple implementation.

There are many papers where VSC systems are analysed, and the surveys are given in [65–71]. Herein, only the linear, discrete-time SMC will be considered, but the next section will present the continuous-time SMC terminology for better understanding of the SMC methodology.

2.3.2 Continuous-time SMC

Consider the following linear, continuous-time system described by

$$\dot{x}(t) = A_c x(t) + B_c u(t) \tag{2.115}$$

where $x(t) \in \mathbb{R}^{n_x}$ is a state vector, $u(t) \in \mathbb{R}^{n_u}$ is a control input vector, and A_c and B_c are the continuous-time system matrices. As it is earlier mentioned, there are minimum two diferent structures defined in VSCS. All such structures are determined by the sign of the vector $g(x(t))$, representing the switching surfaces defined by the switching

[2]The term equivalent control will be explained in the next section in detail.

functions

$$g(x(t)) = Kx(t) \tag{2.116}$$

and

$$g(x(t)) = 0 \tag{2.117}$$

defines a so-called sliding surface. Let $x(0) = x(t_0)$ represents the initial state of the system at time t_0. If for any $x(0)$, located at the switching surface $g(x(t_0))$, all the states of the system are always placed on that surface for $t > t_0$, then the trajectory $x(t)$ describes the sliding mode motion of the system defined by eq. (2.115). This means that the system states move towards the switching surface described by eq. (2.116) whenever they are not on it. Then, once they reach the switching surface, they slide along it, and this surface is called a sliding surface, represented by eq. (2.117). Fig. 2.2 shows the sliding mode motion of a 2^{nd} order system.

As it is already mentioned, the properties of SMC are different for each of three parts of the system motion. The first one is reaching mode, the second one is sliding mode, and the last one is steady-state. In order to determine the condition for moving the system states towards, and for falling onto the sliding surface, the reaching conditions should be defined.

SMC design procedure consists of:

- the design of switching function $g(x(t))$ which provides design of the sliding surface as in eq. (2.117) defining the desired system dynamics together with
- the design of the control law

$$u(t) = \begin{cases} u^+ & \text{for } g(x(t)) > 0 \\ u^- & \text{for } g(x(t)) \leq 0 \end{cases} \tag{2.118}$$

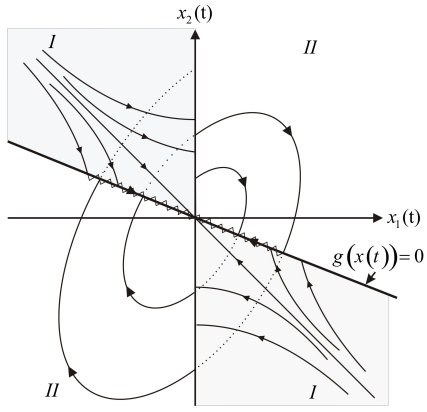

Figure 2.2: 2^{nd} order system sliding mode motion

which drives the state $x(t)$ to the sliding surface in a finite time, and provide that it stays on that surface afterwards.

The motion of the system in sliding mode can be obtained and analyzed by the equivalent control method [72,73], defined from the idea that the trajectories of the system remains on the sliding surface described by eq. (2.117) after they reach it. That motion is defined by

$$\dot{g}(x(t)) = \frac{\partial g(x(t))}{\partial x(t)} A_c x(t) + \frac{\partial g(x(t))}{\partial x(t)} B_c u(t) = 0. \tag{2.119}$$

From eq. (2.119), the equivalent control is calculated by

$$u(t)^{eqc} = -\left(\frac{\partial g(x(t))}{\partial x(t)} B_c\right)^{-1} \frac{\partial g(x(t))}{\partial x(t)} A_c x(t) \tag{2.120}$$

and for a linear time-invariant systems is given by

$$u(t)^{eqc} = -\Big(KB_c\Big)^{-1} KA_c x(t). \tag{2.121}$$

Substituting eq. (2.121) in eq. (2.115) gives the dynamic of the system in sliding mode as

$$\dot{x}(t)^{eqc} = \Big[I - B_c\Big(KB_c\Big)^{-1} K\Big] A_c x(t)^{eqc}. \tag{2.122}$$

SMC can be realized by different switching schemes which have the switching function of predefined order [72,73], the switching function of free order [74], or eventual switching scheme based on a Lyapunov function candidate. When the sliding manifold and sliding motion are defined, one can design the control as

$$u = u(t)^{eqc} + u(t)^{d} \tag{2.123}$$

where

$$u(t)^{d} = -\lambda \text{sgn}(g(x(t))), \quad \lambda > 0 \tag{2.124}$$

provides that trajectory reach the switching manifold. If Lypaunov function candidate has the form

$$V(x(t)) = \frac{1}{2} g(x(t))^2 \tag{2.125}$$

the reaching and existence conditions of sliding mode are given by $\dot{V}(x(t)) < 0$, i.e.

$$g(x(t)\dot{g}(x(t)) < 0 \tag{2.126}$$

Evaluating the time derivative of $V(x(t))$ for the system defined by eq. (2.115) gives

$$\begin{aligned}
\dot{V}(x(t)) &= g(x(t))\Big(K\dot{x}(t)\Big) \\
&= g(x(t))\Big(KA_c x(t) + KB_c u(t)\Big) \\
&= g(x(t))\Big(KA_c x(t) + KB_c[u(t)^{eqc} + u(t)^{d}]\Big) \\
&= g(x(t))\Big(KA_c x(t) + KB_c[-(KB_c)^{-1} KA_c x(t) - \lambda \text{sgn}(g(x(t)))]\Big) \\
&= -g(x(t))KB_c \lambda \text{sgn}(g(x(t))) = -KB_c \lambda |g(x(t)|
\end{aligned} \tag{2.127}$$

Therefore, the reaching and existence conditions, defined by eq. (2.126), are obtained using $K > 0$.

To ensure a finite reaching time, the condition defined by eq. (2.126) is often replaced by

$$g(x(t)\dot{g}(x(t)) \leq -\mu|g(x(t))|, \quad \mu > 0. \tag{2.128}$$

Thus, the finite reaching time t_{rt} can be calculated from $|g(x(t)) - g(x(0))| \leq -\mu t$ as

$$t_{rt} = \frac{|g(x(0))|}{\mu}. \tag{2.129}$$

The reaching mode is commonly a fast phase of the system motion, because the state trajectories reach the sliding surface in a short period of time. The dynamics of the system before the reaching method control approaches [66, 74] was described only for the sliding mode as expressed by the reduced-order system model. To define the reaching phase, which describes the motion of the system before the sliding mode, this law has to satisfy the conditions defined by eq. (2.126).

The ideal sliding mode does not exist and finite switching time between the structures causes the undesirable excitation of high-frequency un-modelled dynamics of the system. This oscillating motion is known as chattering (see Fig. 2.3) and can degrade system response, as well as cause heavy heat losses in electric circuits, or fraying of the mechanical parts of the system.

Among many methods for the suppression of the chattering phenomenon one can use a continuous approximation instead of $\mathrm{sgn}(g(x(t)))$ function as

$$\mathrm{sat}\Big(g(x(t))\Big) = \begin{cases} u^+ & \text{for } \dfrac{g(x(t))}{\epsilon} \geq u^+ \\ u^- & \text{for } \dfrac{g(x(t))}{\epsilon} \leq u^- \\ \dfrac{g(x(t))}{\epsilon} & \text{for } \left|\dfrac{g(x(t))}{\epsilon}\right| < u^+ \end{cases} \tag{2.130}$$

for a design of SMC [66, 75–77]. This approach is called boundary layer control because the switching function does not converge to zero but to close neighborhood defined

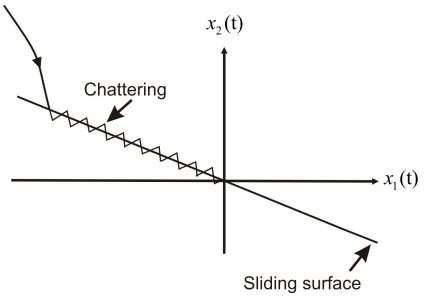

Figure 2.3: Chattering of the 2^{nd} order system trajectory

by an aditional parameter $\epsilon \approx 0$. In [78, 79] the boundary layer is replaced with a sliding sector. Some algorithms uses second (or higher) order sliding mode to eliminate chattering [80, 81] or by the integration of the relay component of the control [82]. Another method for chattering suppression is using of fuzzy sliding mode controllers as in [83, 84].

The next section presents key elements of discrete-time SMC.

2.3.3 Discrete-time SMC

Realisation of discrete-time SMC is very similar to the structure used in continuous-time approach and can be achieved by partial or complete discretisation, which implies:

- discretization of the switching function $g_k = g(x(kT))$, whereas the control signal stays continuous, i.e. $u = u(t)$;
- discretization of the control signal $u_k = u(kT)$, whereas the switching function stays continuous, e.i. $g(t) = g(x(t))$;
- discretization of both switching function and control signal, i.e. $g_k = g(x(kT))$ and $u_k = u(kT)$, respectively.

In this thesis, the latter will be used, i.e. complete discretization of both signals. The discretization affects the characteristics of the discrete-time SMC in the following way. Firstly, ideal sliding of the system states on the sliding surface is not possible due to the non-zero sampling time, which provides different control signal value for the different sample instants, and the constant value of the control signal between to subsequent time instants [55]. This causes the trajectory to stay in a close neighbourhood of the switching surface. The second feature is that the equivalent control cannot be precisely defined so that the system trajectory stays on the sliding surface [85]. These two reasons leads to the definition of so-called quasi-Sliding Mode (qSM) [56].

Definition 1 *The qSM is a motion that satisfies the following conditions:*

- *once the trajectory has crossed the switching surface g_k the first time, it will cross the surface again in every successive time instant, resulting in a zigzag motion about the switching surface g_k;*
- *the size of each successive zigzagging step is non-increasing, and the trajectory stays within a specified band.*

This definition is too restrictive, since moving in a predefined area can also be achieved without the successive crossing of the switching surface in each subsequent step, which is of great importance in the practical reliance of discrete-time SMC, since such a movement does not produce chattering. Therefore, the following definition seems to better describe qSM.

Definition 2 [86]. *qSM is motion in a predefined Δ environment of the sliding surface g_k, such that once the trajectory of the system enters this area it never leaves, i.e. it is always valid that $|g_k| \leq \Delta$, where 2Δ denotes the width of this area around g_k.*

The motion in discrete-time SMC also consists of three phases: the reaching phase, the qSM, and the steady state according to [56], i.e. the reaching phase, switching phase and chattering phase according to [87]. All three ones are described by the following definitions.

Definition 3 *Discrete-time VSCS is in the reaching phase if*

$$\text{sgn}(g_{k+1}) = \text{sgn}(g_k), \quad \forall k \in (0, \varrho) \tag{2.131}$$

and

$$|g_{k+1}| < |g_k| \tag{2.132}$$

where $\varrho > 0$ is a finite number.

Definition 4 *Discrete-time VSS is in chattering phase if*

$$\text{sgn}(g_{k+1}) = -\text{sgn}(g_k), \quad \forall k. \tag{2.133}$$

The existence condition for qSM can be proved using a Lyapunov function candidate of the form

$$V(x_k) = |g_k|, \tag{2.134}$$

and the result of the second Lyapunov method necessary and sufficient conditions for existence of qSM, i.e.

$$|g_{k+1}| < |g_k| \tag{2.135}$$

which is the same result given in eq. (2.132). Eq. (2.135) can be rewritten as in [50] as

$$(g_{k+1} - g_k)\text{sgn}(g_k) < 0, \tag{2.136}$$

$$(g_{k+1} + g_k)\text{sgn}(g_k) \geq 0. \tag{2.137}$$

These inequalities show that trajectory of the system converges to the sliding surface $g_k = 0$, and stays in the area around the sliding surface, changing the side in the every future time instant, which represents the qSM motion of the system. In this way sliding conditions and convergence conditions are defined by eqs. (2.136) and (2.137), respectively.

Let one consider the discrete-time state-space model of the nominal plant is defined as

$$x_{k+1} = Ax_k + Bu_k, \tag{2.138}$$

$$y_k = Cx_k \tag{2.139}$$

where

$$A = e^{A_c T}, \quad B = \int_0^T e^{A_c \lambda} B_c d\gamma. \tag{2.140}$$

A_c and B_c are the matrices of the continuous-time system described by eq. (2.115), and it is assumed that (A_c, B_c) is controllable. This implies that (A, B) is also controllable for all T.

As it is the case with continuous-time SMC, the design of discrete-time SMC consists of two stages. The first one is choosing the appropriate switching function g_k that defines the system dynamics in SMC and then, design of the discrete-time SMC. The reaching and existence of qSM have to be achieved.

The sliding surface can be defined as

$$g_k = Kx_k. \tag{2.141}$$

The coefficients matrix K is chosen to provide sliding mode on the sliding surface $g_k = g_{k+1}$ for all k. The equivalent control of the system (2.138), using eq. (2.141) is obtained by

$$\begin{aligned} g_k &= g_{k+1} \\ g_k &= Kx_{k+1} \\ g_k &= K(Ax_k - Bu_k^{eq}) \end{aligned} \tag{2.142}$$

From above, the equivalent control has the following form

$$u_k^{eq} = -(KB)^{-1}(KAx_k - g_k). \tag{2.143}$$

The discrete-time SMC law is then defined as

$$u_k = u_k^{eq} + u_k^d \tag{2.144}$$

where u_k^d is the discontinuous part of the control law. This part could be designed in different ways. Two of them are used within this thesis and the design procedures will be presented in Chapters 4 - 6.

If the system is not represented by the state-space formulation, and only the input and output signals could be measured, one of the techniques used is discrete-time SMC based on GMVC were the model used for the design of the controller is defiend by eq. (2.19).

One version of this approach introduces the SMC component into GMVC [88]. GMVC is used to replace the discrete-time equivalent control. This control method suppresses chattering using a discrete-time integrator, which provides almost smooth

control action. If the plant is represented by the input-output model described by eq. (2.19), then this control law can be designed as

$$u_k = -\frac{F(z^{-1})y_k - C(z^{-1})r_{k+1} + u_k^d}{E(z^{-1})B(z^{-1}) + Q(z^{-1})} \tag{2.145}$$

where $E(z^{-1})$ and $F(z^{-1})$ are the solutions of the Diophantine equation

$$E(z^{-1})A(z^{-1}) + z^{-1}F(z^{-1}) = C(z^{-1}) \tag{2.146}$$

and the switching function is defined by

$$g_{k+1} = C(z^{-1})(y_{k+1} - r_{k+1}) + Q(z^{-1})u_k \tag{2.147}$$

which is equal to the variable defined by eq. (2.14) in GMVC. The polynomial $C(z^{-1})$ should be stable, i.e. roots should be inside the unit circle of the z-plane. In addition, the polynomial $Q(z^{-1})$ should meet the equality

$$Q(1) = 0 \tag{2.148}$$

and r_{k+1} is the reference signal at time instant $k+1$. There are many different forms of SMC components that can be introduced within this framework. In [2], it is proposed to use

$$u_k^d = \frac{\alpha T}{1 - z^{-1}}\text{sgn}(g_k) \tag{2.149}$$

Substituting eq. (2.145) into eq. (2.19), taking into account eqs. (2.146), (2.147) and (2.149) yields in

$$g_{k+1} = g_k - \alpha T\text{sgn}(g_k) \tag{2.150}$$

An appropriate value for α is chosen by the conditions given in [2].

2.4 Combination of SMC and MPC

When confronted with the often diverse set of requirements of practical control problems, it is a natural approach to try to combine the strengths of different control algorithms. This is also the underlying idea of this thesis, which studies the combination of two advanced control algorithms, MPC and SMC. When uncertainty is present, whether in the form of additive disturbances or model error, the design of MPC can be a challenge because of the complexity of the resulting optimal control problem. A good candidate for improving robustness properties of MPC is introducing SMC which have lower online calculation requirements. Herein will be presented some of the results that represent the starting points for the research presented in this thesis.

For the case when TF models are used in the design of the controller, authors in [89] have suggested the addition of an auxiliary input realized by combining GPC, described in Section 2.2.2 of this thesis, and SMC components. They shoved that the proposed controller improves the closed-loop response of the system, minimizes the size of the control signal during the transient response, and adds extra tuning parameters for the nonlinear part of the control. The SMC component provides robustness with respect to parameter variations, and damping to the transient response. The calculation of the future sliding surface values are obtained only using the past values of the control without considering its future values.

Authors in [90] uses a similar idea, but with included future control movements for more precise prediction of the sliding surface. The discontinuous part of the control is simple and has fewer tuning parameters in comaprison to the one in [89]. It is used to guide the system to the sliding surface. A continuous part is developed in GPC manner, and it is used to keep the controlled variable close to the reference value. It is also demonstrated that proper values of the tuning parameters provide stability of the sliding mode predictive controller when it is applied to the non-minimum phase systems.

In [91,92] the algorithm proposed in [90] is applied for controlling a chemical process and a solar air conditioning plant, which is a non-minimum phase, nonlinear systems with time delay. The cost function is partially optimized with respect to only the predictive part of controller, while sliding mode control is not involved in the optimization problem.

Unfortunately, all these approaches cannot deal with MIMO systems. This is one of the main reasons why the state-space models are dominantly used for the design of the MPC and SMC approaches. Two different approaches in integrating discrete-time SMC and MPC are proposed in [93]. The first one applies direct optimization of a cost function criterion with respect to the equivalent control. The second control method splits the controller into the equivalent control part, ensuring the system to stay on sliding surface once reached, and the reaching control part that guides the system towards the sliding surface. The cost function is optimized with respect to the latter control term.

Hierarchical control schemes, consisting of a high level MPC and a low level SMC, are considered in [94–97], where the SMC component rejects the matched disturbances acting the plant, and reduces uncertainty for the MPC design in that way.

Chapter 3

Sliding Mode based Generalized Predictive Control (SMGPC)

This chapter presents the combination of GPC and SMC techniques in order to improve system robustness to parameter variations. A modification of the SMC component of the design in [89] is proposed to improve the system robustness. The minimum value of the cost function for the perturbed systems is ensured by using the chattering free SMC algorithm. The proposed control algorithm belongs to the group of chattering free sliding mode control laws, and it provides the minimum value of the cost function in the presence of parameter perturbations. Digital simulation results are given to verify the sliding mode based generalized predictive controller.

The chapter is organized as follows. In section 3.1, the control problem is introduced. Sliding Mode based GPC (SMGPC) is presented in section 3.2. The existence condition of Sliding Mode (SM) is thoroughly discussed herein. Section 3.3 presents the results of digital simulation of the system with the proposed control algorithm. Section 3.4 contains some concluding remarks.

3.1 Problem statement

The discrete-time model is considered, with the form as in eq. (2.19)

$$A(z^{-1})y_k = z^{-1}B(z^{-1})u_k, \tag{3.1}$$

with

$$A(z^{-1}) = 1 + a_1 z^{-1} + ... + a_{n_a} z^{-n_a}, \tag{3.2}$$

$$B(z^{-1}) = b_0 + b_1 z^{-1} + ... + b_{n_b} z^{-n_b} \tag{3.3}$$

where z^{-1} denotes the unit delay operator, u_k and y_k are the input and the output of plant, n_a and n_b are the degrees of the polynomials $A(z^{-1})$ and $b(z^{-1})$, respectively. It

is assumed that the control input u_k is bounded, i.e. $|u_k| \leq \bar{U}$ and $\bar{U} = cons$, which typically holds in practical implementations, due to saturation nonlinearities existing in real plants.

The goal of design is to find the control law which will minimize the cost function:

$$J = \mathbf{g}^T\mathbf{g} + \hat{\mathbf{u}}^T\lambda\hat{\mathbf{u}} \tag{3.4}$$

where λ is a control weighting constant and:

$$\mathbf{g} = [g_{k+1} \quad \cdots \quad g_{k+N}]^T \tag{3.5}$$

$$\hat{\mathbf{u}} = [\Delta\hat{u}_k \quad \cdots \quad \Delta\hat{u}_{k+N-1}] \tag{3.6}$$

with N denoting prediction horizon, $\Delta = 1 - z^{-1}$ denoting the difference operator, and:

$$g_{k+j} = C(z^{-1})(y_{k+j} - r_{k+j}) + Q(z^{-1})\Delta u_{k-1} \tag{3.7}$$

representing the variable whose minimum value ensures the good system tracking of the reference input r_k i.e. in the ideal case the zero value of the tracking error:

$$e_k = y_k - r_k. \tag{3.8}$$

The polynomials $C(z^{-1})$ and $Q(z^{-1})$ are given by:

$$C(z^{-1}) = c_0 + c_1 z^{-1} + ... + c_{n_c} z^{-n_c}, \tag{3.9}$$

$$Q(z^{-1}) = q_0 + q_1 z^{-1} + ... + q_{n_q} z^{-n_q}, \tag{3.10}$$

having the degrees n_c and n_q, respectively, and should be selected to assign the desired closed-loop systems dynamics. The variable $\hat{u}_k$ is obtained from the control input as:

$$\hat{u}_k = C(z^{-1})u_k. \tag{3.11}$$

3.2 Sliding Mode based Generalized Predictive Control Design

The basic idea of existing GPC strategies with SM is to use GPC as a replacement for the so-called equivalent control in VSS with SM [72, 98]. The basic GPC method and design procedure are represented in subsection 2.2.2 and this section will describe how to design the SMGPC.

If the switching function of the SMC is defined as

$$\hat{g}_{k+1} = \Upsilon(z^{-1})y_k - \Psi(z^{-1})r_{k+N}, \tag{3.12}$$

note that

$$\hat{g}_{k+1} = 0 \tag{3.13}$$

defines the sliding surface in our case, and:

$$g_{k+1} = \hat{g}_{k+1} + \Phi(z^{-1})\Delta u_k. \tag{3.14}$$

Matrices $\Upsilon(z^{-1}), \Psi(z^{-1}), \Phi(z^{-1})$ are defined as in Section 2.2.2.

The control law will be found next, and will establish the sliding motion in the vicinity of (3.13) and provide $g_{k+1} = 0$ at the same time. This sliding mode based control algorithm can be expressed now in the following form

$$\Delta u_k = -\Phi^{-1}(z^{-1})\{\Upsilon(z^{-1})y_k - \Psi(z^{-1})r_{k+N} - \hat{g}_k + \min(|\hat{g}_k|, \alpha)\mathrm{sgn}(\hat{g}_k)\}. \tag{3.15}$$

Theorem 3.2.1. *The system (3.1) with the control law (3.15) guarantees $g_{k+1} = 0$ and vanishing of the tracking error if*

$$\alpha > 3\Lambda = \max|\Phi(z^{-1})\Delta u_{k-1}|. \tag{3.16}$$

Proof. As the input signal is bounded by assumption, there is a constant α always satisfying (3.16). Substituting eq. (3.15) into eq. (3.14), taking into account eq. (3.12), yields:

$$g_{k+1} = \hat{g}_{k+1} - \min(|\hat{g}_k|, \alpha)\mathrm{sgn}(\hat{g}_k), \tag{3.17}$$

i.e.

$$g_{k+1} = g_k - \min(|\hat{g}_k|, \alpha)\mathrm{sgn}(\hat{g}_k) - \Phi(z^{-1})\Delta u_k. \tag{3.18}$$

Suppose that $g_k > 0$, $\hat{g}_k > 0$ and $\hat{g}_k > \alpha$. Then, g_k converges to the domain:

$$\sum = \{g_k : |g_k| < \alpha + \Lambda\} \tag{3.19}$$

and enters it at $k = K_0$ determined by:

$$K_0 = int((|g_0| - \alpha - \Lambda)/(\alpha - \Lambda)) + 1, \tag{3.20}$$

where g_0 denotes the initial value of eq. (3.14). Let $g_k = \alpha + \Lambda$, then $\hat{g}_k$ could be still greater than α, but in the next step $\hat{g}_{k+1} < 3\Lambda < \alpha$. It means that immediately after the entrance in the domain defined by eq. (3.19), $\hat{g}_k < \alpha$ and eq. (3.18) become

$$g_{k+1} = g_k - \hat{g}_k - \Phi(z^{-1})\Delta u_{k-1} = 0. \tag{3.21}$$

Assume that $\hat{g}_k > 0$ and $g_k < 0$. In that case, $\Phi(z^{-1})\Delta u_{k-1}$ is negative and

$$\hat{g}_k = |\Phi(z^{-1})\Delta u_{k-1}| < \alpha \tag{3.22}$$

so (3.21) occurs. The proof is similar for $g_k < 0$. □

Corollary 2.1. The control law, defined by eqs. (3.15) and (3.16), ensures the existence of a quasi-sliding mode in eq. (3.1) in the vicinity of sliding surface $\hat{g}_{k+1} = 0$.

Proof. The implementation of eq. (3.15) into eq. (3.14) gives

$$\hat{g}_{k+1} = \hat{g}_k - \min(|\hat{g}_k|, \alpha)\text{sgn}(\hat{g}_k) - \Phi(z^{-1})\Delta u_k. \tag{3.23}$$

If α is selected in accordance with eq. (3.16), $\hat{g}_k$ reaches the domain defined by eq. (3.19) with $\hat{g}_0$ representing the initial value of eq. (3.12). In eq. (3.18) $\hat{g}_k < \alpha$, so $\hat{g}_{k+1} = -\Phi(z^{-1})\Delta u_k$ and

$$\hat{g}_{k+1} < \Lambda \tag{3.24}$$

for every value of k.

Corollary 1 presents the results of the chattering-free discrete-time SMC [59], obtained by the discretization process of the well-known chattering-free power rate reaching law method [74]. In this chapter, a similar chattering-free control law is obtained, trying to ensure $g_{k+1} = 0$ by using the switching function $\hat{g}_k$ of SMC, defined by eq. (3.12).

3.3 Digital simulation results

In order to verify the proposed sliding mode based generalized predictive controller, digital simulations are performed by using the Van der Vusse reactor as a plant. This chemical process is very often utilized as a benchmark problem for desiging process control algorithms. The example and the parameter values of the reactor are taken from [89] and [99]. The normalized model of process is given by:

$$\dot{x}_1 = -50x_1 - 10{x_1}^2 + u(10 - x_1), \tag{3.25}$$

$$\dot{x}_2 = 50x_1 - 100x_2 + u(-x_2), \tag{3.26}$$

$$y = x_2, \tag{3.27}$$

where x_1 and x_2 denote the concentrations of components A and B, respectively, and u is an inlet flow rate. The operating point is determined by $X_{10} = 3.0$, $X_{20} = 1.12$ and $U_0 = 34.4$.

To obtain the discrete-time plant model described by eq. (3.1), linearization of the nonlinear process defined by eqs. (3.25)-(3.27) has been done around the operating point, and discretization has been performed with the sampling period $T = 0.005h$. The results are the polynomials:

$$A(z^{-1}) = 1 - 0.997z^{-1} + 0.248z^{-2}, \tag{3.28}$$

$$B(z^{-1}) = -1.29 * 10^{-3} + 3.73 * 10^{-3}z^{-1}. \tag{3.29}$$

The zero initial conditions of the plant are taken and the polynomials $C(z^{-1})$ and $Q(z^{-1})$ are chosen as:

$$C(z^{-1}) = 1 + 151.667z^{-1} - 143.502z^{-2} + 33.675z^{-3}, \quad (3.30)$$

$$Q(z^{-1}) = -879.661 + 828.859z^{-1} - 194.331z^{-2} + 0.0125z^{-3}. \quad (3.31)$$

yielding the closed-loop poles: $p_1 = 0.1$, $p_2 = 0.2$, $p_3 = 0.4$, $p_4 = 0.4$, $p_5 = 0.5$, $p_6 = 0.6$, $p_7 = 0.7$. The prediction horizon of the proposed controller is $N = 5$ and $\alpha = 1$. The reference input is $r_k = 0.62$ for $k = 1, 2, \ldots$, and the system starts from the steady state corresponding to the initial reference $r_0 = X_{20} = 1.12$.

Figure 3.1 presents the output signal of the Van der Vusse reactor with GPC. The system response is not satisfactory since the coefficients of polynomials $A(z^{-1})$ and $B(z^{-1})$ caused by non-linearities significantly differs from the 'nominal' values used in the calculation of GPC parameters. The control signal defined by eq. (2.40) is shown in Fig. 3.2.

The implementation of the proposed sliding mode based GPC (SMGPC) in the control of Van der Vusse reaction process yields the results presented in Figs. 3.3 - 3.6. The output response is given in Fig. 3.3, and the system response is much better comparing to the response of system with GPC. The control signal defined by eq. (3.15) is depicted in Fig. 3.4. As one can see, there is no high frequency component in the control signal, so there is no chattering phenomenon at all.

The zero value of g_k is ensured as it is shown in Fig. 3.5. The quasi-sliding mode is reached on sliding surface defined by the switching function $\hat{g}_k$ (Fig. 3.6).

In order to analyze the robustness of the proposed SMGPC, 20% perturbation of the plant parameters is considered in digital simulation. Figs. 3.7 - 3.10 show the responses of the perturbed system with the proposed control. The variations of plant parameters cause the oscillation in output response (Fig. 3.7). There is no chattering in the system, as the control contains only low frequency components (Fig. 3.8).

The zero value of g_k is still ensured (see Fig. 3.9), whereas the quasi-sliding motion occurs in the vicinity of $\hat{g}_k$, determined by eq. (3.24).

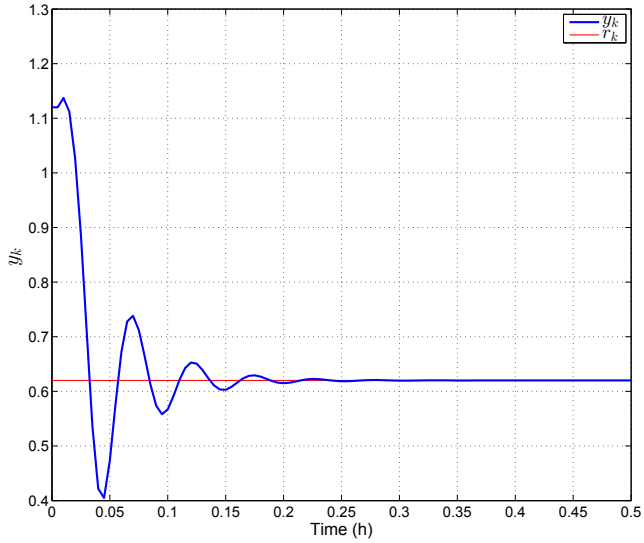

Figure 3.1: Output y_k of system with GPC.

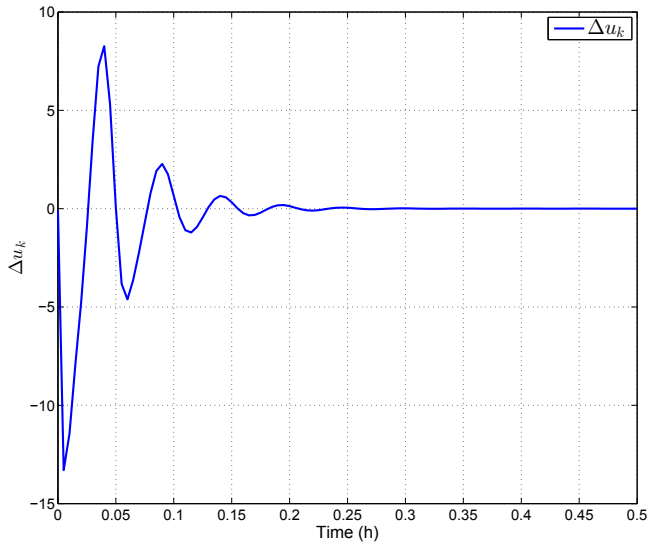

Figure 3.2: Control signal Δu_k of system with GPC

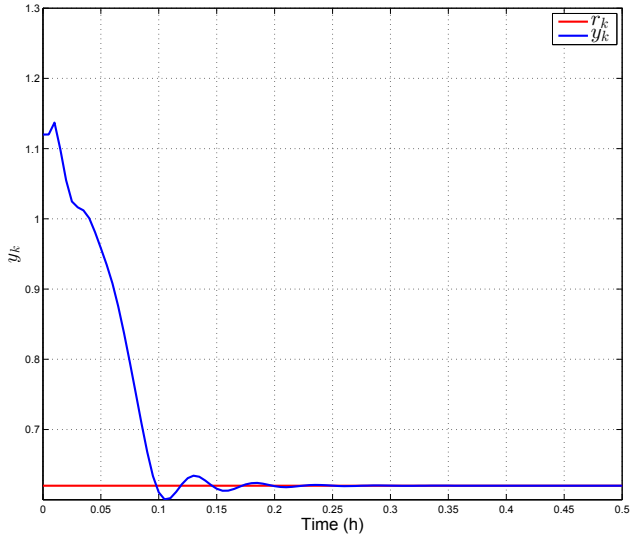

Figure 3.3: Output y_k of system with SMGPC

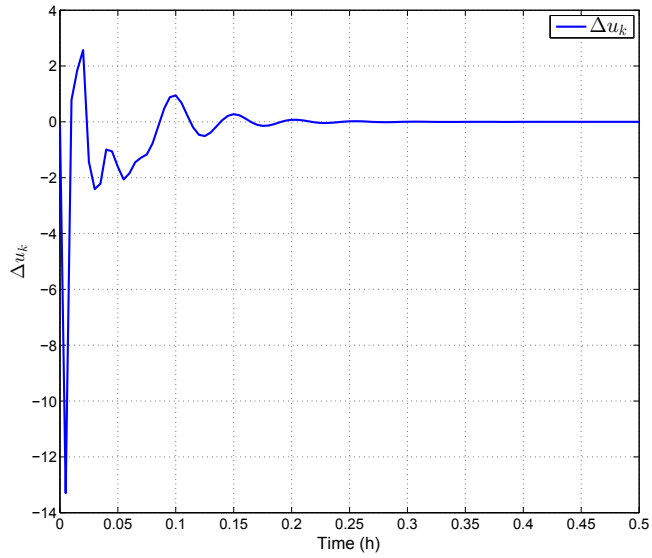

Figure 3.4: Control signal Δu_k of system with SMGPC

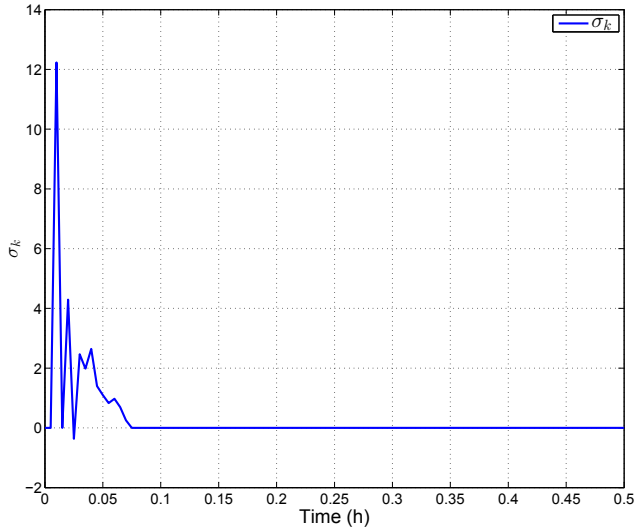

Figure 3.5: g_k of system with SMGPC

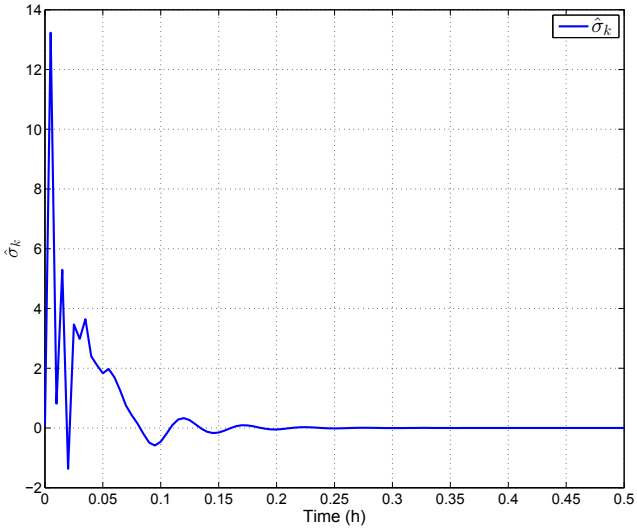

Figure 3.6: Switching function $\hat{g}_k$ of system with SMGPC

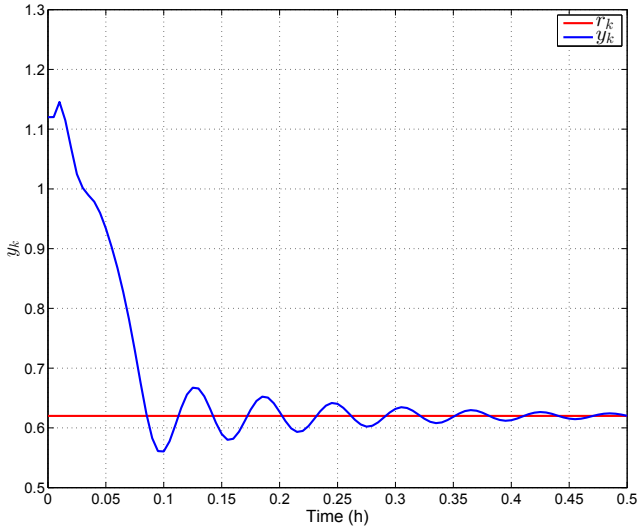

Figure 3.7: Output y_k of perturbed system with SMGPC

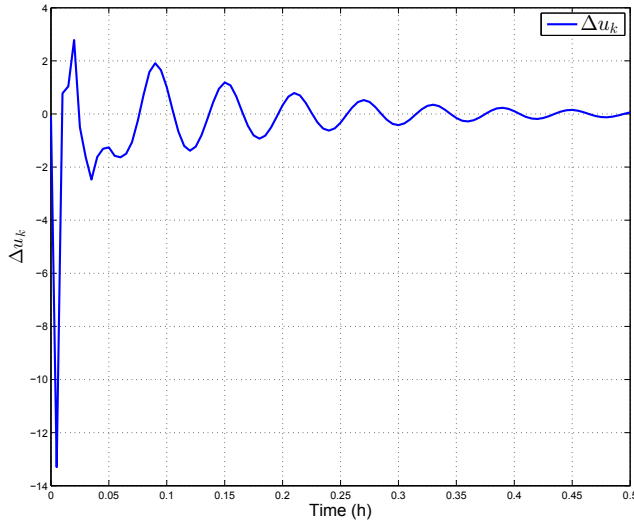

Figure 3.8: Control signal Δu_k of perturbed system with SMGPC

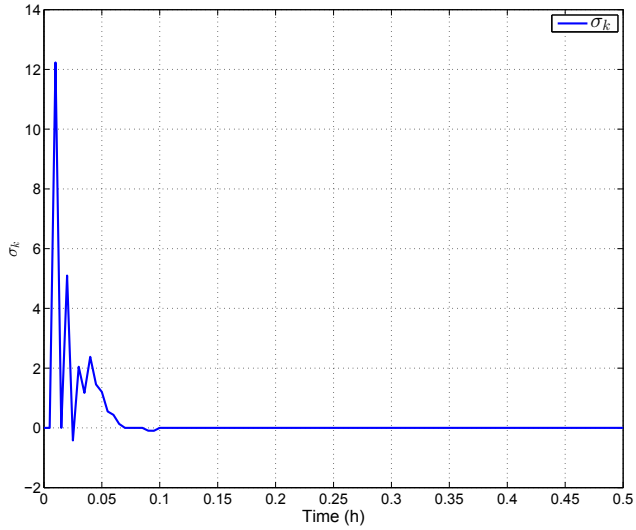

Figure 3.9: g_k of perturbed system with SMGPC

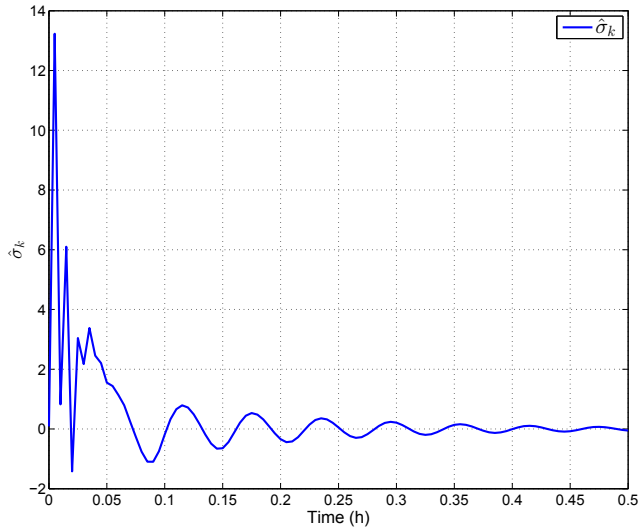

Figure 3.10: Switching function $\hat{g}_k$ of perturbed system with SMGPC

3.4 Conclusion

A novel sliding mode based generalized predictive control is presented in this chapter. The advantages of both sliding mode control and generalized predictive control are combined in order to obtain the control algorithm that would improve the robustness of system to parameter perturbations[1]. The given control law ensures the cost function minimum in the presence of internal disturbances. As the main advantage of model predictive control, compared to classical optimal control, is the ability to handle constraints in both inputs and states/outputs, the future work should consider the inclusion of constraints in generalized predictive control formulation.

[1] All files for the controller design can be found on http://automatika.elfak.ni.ac.rs/mspasic/

Chapter 4

Tube MPC with an Auxiliary SMC

This chapter studies TMPC with a SMC as an auxiliary controller. It is shown how to calculate the tube widths under SMC control, and thus how much the constraints of the nominal MPC have to be tightened in order to achieve robust stability and constraint fulfilment.

The chapter is organized as follows. In Section 4.1, the control problem is introduced. Section 4.2 briefly describes two proposed discrete-time sliding mode control approaches. The algorithms for calculating the constraints tightening is presented in Section 4.3. The new TMPC with an auxiliary SMC has been applied to the real DC servo system [100], and the digital simulation and experimental results are given in Section 4.4. Section 4.5 contains some concluding remarks.

4.1 Problem description

Consider the discrete time system described by the model

$$x_{k+1} = Ax_k + Bu_k + Ew_k, \tag{4.1}$$

with the system state $x \in \mathbb{R}^{n_x}$, the input $u \in \mathbb{R}^{n_u}$, and the disturbance $w \in \mathbb{R}^{n_w}$. There are also constraints on the allowable state

$$x \in \mathbb{X} = \{x | Fx \leq f\}, \tag{4.2}$$

constraints on the allowable input

$$u \in \mathbb{U} = \{u | \Gamma u \leq \gamma\}, \tag{4.3}$$

and constraints on the possible range of disturbances

$$w \in \mathbb{W} = \{w | Hw \leq h\}. \tag{4.4}$$

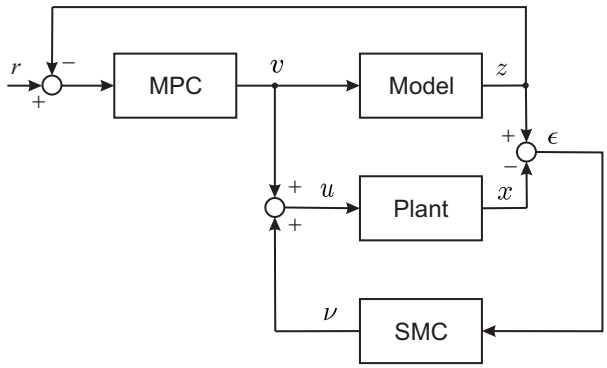

Figure 4.1: Control scheme

It follows from the description above that the sets $\mathbb{X}$,$\mathbb{U}$, and $\mathbb{W}$ are polyhedral; it will be also assumed that they are bounded (and thus that the sets are polytopic), of full dimension, and contain the origin in their interior.

In the following, the system state is split into two components, a nominal component z and a deviation from nominal ϵ

$$x = z + \epsilon. \tag{4.5}$$

Similarly, the input is split into the input from the nominal MPC v, and the input ν from the auxiliary controller

$$u = v + \nu. \tag{4.6}$$

The dynamics, described by eq. (4.1), may therefore be split into the nominal dynamics and the deviation from nominal

$$z_{k+1} = Az_k + Bv_k \tag{4.7}$$
$$\epsilon_{k+1} = A\epsilon_k + B\nu_k + Ew_k \tag{4.8}$$

Clearly, eqs. (4.7) and (4.8) add to eq. (4.1). The control scheme is illustrated in Figure 4.1.

At each timestep, the nominal MPC solves the problem

$$\min_{\mathbf{z},\mathbf{v}} J(\mathbf{z},\mathbf{v}) \tag{4.9}$$
$$\text{subject to}$$
$$z_{k+i} \in \{z_{k+i} | Fz_{k+i} \leq f - \delta_i^z\} \quad i \in \{0,1,\ldots,N\},$$
$$v_{k+i} \in \{v_{k+i} | \Gamma v_{k+i} \leq \gamma - \delta_i^v\} \quad i \in \{0,1,\ldots,N\}.$$

The function $J(\mathbf{z}, \mathbf{v})$ is the MPC cost function[1], N is the length of the prediction horizon for the MPC, $\mathbf{z}$ is the vector of present and future nominal states in the prediction horizon, $\mathbf{z}^T = \begin{bmatrix} z_k^T & z_{k+1}^T & \dots & z_{k+N}^T \end{bmatrix}$, and $\mathbf{v}$ is the vector of present and future inputs from the nominal MPC in the prediction horizon, $\mathbf{v}^T = \begin{bmatrix} v_k^T & v_{k+1}^T & \dots & v_{k+N}^T \end{bmatrix}$. The vector δ_i^z quantifies how much the nominal state constraints have to be restricted at time $k+i$ in order to ensure that the true state adheres to the original constraints, while the vector δ_i^v quantifies how much the constraints on the nominal MPC input have to be restricted at time $k+i$ in order to ensure that the total input adheres to the original constraints. The simplest TMPC formulations treat δ_i^z and δ_i^v as constants over the prediction horizon, whereas other formulations allow these to vary to account for the fact that the disturbance will typically be able to drive the true state further from the nominal state (also under the action of the auxiliary control) over a time period of several timesteps than over a single timestep.

Remark. A special terminal set for the state is a common ingredient in MPC formulations guaranteeing closed loop stability. Such a terminal set is ignored in eq. (4.9) for reasons of notational simplicity, but it adding such a terminal set would be straight forward.

From eq. (4.9), it is clear that δ_i^z and δ_i^v have to be found in order to be able to formulate the nominal MPC. This will be addressed in Section 4.3.

4.2 Discrete-time Sliding Mode Control

To design the auxiliary discrete-time SMC, the deviated system dynamics is considered and described by eq. (4.8). Two control algorithms are implemented herein. The first one is a traditional relay based sliding mode control defined by

$$\nu_k = -(KB)^{-1}(KA\epsilon_k - g_k + \Delta_u \text{sgn}(g_k)) \tag{4.10}$$

where

$$g_k = K\epsilon_k \tag{4.11}$$

denotes the switching function and

$$g_k = 0 \tag{4.12}$$

is the equation for the sliding surface or the intersection of sliding surfaces if $n_u > 1$. Notice that $K\epsilon_k$ is usually selected as an auxiliary control in TMPC and a matrix K has dimension $n_u \times n_x$. Here $\text{sgn}(g_k)$ is understood to be a vector with elements ± 1,

[1]The cost function will not be specified at present, but it is naturally assumed a sensible cost function ensuring that the control of the nominal system is stable, and one which allows the optimization problem to be solved efficiently.

and Δ_u is a diagonal matrix with constants representing the relay outputs. The sliding surface, i.e. K, should be selected so that the system [55]

$$\begin{aligned} \epsilon_{k+1} &= (A - B(KB)^{-1}K(A - I))\epsilon_k \quad (4.13) \\ K\epsilon_k &= 0 \quad (4.14) \end{aligned}$$

is stable. Eqs. (4.13) and (4.14), describing system dynamics in sliding mode, are obtained by implementing the well-known equivalent control

$$\nu_k^{eqc} = -(KB)^{-1}(KA\epsilon_k - g_k) \quad (4.15)$$

in eq. (4.8). Substituting eq. (4.10) in eqs. (4.8) and (4.11) yields

$$g_{k+1} = g_k - \Delta_u \mathrm{sgn}(g_k) + KEw_k \quad (4.16)$$

defining the switching function dynamics at time instant k, whereas in the prediction horizon it is determined by

$$\begin{aligned} g_{k+i+1} &= g_{k+i} - \Delta_u \mathrm{sgn}(g_{k+i}) + KEw_{k+i}, \quad (4.17) \\ i &\in \{0, 1, \ldots, N\} \end{aligned}$$

In order to provide stable switching function dynamics, Δ_u should be calculated according to the following theorem.

Theorem 4.2.1. *If Δ_u is chosen to satisfy the following inequality*

$$\Delta_u \underline{1} > \Omega > \max|KEw_k|, \quad (4.18)$$

where Ω is a positive real vector and $\underline{1}$ is a vector of 1's, then, for every initial state g_k, there exists a positive integer number $k_0 = k_0(g_k) < N$, such that the system phase trajectory, described by eqs. (4.17) and (4.18), enters the domain defined by

$$G = \{g_{k+i} : |g_{k+i}| < \Delta_u \underline{1} + \Omega\}, \quad (4.19)$$

after k_0 timesteps and remains in this domain for all $i > k_0$.

Proof. See Appendix A. □

However, relay feedback is known to often result in very fast switching, which for some applications will not be desirable. A common remedy is then to replace the 'infinite gain' at the switching surface with a steep linear function, leading to a chattering free SMC. The second auxiliary discrete-time SMC, used in this chapter, is so-called robust discrete-time chattering free sliding mode control [59]

$$\begin{aligned} \nu_k = &- (KB)^{-1}\big(KA\epsilon_k - g_k \\ &+ \min(I|g_k|, \Delta_u)\mathrm{sgn}(g_k)\big) \quad (4.20) \end{aligned}$$

Implementing eq. (4.20) in eq. (4.8), the switching function dynamics becomes

$$g_{k+1} = g_k - \min(I|g_k|, \Delta_u)\text{sgn}(g_k) + KEw_k \tag{4.21}$$

and, inside the prediction horizon it is formulated by

$$\begin{aligned} g_{k+i+1} &= g_{k+i} - \min(I|g_{k+i}|, \Delta_u)\text{sgn}(g_{k+i}) \\ &+ KEw_{k+i}, \quad i \in \{0, 1, \ldots, N\} \end{aligned} \tag{4.22}$$

The next theorem gives sufficient conditions for stable sliding motion.

Theorem 4.2.2. *The system phase trajectory, described by eqs. (4.22) and (4.18), reaches the domain G defined by eq. (4.19) in $k_0 = k_0(g_k) < N$ timesteps for every initial g_k, and remains in it for all $i > k_0$.*

Proof. See Appendix B. □

4.3 Calculating the required constraint tightening with SMC-based auxiliary controllers

This section describes how to calculate the required constraint tightening for TMPC for each of the SMC controls defined by eqs. (4.10) and (4.20).

4.3.1 Constraint tightening for traditional SMC

Denote the relay term in eq. (4.10) as

$$\vartheta_k = \Delta_u \text{sgn}(K\epsilon_k), \tag{4.23}$$

To proceed, for each element ϑ_j of ϑ a binary variable s_j is defined, such that $\vartheta_j > 0 \Rightarrow s_j = 1$, and $s_j = 0$ otherwise. Also needed are upper and lower bounds on each component of the vector $K\epsilon$. From eqs. (4.2) and (4.5), it is clearly safe to assume $F\epsilon \leq f$, and the lower bounds m_j and upper bounds μ_j on element j of $K\epsilon$ can be found from the LPs

$$m_j = \min_{F\epsilon \leq f} K_j\epsilon \tag{4.24}$$

and

$$\mu_j = \max_{F\epsilon \leq f} K_j\epsilon \tag{4.25}$$

where K_j is row j of K. Let $\underline{1}$ denote a vector of 1's. Equation (4.23) is then implied by [101]

$$\vartheta_k = \Delta_u S - \Delta_u(\underline{1} - s) = \Delta_u(2s - \underline{1}), \tag{4.26}$$

where the value of the binary variables s follow from the constraints

$$m_j(1 - s_j) < \quad K_j\epsilon \tag{4.27}$$
$$-\mu_j s_j < \quad -K_j\epsilon \tag{4.28}$$

Note that numerical optimization solvers cannot distinguish between strict and non-strict inequalities. The formulation above will leave the value of s_j undecided if $K_j\epsilon = 0$. It will then be left for the optimization routine to choose the optimal value.

The furthest from the origin the disturbance sequence $\{w_k\}$ may drive the deviation state ϵ_k in the direction of the state constraint $F_l x_k \leq f_l$ over a horizon of N timesteps can then be found by solving

$$\begin{aligned}
&\delta f_{j,N} = \max_{w_k, s_k, \epsilon_k} F_l \epsilon_N \\
&\text{subject to} \\
&\epsilon_0 = 0 \\
&Hw_k \leq h;\ k = 0, \ldots, N-1 \\
&\epsilon_{k+1} = \overline{A}\epsilon_k + \overline{B}\Delta_u(2s_k - \underline{1}) + Ew_k; \\
&\qquad k = 0, \ldots, N-1 \\
&\overline{A} = A - B(KB)^{-1}K(A - I) \\
&\overline{B} = -B(KB)^{-1} \\
&diag\{m_j\}(\underline{1} - s_k) < K\epsilon_k;\ k = 0, \ldots, N-1 \\
&-diag\{\mu_j\}s_k < -K\epsilon_k;\ k = 0, \ldots, N-1 \\
&s_k \in \{0, 1\}^{n_u}
\end{aligned} \tag{4.29}$$

For each state constraint j, this optimization should be solved for a number of horizon lengths N. For each timestep i, the elements of δ_i^z are given by $\delta f_{j,i}$. If the system under the relay feedback is stable, $\delta f_{j,N}$ will approach an upper bound as N grows large.

4.3.2 Constraint tightening for chattering free SMC

Instead of eq. (4.23), the following control law is used

$$\vartheta_j = \min(|K_j\epsilon|, \Delta_{uj})\text{sgn}(K_j\epsilon) \tag{4.30}$$

where Δ_{uj} denotes the j'th element on the main diagonal of the diagonal matrix Δ_u, and K_j as before refers to row j of K. Eq. (4.30) is rewritten as

$$\vartheta_j = \text{sat}(K_j x) = \begin{cases} \Delta_{uj} & \text{if } K_j\epsilon \geq \Delta_{uj} \\ K_j\epsilon & \text{if } -\Delta_{uj} \leq K_j\epsilon \leq \Delta_{uj} \\ -\Delta_{uj} & \text{if } K_j\epsilon \leq -\Delta_{uj} \end{cases} \tag{4.31}$$

To capture this behaviour, two binary variables, s_j and t_j are needed for each auxiliary input ϑ_j, such that

$$K_j\epsilon < -\Delta_{uj} \quad \rightarrow s_j = 0 \tag{4.32}$$

$$K_j\epsilon > -\Delta_{uj} \quad \rightarrow s_j = 1 \tag{4.33}$$

$$K_j\epsilon < \Delta_{uj} \quad \rightarrow t_j = 0 \tag{4.34}$$

$$K_j\epsilon > \Delta_{uj} \quad \rightarrow t_j = 1 \tag{4.35}$$

Define

$$q_j = K_j\epsilon - m_j \tag{4.36}$$

where m_j is calculated as in eq. (4.24). It is noted that q_j is non-negative in the domain of interest. The actual input from the auxiliary controller may then be calculated from the expression

$$\vartheta_j = -(1 - s_j)\Delta_{uj} + (s_j - t_j)(q_j + m_j) + t_j\Delta_{uj} \tag{4.37}$$

where is also noted that $s_j \geq t_j$. The difficulty in the above equation lies in the bilinear terms $s_j q_j$ and $t_j q_j$, both being the product of a binary variable and a non-negative real. To proceed, the auxiliary variables $\sigma_j = s_j q_j$ and $\tau_j = t_j q_j$ are introduced. From [102], it can be seen that the set

$$\mathcal{R} = \{(q_j, s_j, \sigma_j) : \sigma_j = s_j q_j, 0 \leq q_j \leq a_j, s_j \in \{0, 1\}\} \tag{4.38}$$

can equivalently be expressed as

$$\begin{aligned} \mathcal{M} = \quad & \{(q_j, s_j, \sigma_j) : 0 \leq \sigma_j \leq a_j s_j, \\ & q_j + a_j s_j - a_j \leq \sigma_j \leq q_j, s_j \in \{0, 1\}\} \end{aligned} \tag{4.39}$$

and similarly for (q_j, t_j, τ_j). Recognizing that in this case $a_j = \mu_j - m_j$, and introducing

$$m_{1j} = m_j + \Delta_{uj} \tag{4.40}$$

$$\mu_{1j} = \mu_j + \Delta_{uj} \tag{4.41}$$

$$m_{2j} = m_j - \Delta_{uj} \tag{4.42}$$

$$\mu_{2j} = \mu_j - \Delta_{uj} \tag{4.43}$$

Defining the diagonal matrices $\Lambda = diag(a_j)$, $\underline{M}_1 = diag(m_{1j})$, $\bar{M}_1 = diag(\mu_{1j})$, $\underline{M}_2 = diag(m_{2j})$, and $\bar{M}_2 = diag(\mu_{2j})$, and forming the column vectors $m = \text{vec}(m_j)$, $s_k = \text{vec}(s_{kj})$, $t_k = \text{vec}(t_{kj})$, $\sigma_k = \text{vec}(\sigma_{kj})$, and $\tau_k = \text{vec}(\tau_{kj})$, the optimization formulation is obtained as

$$\delta f_{l,N} = max_{w_k,\vartheta_k,\sigma_k,\tau_k,s_k,t_k,\epsilon_k} F_l \epsilon_N \tag{4.44}$$

$$\text{subject to} \tag{4.45}$$

$$\epsilon_0 = 0 \tag{4.46}$$

$$Hw_k \leq h; \quad k = 0, \ldots, N-1 \tag{4.47}$$

$$\epsilon_{k+1} = \overline{A}\epsilon_k + \overline{B}\vartheta_k + Ew_k; \quad k = 0, \ldots, N-1 \tag{4.48}$$

$$\vartheta_k = -\Delta_u(\underline{1} - s_k) + M(s_k - t_k) + \sigma_k - \tau_k \tag{4.49}$$
$$+\Delta_u t_k; \quad k = 0, \ldots, N-1$$

$$\underline{M}_1(\underline{1} - s_k) < K\epsilon_k + \Delta_u \underline{1}; \quad k = 0, \ldots, N-1 \tag{4.50}$$

$$-\bar{M}_1 s_k < -K\epsilon_k - \Delta_u \underline{1}; \quad k = 0, \ldots, N-1 \tag{4.51}$$

$$\underline{M}_2(\underline{1} - t_k) < K\epsilon_k - \Delta_u \underline{1}; \quad k = 0, \ldots, N-1 \tag{4.52}$$

$$-\bar{M}_2 t_k < -K\epsilon_k + \Delta_u \underline{1}; \quad k = 0, \ldots, N-1 \tag{4.53}$$

$$\sigma_k > 0; \quad k = 0, \ldots, N-1 \tag{4.54}$$

$$\tau_k > 0; \quad k = 0, \ldots, N-1 \tag{4.55}$$

$$\sigma_{1k} < \Lambda s_k; \quad k = 0, \ldots, N-1 \tag{4.56}$$

$$\tau_k < \Lambda t_k; \quad k = 0, \ldots, N-1 \tag{4.57}$$

$$\sigma_k < K\epsilon_k - m; \quad k = 0, \ldots, N-1 \tag{4.58}$$

$$\tau_k < Kx_k - m; \quad k = 0, \ldots, N-1 \tag{4.59}$$

$$K\epsilon_k + \Lambda s_k - \Lambda \underline{1} - m < \sigma_k; \quad k = 0, \ldots, N-1 \tag{4.60}$$

$$K\epsilon_k + \Lambda t_k - \Lambda \underline{1} - m < \tau_k; \quad k = 0, \ldots, N-1 \tag{4.61}$$

$$s_k \in \{0,1\}^{n_u}, \qquad t_k \in \{0,1\}^{n_u} \tag{4.62}$$

Clearly, with ν_k as in eqs. (4.10) and (4.20) taking into account $F\epsilon \leq f$ as specified above, we have

$$\delta_i^v = max(\nu_k) \; \forall i. \tag{4.63}$$

4.4 Digital simulation and experimental results

The validation of the proposed control methods is performed by using the modular servo system [100] shown in Figure 4.2. The objective is to control the angular position of the DC motor shaft. The system consists of the following components: a tachogenerator, a DC motor, an encoder and an inertia load. This modular experimental setup supports

real-time design and implementation of advanced control algorithms, and is interfaced with the MATLAB/Simulink using specific RT-DAC4/USB board for transferring the measured signals from the tachogenerator and encoder, and the control signals to the power interface unit. The angular position θ of the DC motor shaft is measured by the incremental encoder, and the angular velocity ω is proportional to the voltage produced by the tachogenerator. The DC motor is controlled by a PWM signal with the scaled input voltage

$$U(t) = V(t)/V_{max} \tag{4.64}$$

where $|U(t)| \leq 1$ and $V_{max} = 12[V]$.

In order to identify the model of the system, the identification tool within Modular Servo Toolbox, which operates directly in the MATLAB/Simulink environment, is used. The identification procedure is also given in [100]. The following transfer function is obtained

$$G(s) = \frac{\theta(s)}{u(s)} = \frac{K_s}{s(T_s s + 1)} \tag{4.65}$$

where $K_s = 184.73$ and $T_s = 1.3s$.

By denoting $x_1 = \theta$ and $x_2 = \omega$, the state space model of servo system is

$$\begin{aligned} \dot{x}_1 &= x_2 \\ \dot{x}_2 &= ax_2 + bu + w \end{aligned} \tag{4.66}$$

where $a = -1/T_s$ and $b = K_s/T_s$, and w represents the Coulomb friction defined by

$$w = F_c \text{sgn}(x_2) \tag{4.67}$$

treated as the unmodeled disturbance.

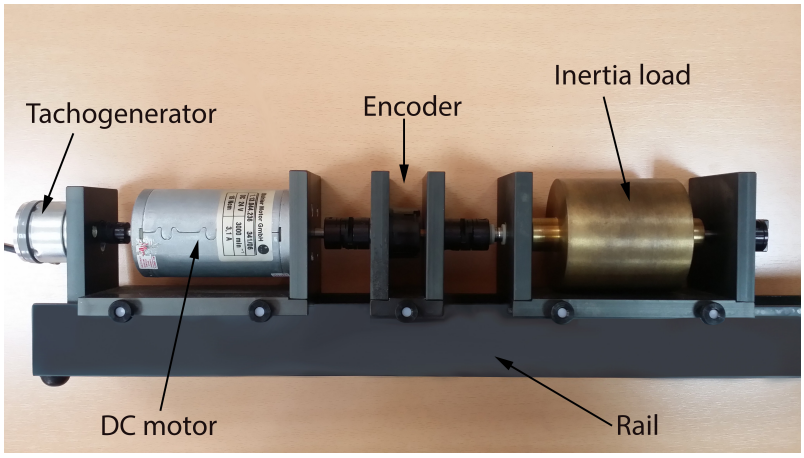

Figure 4.2: DC servo system setup

The sampling period is set to $T = 0.01s$, and the discrete-time state space model is given by

$$\begin{aligned} x_{k+1} &= Ax_k + Bu_k + Ew_k \\ y_k &= Cx_k \end{aligned} \tag{4.68}$$

with

$$\begin{aligned} A = \begin{bmatrix} 1 & 0.01 \\ 0 & 0.9923 \end{bmatrix}, \quad B &= \begin{bmatrix} 0.0071 \\ 1.4155 \end{bmatrix}, \quad E = \begin{bmatrix} 0 \\ 1 \end{bmatrix} \\ C &= \begin{bmatrix} 1 & 0 \end{bmatrix}. \end{aligned} \tag{4.69}$$

The weight matrices are chosen as

$$Q = \begin{bmatrix} 50 & 0 \\ 0 & 1 \end{bmatrix} \tag{4.70}$$

$$R = 1000 \tag{4.71}$$

and the prediction horizon of $N = 20$ is considered.

The dynamics described by eq. (4.68) is split into the nominal one, eq. (4.7), and the deviation from the nominal, eq. (4.8).

Three sets of the digital simulations and real-time experiments are conducted in order to validate the proposed TMPC control methods. The reference signal is defined by

$$r = \begin{cases} 0 & \text{if Time steps} < 50 \\ 40 & \text{if } 50 \leq \text{Time steps} \leq 500 \\ 0 & \text{if Time steps} > 500 \end{cases} \tag{4.72}$$

In all three sets, the nominal MPC, v, is calculated by the nominal model only, and SMC, ν, is used as the auxiliary controller to eliminate the disturbance.

A. Nominal MPC

In order to show the system response, when only the nominal MPC is applied, the first set of the digital simulation and real-time experiment is conducted. The following control

$$-1 \leq u \leq 1 \tag{4.73}$$

and the state

$$-50 \leq x_1 \leq 50 \tag{4.74}$$
$$-34 \leq x_2 \leq 34$$

constraints are defined.

Initially, the nominal MPC, shown in Figure 4.3, is applied to the nominal model. The digital simulation results, together with the corresponding experimental results, are depicted in Figures 4.4 and 4.5.

It is shown that both nominal and real states respect the constraints defined by eq. (4.74), but there is discrepancy between the responses of the nominal model and real plant. This demonstrates the lack of robustness of the nominal MPC when it is applied to the real-time DC servo system in the presence of disturbance.

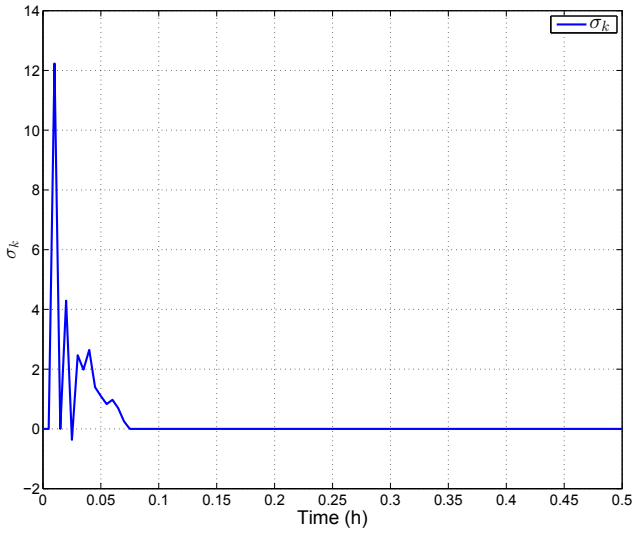

Figure 4.3: Nominal MPC signal

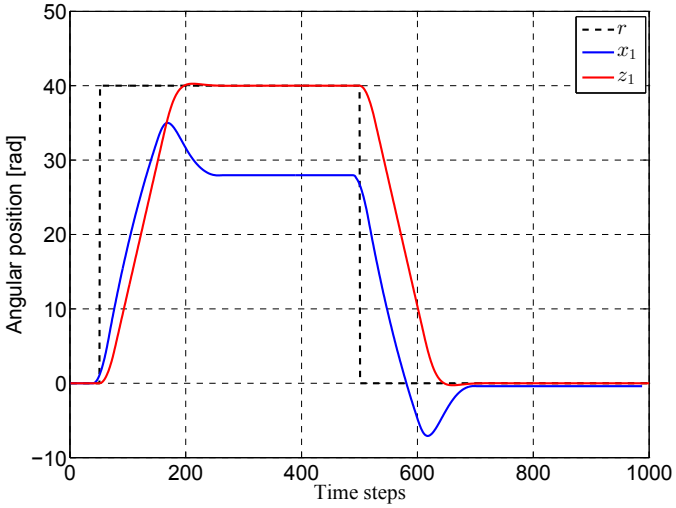

Figure 4.4: The angular position z_1 of the nominal model, and x_1 of the real plant for the nominal MPC

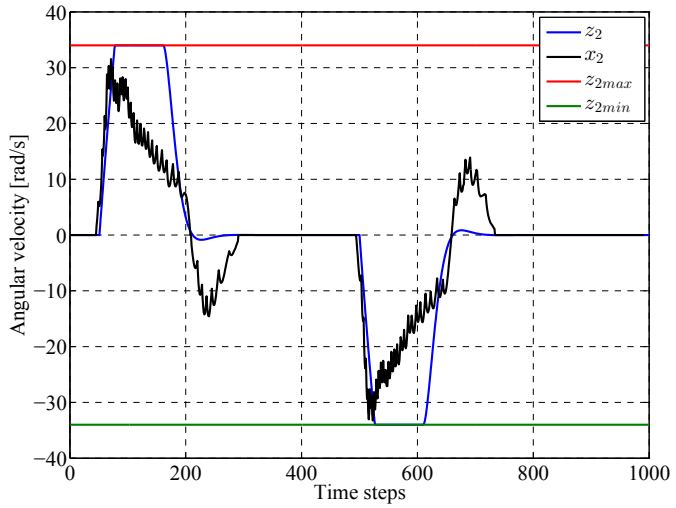

Figure 4.5: The angular velocity z_2 of the nominal model, and x_2 of the real plant for the nominal MPC

B. Tube MPC with traditional SMC

The traditional SMC defined by eq. (4.10), as an auxiliary controller of TMPC, is applied to cope with the disturbance. The two control components are now constrained separately.

The constraints for the nominal MPC and SMC are defined by

$$-0.7 \leq v_k \leq 0.7 \tag{4.75}$$

$$-0.3 \leq \nu_k \leq 0.3 \tag{4.76}$$

which satisfy eq. (4.73), i.e. $-1 \leq v+\nu \leq 1$. The new state constraints are calculated by using the tightening procedure described in Section 4.3. The tightened state constraints used for the nominal system are now defined by

$$-45 \leq z_1 \leq 45 \tag{4.77}$$

$$-25 \leq z_2 \leq 25$$

and the real system has to satisfy constraints defined by eq. (4.74). First, the digital simulation is performed, where nominal MPC signal is applied to the nominal model. Obtained results are shown in Figures 4.6 and 4.7.

It can be seen that the nominal states respect constraints defined by eq. (4.77). The nominal MPC signal also respects the constraints defined by eq. (4.75), which is illustrated in Figure 4.8. Then, the TMPC with the traditional auxiliary SMC is applied to the real-time DC servo system in order to eliminate the disturbance. The parameters of the SMC component are $\Delta_u = 0.3$ and $K = [-0.0118 - 0.0071]$. The real-time system responses are also presented in Figures 4.6 and 4.7.

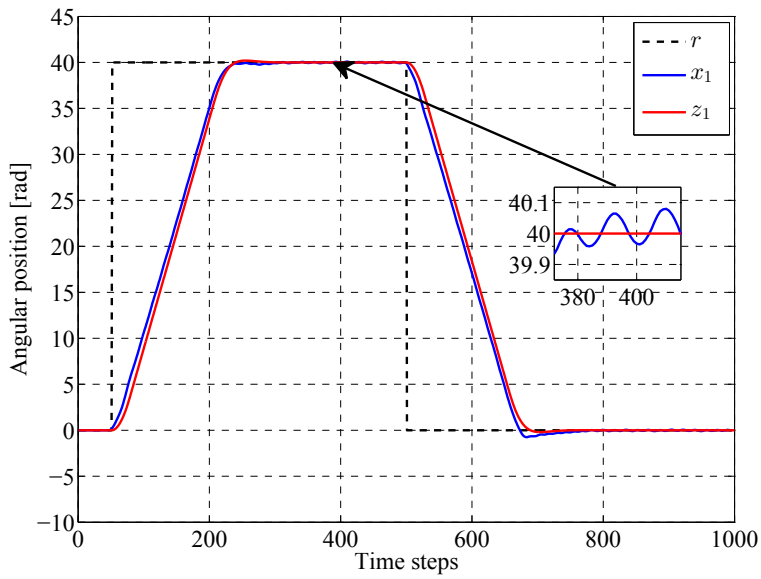

Figure 4.6: The angular position z_1 of the nominal model for the nominal MPC, and x_1 of the real plant for the proposed control

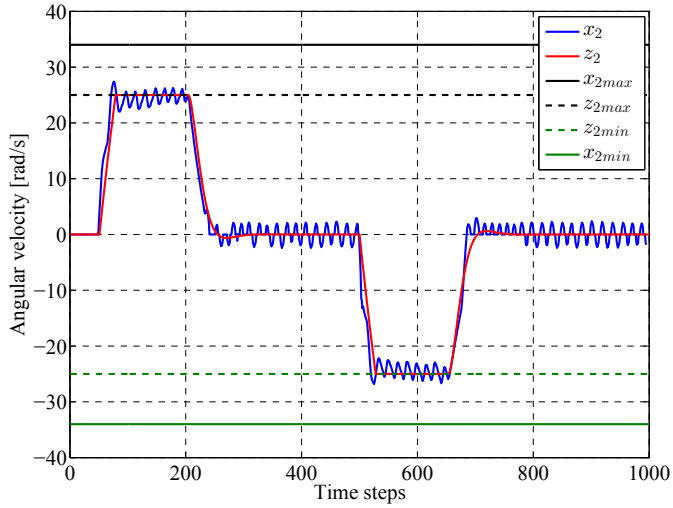

Figure 4.7: The angular velocity z_2 of the nominal model for the nominal MPC , and x_2 of the real plant for the proposed control

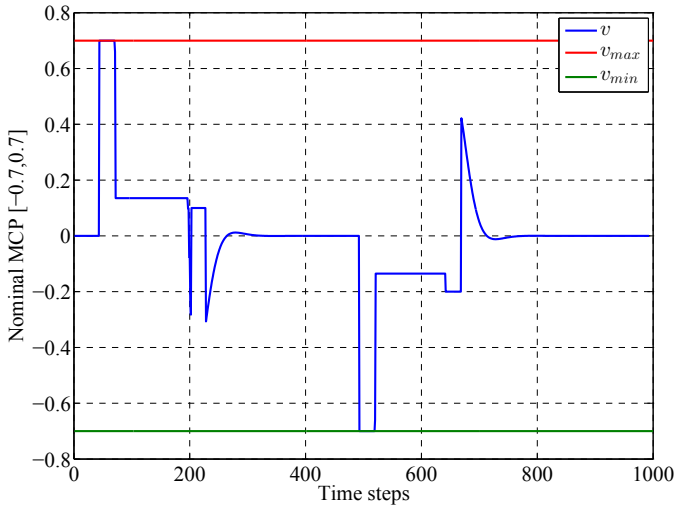

Figure 4.8: Nominal MPC component of the proposed control

In Figure 4.9 the SMC component of the TMPC is presented. Comparing the previous two experimental results, it is shown that the disturbance is rejected, but there is a little chattering in the output signal. The next experiment demonstrates how to eliminate the chattering phenomenon.

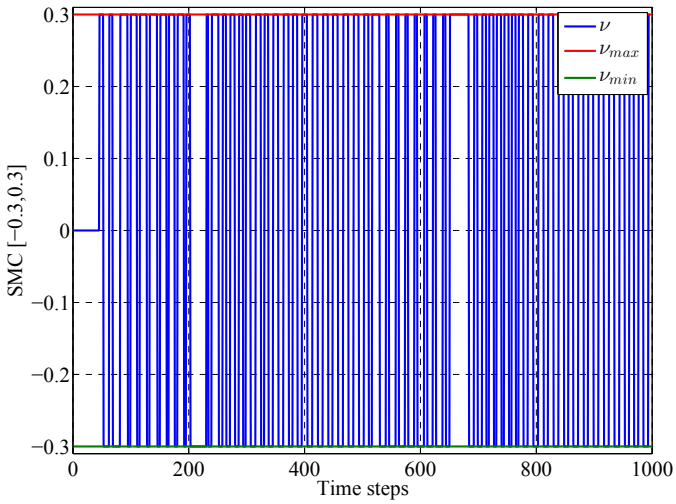

Figure 4.9: Traditional SMC component of the proposed control

C. Tube MPC with chattering free SMC

The same control and state constraints, defined by eqs. (4.75), (4.76) and (4.77), respectively, are used herein. The nominal MPC is applied to the nominal model first. The obtained nominal and real-time system responses are illustrated in Figures 4.10 and 4.11. After that, TMPC with the chattering free SMC is applied to the real DC servo system. The SMC component is defined by eq. (4.20) and the parameters are $\Delta_u = 0.3$ and $K = [-0.0118 - 0.0071]$. Figure 4.10 shows that the chattering is eliminated.

The oscillations in SMC component between 0 and 200, as well as 500 and 700 timesteps in Figure 4.13 originate from noise existing in angular velocity signal taken from tachogenerator (Figure 4.11). Therefore, they are not caused by chattering phenomenon. As in the previous experiments, all states and control signals respect the defined constraints.

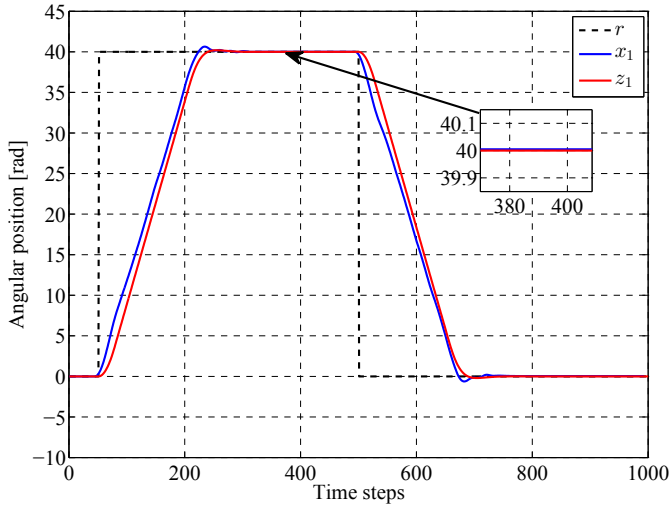

Figure 4.10: The angular position z_1 of the nominal model for the nominal MPC, and x_1 of the real plant for the proposed control

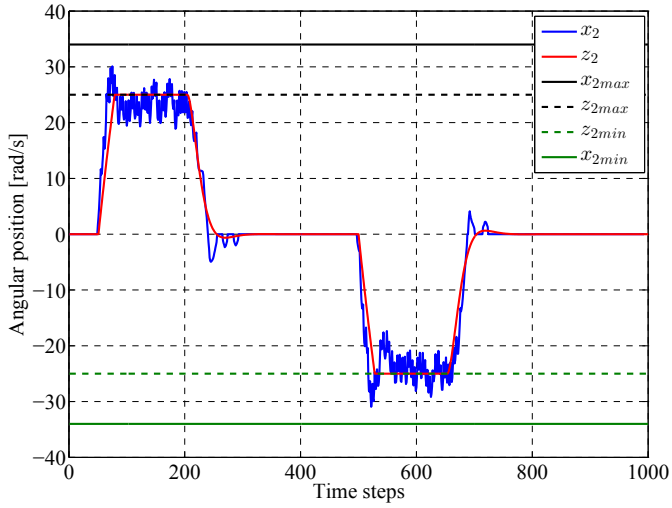

Figure 4.11: The angular velocity z_2 of the nominal model for the nominal MPC, and x_2 of the real plant for the proposed control

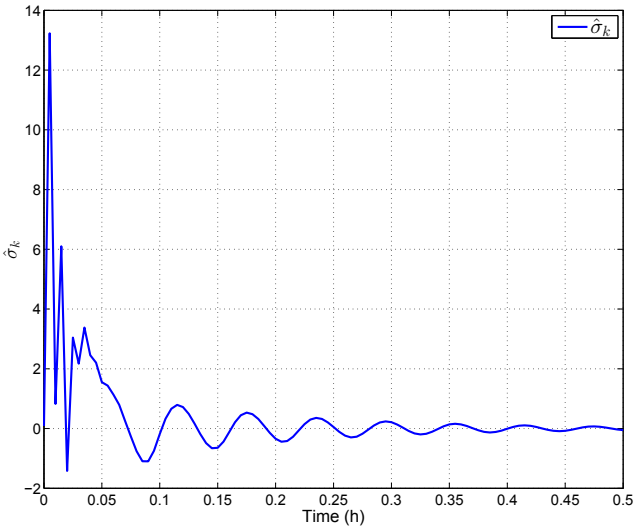

Figure 4.12: Nominal MPC component of the proposed control

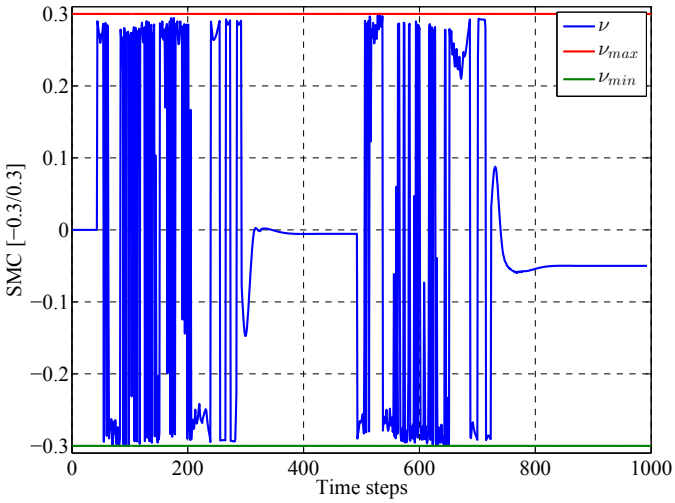

Figure 4.13: Chattering free SMC component of the proposed control

4.5 Conclusion

In this chapter, the TMPC with a SMC as an auxiliary controller is studied in order to improve the robustness of the overall system. Due to the presence of the SMC component, it is necessary to tighten the constraints of the nominal MPC part. The online calculations for SMC are not time consuming and the use of the SMC in a TMPC setting allows for the use of a simple nominal MPC which also has modest online calculation requirements. The traditional and chattering-free SMC algorithms are introduced in TMPC in order to reject disturbances and to achieve better performances of the real system. Procedures for calculating the required constraint tightening are derived for the both cases. The good characteristics of the proposed control algorithms [2] are demonstrated by conducting several digital simulations and real-time experiments on a DC servo system.

[2] All files for the controllers design can be found on http://automatika.elfak.ni.ac.rs/mspasic/

Chapter 5

Tube Model Predictive Control based on Laguerre functions with an Auxiliary Sliding Mode Controller

This chapter deals with Tube Model Predictive Control (TMPC) based on Laguerre functions with a Sliding Mode Controller (SMC) as an auxiliary controller. Two types of SMC are implemented: the traditional one and the robust chattering-free discrete-time SMC. It is shown how much the constraints of the nominal Laguerre functions based MPC have to be tightened in order to achieve robust stability and control constraints fulfilment. The proposed approach is verified by experimental results.

This Chapter is organized as follows. In Section 5.1, the control problem is introduced. The Laguerre functions based MPC design is presented in Section 5.2. Section 5.3 describes two proposed discrete-time sliding mode control algorithms used for the design of MPCBLF. The novel TMPC based on Laguerre functions with an auxiliary SMC has been applied to a real DC servo system [100], and the experimental results are given in Section 5.4. Concluding remarks are given in Section 5.5.

5.1 Problem description

The model of the considered discrete time system is described by

$$x_{k+1} = Ax_k + Bu_k + Ew_k, \tag{5.1}$$

the system state , the input, and disturbance are defined as in eq. (4.1). The constraints on the input and possible range of disturbance are defined as in eqs. (4.3) and (4.4) as well. The input increment Δu_k is also determined at time k, *i.e.*, $\Delta u_k = u_k - u_{k-1}$.

It follows from those descriptions that the sets $\mathbb{U}$, and $\mathbb{W}$ are polyhedral and it is also assumed that they are bounded (and thus that the sets are polytopic), of full dimension,

and contain the origin in their interior as in the previous chapter.

If the system state is split into a nominal component z and a deviation from the nominal ϵ (eq. (4.5)), and the control is split into the input from the nominal Laguerre functions based MPC v, and the input ν from the auxiliary controller

$$u = v + \nu, \tag{5.2}$$

then the dynamics of the system described by eq. (5.1), may therefore be split into the nominal dynamics z_{k+1} and the deviation from nominal ϵ_{k+1} as in eqs (4.7) and (4.8).

$$z_{k+1} = Az_k + Bv_k, \tag{5.3}$$
$$\epsilon_{k+1} = A\epsilon_k + B\nu_k + Ew_k. \tag{5.4}$$

At each timestep, the nominal Laguerre functions based MPC solves the problem

$$\min_{\mathbf{v}} J(\mathbf{v}), \tag{5.5}$$
$$\text{subject to}$$
$$v_{k+i} \in \{v_{k+i} | \Gamma v_{k+i} \leq \gamma - \delta_i^v\}. \tag{5.6}$$

Here, $J(\mathbf{v})$ is the Laguerre functions based MPC cost function and it is also assumed a sensible cost function ensuring that the control of the nominal system is stable, and the one which allows the optimization problem to be solved efficiently. The vector $\mathbf{v}$ consists of present and future inputs from the nominal Laguerre functions based MPC in the prediction horizon and N is the length of the prediction horizon. All the parameters are defined as in Section 4.1.

From (5.5), it is clear that δ_i^v have to be found in order to be able to formulate the nominal MPC.

5.2 MPC based on Laguerre functions

Discrete-time Laguerre functions are obtained using the inverse z-transform of Laguerre networks and can be represented in a vector form

$$L_k = [l_{1k} \quad l_{2k} \quad ... \quad l_{Nk}]^T. \tag{5.7}$$

The difference equation of discrete-time Laguerre functions is defined as

$$L_{k+1} = A_l L_k \tag{5.8}$$

where the matrix A_l, containing the parameters a (as defined in section 2.2.4) and $\beta = 1 - a^2$ of the Laguerre functions , is given in the following form

$$A_l = \begin{bmatrix} a & 0 & 0 & ... & 0 \\ \beta & a & 0 & ... & 0 \\ -a\beta & \beta & a & ... & 0 \\ -a^{N-2}\beta & -a^{N-3}\beta & ... & -a^{N-N}\beta & a \end{bmatrix} \tag{5.9}$$

with the vector of initial condition represented by

$$L(0)^T = \sqrt{\beta}[1 \quad -a \quad a^2 \quad -a^3 \quad ... \quad (-1)^{N-1}a^{N-1}]. \tag{5.10}$$

In order to design Laguerre functions based MPC, an augmented state-space model needs to be used. If the states difference is defined as

$$z_{k+1} - z_k = A(z_k - z_{k-1}) + B(v_k - v_{k-1}), \tag{5.11}$$

and if Δz and Δv are introduced as

$$\Delta z_k = z_k - z_{k-1}, \tag{5.12}$$

$$\Delta v_k = v_k - v_{k-1}, \tag{5.13}$$

the augmented state-space model is obtained by connecting Δz_k to the output y_k

$$\begin{aligned} \begin{bmatrix} \Delta z_{k+1} \\ y_{k+1} \end{bmatrix} &= \begin{bmatrix} A & \mathbf{0}^T \\ CA & 1 \end{bmatrix} \begin{bmatrix} \Delta z_k \\ y_k \end{bmatrix} + \begin{bmatrix} B \\ CB \end{bmatrix} \Delta v_k, \\ y_k &= \begin{bmatrix} \mathbf{0} & 1 \end{bmatrix} \begin{bmatrix} \Delta z_k \\ y_k \end{bmatrix}. \end{aligned} \tag{5.14}$$

The new matrices can be denoted as

$$z_k{}^{aug} = \begin{bmatrix} \Delta z_k \\ y_k \end{bmatrix} \quad , \quad A^{aug} = \begin{bmatrix} A & \mathbf{0}^T \\ CA & 1 \end{bmatrix},$$

$$B^{aug} = \begin{bmatrix} B \\ CB \end{bmatrix} \quad , \quad C^{aug} = \begin{bmatrix} \mathbf{0} & 1 \end{bmatrix}.$$

The nominal augmented state-space system model is now described by

$$\begin{aligned} z_{k+1}{}^{aug} &= A^{aug} z_k{}^{aug} + B^{aug} \Delta v_k, \\ y_k &= C^{aug} z_k{}^{aug}. \end{aligned} \tag{5.15}$$

The constraints on the input signal and its increment are defined in the form of a set of linear inequalities

$$v^{\min} \leqslant v_{k+i} \leqslant v^{max}, \tag{5.16}$$

$$\Delta v^{\min} \leqslant \Delta v_{k+i} \leqslant \Delta v^{max}, \tag{5.17}$$

where $v^{\min}, v^{max}, \Delta v^{\min}$, and Δv^{max} represents the lower and upper limits on the input and the increment of the input signals, respectively.

The control increment Δv_{k+i} is captured by a set of Laguerre functions (5.7), i.e.

$$\Delta v_{k+i} = \sum_{j=1}^{N} c_{j_k} l_{j_i}, \tag{5.18}$$

where k and i are the initial time and future sampling instants, respectively, N is the number of Laguerre terms, and c_j are Laguerre coefficients. The main goal of using such parameterization of the control input over the prediction horizon is that it is calculated with only few Laguerre terms, i.e. Laguerre coefficients, which provides smaller optimization problem.

Equation (5.18) can be written in vector form as

$$\Delta v_{k+i} \quad = \quad {L_i}^T \eta_k, \tag{5.19}$$

where $\eta_k = [c_{1k} \quad c_{2k} \quad ... \quad c_{Nk}]^T$ is a vector of Laguerre coefficients. In order to calculate the control increment Δv_k defined as in (5.19), the optimal Laguerre parameters η have to be calculated and have to satisfy the new set of constraints defined by

$$\Theta \eta_k \leqslant \Pi, \tag{5.20}$$

where

$$\Theta = \begin{bmatrix} M_1 \\ -M_1 \\ M_2 \\ -M_2 \end{bmatrix}, \quad \Pi = \begin{bmatrix} \Delta v^{max} \\ -\Delta v^{\min} \\ v^{max} - v_{k-1} \\ -v^{\min} + v_{k-1} \end{bmatrix}, \tag{5.21}$$

and

$$M_1 = \begin{bmatrix} {L_{i_1}}^T & {0_2}^T & ... & 0^T \\ {0_2}^T & {L_{i_2}}^T & ... & 0^T \\ \vdots & \vdots & \ddots & \vdots \\ {0_2}^T & {0_2}^T & ... & {L_{i_{n_u}}}^T \end{bmatrix}, \tag{5.22}$$

$$M_2 = \begin{bmatrix} \sum_{j=0}^{i-1} {L_{j_1}}^T & {0_2}^T & ... & {0_m}^T \\ {0_2}^T & \sum_{j=0}^{i-1} {L_{j_2}}^T & ... & {0_m}^T \\ \vdots & \vdots & \ddots & \vdots \\ {0_2}^T & {0_2}^T & ... & \sum_{j=0}^{i-1} {L_{j_{n_u}}}^T \end{bmatrix},$$

where n_u is the number of inputs.

The constraints defined by eq. (5.20) are linear in the decision variables and the provided objective function is convex. There are a number of optimization routines that can handle this type of optimization problems [103].

The Laguerre functions based MPC signal v_k is applied to the nominal system described by eq. (5.3) and to the plant defined by eq. (5.1). The deviation from nominal system dynamics is then eliminated using the auxiliary SMC. The design of proposed SMC is described in sequel.

5.3 Auxiliary Sliding Mode Controller Design

To design the auxiliary discrete-time SMC, the deviation from nominal system dynamics described by eq. (5.4) is considered. The proposed control law is given by

$$\nu_k = -(KB)^{-1}(KA\epsilon_k - g_k + \tau(g_k)), \tag{5.23}$$

where

$$g_k = K\epsilon_k \tag{5.24}$$

denotes the switching function and

$$g_k = 0 \tag{5.25}$$

is the equation for the sliding surface or the intersection of sliding surfaces if $n_u > 1$. Two control algorithms are proposed: the traditional relay based sliding mode control

$$\tau(g_k) = \Delta_u \text{sgn}(g_k)) \tag{5.26}$$

and the robust discrete-time chattering free sliding mode control [59]

$$\tau(g_k) = \min(I|g_k|, \Delta_u)\text{sgn}(g_k). \tag{5.27}$$

Here $\text{sgn}(g_k)$ is understood to be a vector with elements ± 1, Δ_u is a diagonal matrix with constants representing the relay outputs and the min function produces a diagonal matrix output by applying the scalar min operation to the diagonal elements of the inputs. Substituting eq. (5.23) into eq. (5.4) and taking account eq. (5.24) yields

$$g_{k+1} = g_k - \tau(g_k) + KEw_k \tag{5.28}$$

defining the switching function dynamics at time instant k, whereas in the prediction horizon it is defined by

$$\begin{aligned} g_{k+i+1} &= g_{k+i} - \tau(g_{k+i}) + KEw_{k+i}, \\ i &\in \{0, 1, \ldots, N\} \end{aligned} \tag{5.29}$$

To provide stable switching function dynamics, Δ_u should satisfy the Theorems 4.2.1 and 4.2.2 as well.

Clearly, with ν_k as in eq. (5.23), taking into account eqs. (5.2) and (5.6), it is obtained that

$$\delta_i^v = max(\nu_k) \; \forall i. \tag{5.30}$$

5.4 Experimental results

The proposed control algorithms are verified on the modular servo system described in [100]. The transfer function of the DC servo system has the following form

$$G(s) = \frac{\theta(s)}{u(s)} = \frac{K_s}{s(T_s s + 1)}, \tag{5.31}$$

where $K_s = 184.73$ and $T_s = 1.3s$.

By choosing $T = 0.01s$ for a sampling period, the parameters of the discrete-time state-space model described by eq. (5.1) is calculated as

$$A = \begin{bmatrix} 1 & 0.01 \\ 0 & 0.9923 \end{bmatrix}, \quad B = \begin{bmatrix} 0.0071 \\ 1.4155 \end{bmatrix}, \quad C = \begin{bmatrix} 1 & 0 \end{bmatrix}.$$

The parameters for design of Laguerre functions based MPC (5.14) are: prediction horizon $N_p = 50$, number of the Laguerre terms $N = 4$, Laguerre function parameter $a = 0.4$. The parameters of the SMC components for the both auxiliary controllers are $\Delta_u = 0.3$ and $K = [-0.0118 \; -0.0071]$, and the reference signal is defined by

$$r = \begin{cases} 0 & \text{if Time steps} < 50 \\ 40 & \text{if } 50 \leq \text{Time steps} \leq 500 \\ 0 & \text{if Time steps} > 500 \end{cases}. \tag{5.32}$$

First, only the Laguerre functions based MPC is applied to the DC servo system with the following constraints on control and its increment

$$-1 \leq u_k \leq 1, \quad -0.5 \leq \Delta u_k \leq 0.5. \tag{5.33}$$

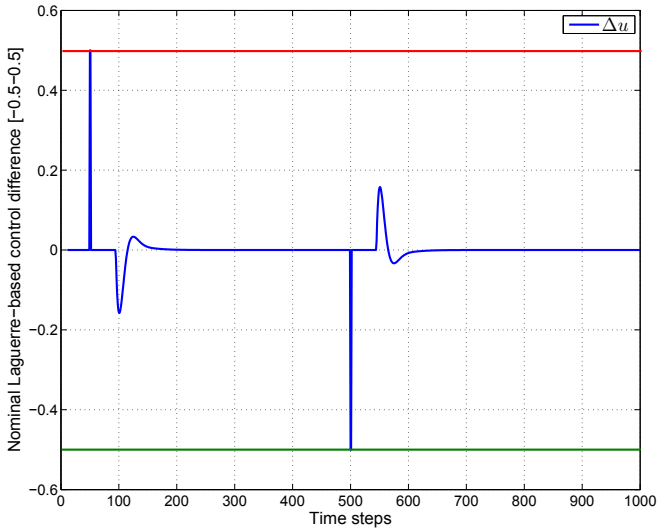

Figure 5.1: Laguerre functions based MPC signal increment Δu

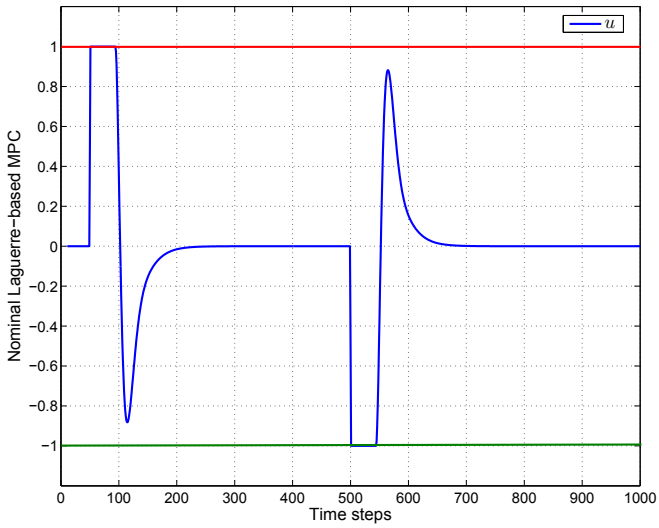

Figure 5.2: Laguerre functions based MPC signal u

The results are given in Figs. (5.1), (5.2) and (5.3). It is obvious that the control signal respects both constraints defined by eq. (5.33), but there is huge difference in the responses of the nominal model and the real plant.

The constraints on the components of the control input signal and its increments for

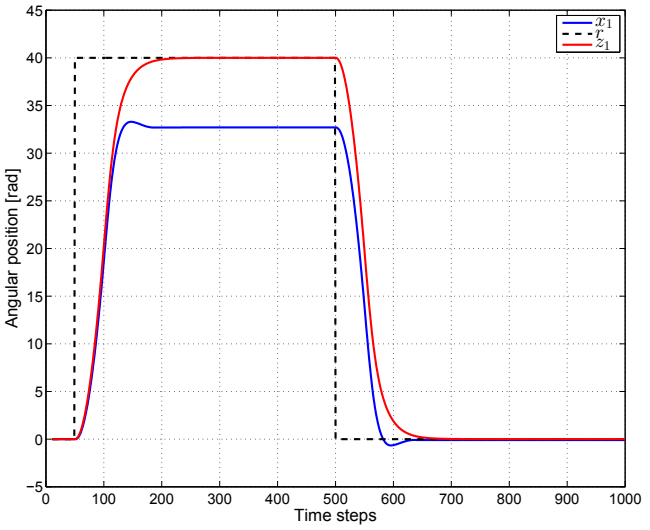

Figure 5.3: The angular position z_1 of the nominal model, and x_1 of the real plant for the Laguerre functions based MPC

the Laguerre functions based MPC with auxiliary SMC are defined by

$$\begin{aligned} -0.7 \leq v_k \leq 0.7, \\ -0.2 \leq \Delta v_k \leq 0.2, \\ -0.3 \leq \nu_k \leq 0.3, \end{aligned} \tag{5.34}$$

which satisfy eq. (5.33), i.e. $-1 \leq v + \nu \leq 1$.

The Laguerre functions based MPC signal and its increment, respecting constraints defined by eq. (5.35), are presented in Figs. (5.4) and (5.5).

The traditional SMC defined by (5.23), as an auxiliary controller of TMPC, applied to cope with the disturbance, is depicted in Fig. (5.6). The response of DC servo system with Laguerre functions based MPC with auxiliary traditional SMC is given in Fig. (5.7). It is clear that the disturbance is rejected, but there is a chattering in the SMC controller signal, leading to slight oscillations in the real state x_1.

The next experiment, which uses the control law defined by eq. (5.23) with eq. (5.27) shown in Fig. (5.8), alleviates the chattering phenomenon significantly in DC servo system response, given in Fig. (5.9).

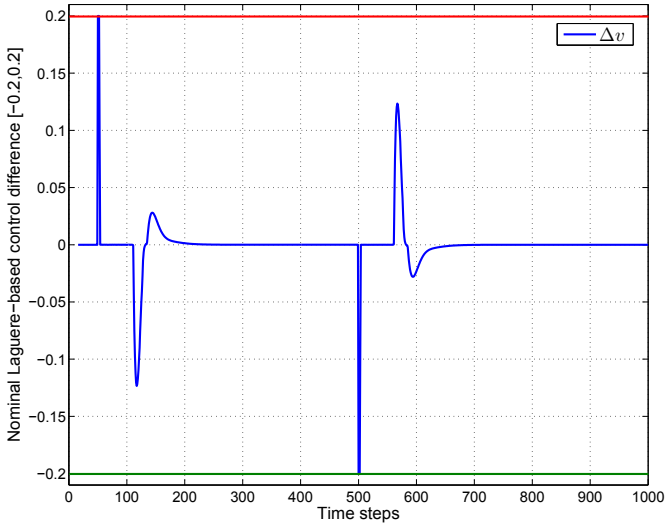

Figure 5.4: Laguerre functions based MPC signal increment Δv when the auxiliary SMC controller is introduced

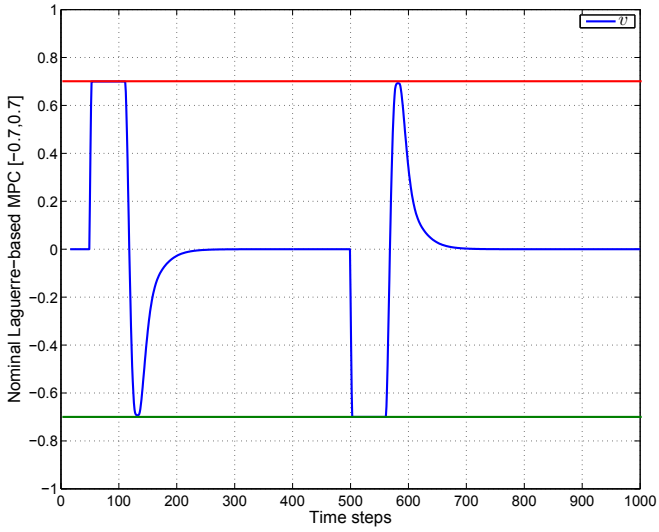

Figure 5.5: Laguerre functions based MPC signal v

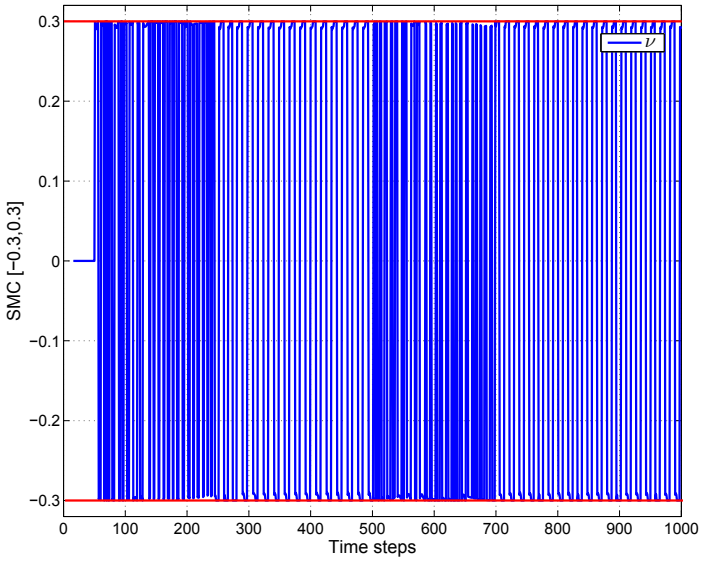

Figure 5.6: Traditional SMC component of the proposed control as an auxiliary controller

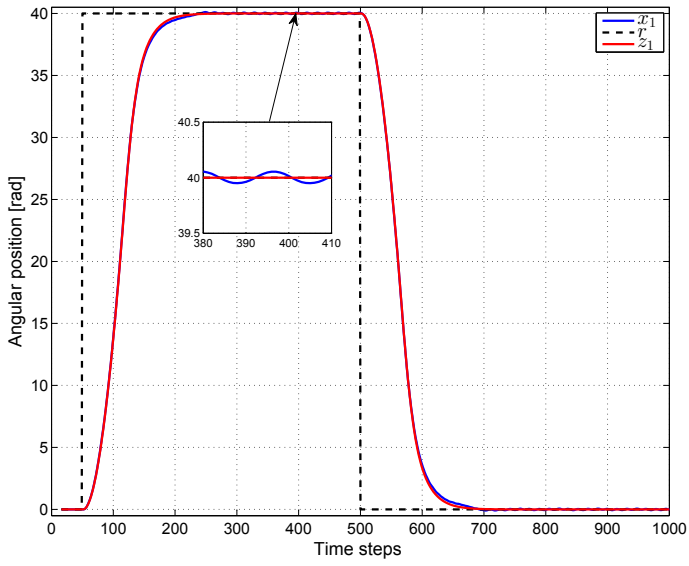

Figure 5.7: The angular position z_1 of the nominal model for the Laguerre functions based MPC, and x_1 of the real plant for the proposed control

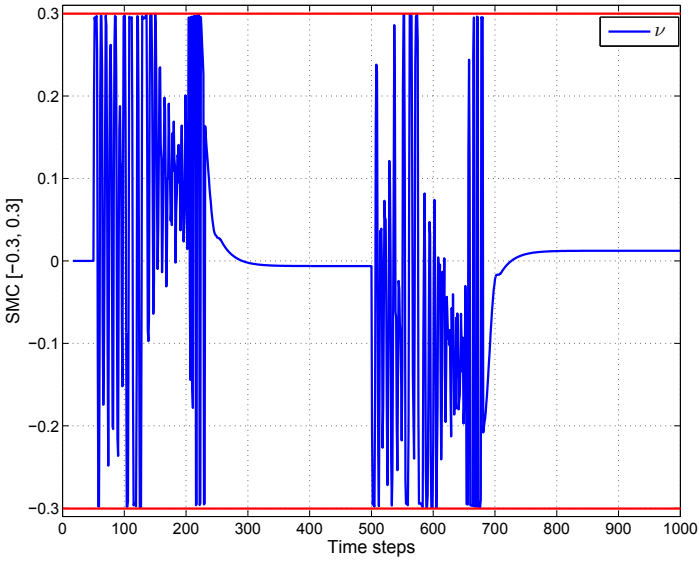

Figure 5.8: Chattering free SMC component of the proposed control as an auxiliary controller

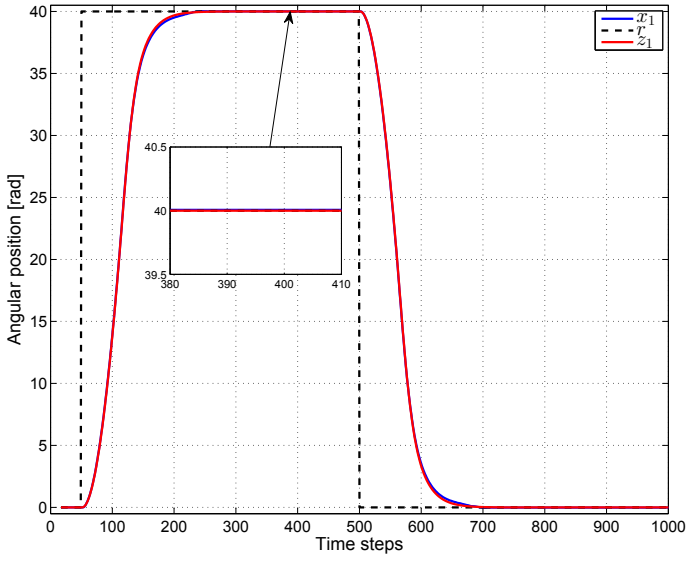

Figure 5.9: The angular position z_1 of the nominal model for the nominal MPC, and x_1 of the real plant for the proposed control

5.5 Conclusion

In this chapter, the TMPC based on Laguerre functions with a SMC as an auxiliary controller is studied in order to improve the robustness of the overall system. Due to the presence of the SMC component, it is necessary to tighten the constraints on the control input and its increment of nominal MPC component. The online solving of constrained optimization problem for MPCBLF is not time consuming and the realisation of SMC is rather simple. The traditional and chattering-free SMC algorithms are introduced as auxiliary control part to alleviate disturbances and to achieve better real system performances. The proposed control laws demonstrate the good system characteristics, which is shown by conducting several real-time experiments on the modular DC servo system. Using the Laguerre functions based MPC parameters, the size of the optimization problem is reduced while allowing for large prediction horizons. The obtained results demonstrate that the performance of the modular DC servo system is very good. Furthermore, better tracking results compared to the ones presented in [4] are obtained.

Chapter 6

Predictive Sliding Mode Control based on Laguerre Functions

This chapter deals with Predictive Sliding Mode Control (PSMC) that uses Laguerre functions in the design of a control input signal. Two types of PSMC algorithms are considered: one originating from the discrete-time equivalent control method approach, and another containing an additional sliding mode control component that provides the robustness and determines the system dynamics in reaching mode. A one-step-delayed disturbance estimator is introduced to account for system nonlinearities and unknown disturbances, as well as to ensure better system steady-state accuracy. The proposed algorithms are demonstrated by conducting several real-time experiments on a modular DC servo system. Robustness of the closed loop, affected by tuning parameter values, is demonstrated as well.

6.1 Problem Formulation

6.1.1 Mathematical Model of Plant

Consider a discrete-time state-space model of plant given by

$$x_{k+1} = Ax_k + Bu_k + d_k, \tag{6.1}$$

$$y_k = Cx_k \tag{6.2}$$

where $x_k \in \mathbb{R}^{n_x}$, $u_k \in \mathbb{R}^{n_u}$, and $d_k \in \mathbb{R}^{n_x}$ represent vectors of system state, control input signals and disturbances, respectively. To introduce integral action in the controller, the following augmented state-space model is obtained

$$x_{e,k+1} = A_e x_{e,k} + B_e \Delta u_k + \delta_k \tag{6.3}$$

$$y_k = C_e x_{e,k} \tag{6.4}$$

where the control increment $\Delta u_k = u_k - u_{k-1}$ is used as an optimization variable and

$$x_{e,k} = \begin{bmatrix} x_k \\ u_{k-1} \end{bmatrix}; \delta_k = \begin{bmatrix} I \\ 0 \end{bmatrix} d_k; \tag{6.5}$$

$$A_e = \begin{bmatrix} A & B \\ 0 & I \end{bmatrix}; B_e = \begin{bmatrix} B \\ I \end{bmatrix}; C_e = \begin{bmatrix} C & 0 \end{bmatrix}. \tag{6.6}$$

It is assumed that the pair (A_e, B_e) is controllable.

6.1.2 Sliding Mode Control

The design procedure for the sliding mode control of discrete-time systems can be carried out in two steps. The first one involves the selection of a switching function

$$G_k = K x_{e,k} \tag{6.7}$$

where $rank(K) = n_u$. Note that $G_k = 0$ denotes a so-called sliding surface, also known as a sliding manifold, defining the system behaviour in a desired manner. In the second step, the discrete-time control signal Δu_k is selected such that the reaching and existence conditions of sliding mode are satisfied.

To determine the system dynamics in sliding mode, the equivalent control method is used [72, 73]. Starting with $G_{k+1} = K x_{e,k+1} = 0$, taking into account eq. (6.3), the equivalent control input signal is obtained in the form of

$$\Delta u^{eq}{}_k = -(KB_e)^{-1} K (A_e x_{e,k} + \delta_k). \tag{6.8}$$

Substituting eq. (6.8) into eq. (6.3), the system dynamics in sliding mode is defined by

$$x_{e,k+1} = (A_e - B_e (GB_e)^{-1} G A_e) x_{e,k}. \tag{6.9}$$

in the absence of any disturbance. If the system state is close to the sliding manifold, the equivalent control can drive the system along the sliding surface. However, since δ_k is not available, a one-step-delayed estimator obtained from eq. (6.3) as

$$\hat{\delta}_k = \delta_{k-1} = x_{e,k} - A_e x_{e,k-1} + B_e \Delta u_{k-1} \tag{6.10}$$

is usually utilized in design of Δu_k

$$\Delta u_k = -(KB_e)^{-1} K (A_e x_{e,k} + \hat{\delta}_k). \tag{6.11}$$

Substituting eq. (6.11) into eq. (6.3), using eq. (6.7), the switching function dynamics is described by

$$G_{k+1} = K(\delta_k - \delta_{k-1}). \tag{6.12}$$

This control approach belongs to the class of deadbeat controllers with some drawbacks. The control input signal defined by eq. (6.11) drives the system state to the sliding manifold at one sampling period T, so it may enter saturation because of its high calculated values. Therefore, the system dynamics in reaching mode is not defined at all. Oscillatory motion may also occur in perturbed systems (when the model used is in error) due to such large control input values, since the system is overcompensated and the system state crosses the sliding surface at the very next time instants. Finally, if the disturbance depends on the control input

$$\delta_k = \delta^*{}_k + (\Delta B_e)\Delta u_k \tag{6.13}$$

where ΔB_e represents the error in B_e and $\delta^*{}_k$ is independent of the control input, the system can either go unstable or produce chattering [63, 85]. In the latter case, the switching function dynamics is defined by

$$G_{k+1} = -K\Delta B_e(GB_e)^{-1}[2G_k - G_{k-1}] + O(T^2) \tag{6.14}$$

and for significant error in the control matrix ΔB_e, the poles of the equation (6.14) can be outside the unit disk in the z-plane. However, it is typically neither necessary nor optimal to force the system to reach the sliding mode at the very next instant. Therefore, in order to avoid high control input signals and to determine switching function dynamics in reaching mode, the additional control component is introduced into the control algorithm yielding

$$\begin{aligned} \Delta u_k = \; & - \; (KB_e)^{-1}K(A_e x_{e,k} + \hat{\delta}_k - x_{e,k} \\ & + \; \min\big(\,|G_k|\,, diag(\mathbf{K})\big)\mathrm{sgn}(G_k) \end{aligned} \tag{6.15}$$

and defining the switching function dynamics in the following form

$$\begin{aligned} G_{k+1} = G_k \; & - \; \min\big(\,|G_k|\,, diag(\mathbf{K})\big)\mathrm{sgn}(G_k) \\ & + \; K(\delta_k - \delta_{k-1}) \end{aligned} \tag{6.16}$$

where $\mathbf{K} \in \mathbb{R}^{n_u}$ is a gain vector. The control signal defined by eq. (6.15) will drive the system state to the sliding manifold in a finite number of sampling instants if

$$\mathbf{K} > \Delta \tag{6.17}$$

where

$$|K(\delta_k - \delta_{k-1})| < \Delta \tag{6.18}$$

and Δ is a positive vector [104].

Unfortunately, if the disturbance has the form of eq. (6.13), the system may become unstable in this case as well. In order to cope with the later issue and to incorporate and solve the problem of control signal saturation in SMC design, model predictive control (MPC) is used due to its ability to deal with constraints and stability problem caused by model error. In this chapter, unlike the algorithm described in [93], Laguerre functions based MPC is proposed to reduce the number of decision variables making the optimization problem smaller.

6.2 Predictive SMC based on Laguerre functions

The procedure for using Laguerre functions in the design of MPC is already described in section 5.2. The control increment is denoted as Δu and is defined by

$$\Delta u_{k+i} = {L_i}^T \ \eta_k \tag{6.19}$$

already defined in section 5.2. Herein will be shown how to introduce that approach in the PSMC design.

The PSMC based on the equivalent control method is considered first. The future values of the switching function can be obtained by extending eq. (6.7) within the prediction horizon as follows

$$\begin{aligned}
G_{k+1} &= Kx_{e,k+1} = K(A_e x_{e,k} + B_e \Delta u_k + \delta_k) \\
G_{k+2} &= Kx_{e_{k+2}} = K(A_e x_{e,k+1} + B_e \Delta u_{k+1} + \delta_{k+1}) \\
&= K({A_e}^2 x_{e,k} + A_e B_e \Delta u_k + A_e \delta_k + B_e \Delta u_{k+1}) \\
&\ \ \vdots \\
G_{k+N_p} &= Kx_{e_{k+N_p}} \\
&= K(A_e x_{e,k+N_p-1} + B_e \Delta u_{k+N_p-1} + \delta_{k+N_p-1}) \\
&= K({A_e}^{N_p} x_{e,k} + \sum_{i=0}^{N_p-1} {A_e}^i B_e \Delta u_{k+N_p-i-1}) \\
&+ K \sum_{i=0}^{N_p-1} {A_e}^i \delta_{k+N_p-i-1}
\end{aligned} \tag{6.20}$$

Substituting eq. (6.19) into eq. (6.20) one obtain the prediction of the future switching

function as

$$\begin{aligned} G_{k+m} &= K{A_e}^m x_{e,k} + K(\sum_{i=0}^{m-1} A_e^{m-i-1} B_e {L_i}^T)\eta_k \\ &+ K(\sum_{i=0}^{m-1} {A_e}^i \delta_{k+m-i-1}). \end{aligned} \tag{6.21}$$

The design goal is to find optimal η_k by minimising a cost function

$$J = \sum_{m=1}^{N_p} {G_{k+m}}^T G_{k+m} + {\eta_k}^T R \eta_k \tag{6.22}$$

subject to the constraints defined by eq. (5.20), where $R > 0$ is a weighting matrix. The control input increment Δu_k is then calculated using eq. (6.19). Unfortunately, the latter control input does not define the system dynamics in reaching mode. That is why PSMC, based on the control approach described by eq. (6.15), is considered in the sequel.

One should expand the difference $\Delta G_{k+m} = G_{k+m} - G_{k+m-1}$ in the prediction horizon ($m = \overline{1, N_p}$) first. This gives

$$\begin{aligned} \Delta G_{k+1} &= K x_{e,k+1} - K x_{e,k} + K\delta_k \\ &= K(A_e - I)x_{e,k} + K B_e \Delta u_k + K\delta_k \\ \Delta G_{k+2} &= K x_{e_{k+2}} - K x_{e,k+1} \\ &= K(A_e x_{e,k+1} + B_e \Delta u_{k+1} + \delta_{k+1}) \\ &- K(A_e x_{e,k} + B_e \Delta u_k + \delta_k) \\ &= K(A_e - I)A_e x_{e,k} + K(A_e - I)B_e \Delta u_k \\ &+ K B_e \Delta u_{k+1} + K(A_e - I)\delta_k + K\delta_{k+1} \\ &\cdot \\ &\cdot \\ &\cdot \end{aligned}$$

$$
\begin{aligned}
&\vdots \\
&\vdots \\
&\vdots \\
\Delta G_{k+N_p} &= K x_{e_{k+N_p}} - K x_{e_{k+N_{p-1}}} \\
&= K(A_e - I) {A_e}^{N_{p-1}} x_{e,k} \\
&+ K \sum_{i=0}^{N_p-1} {A_e}^i B_e \Delta u_{k+N_p-i-1} \\
&- K \sum_{i=0}^{N_p-2} {A_e}^i B_e \Delta u_{k+N_p-i-2} \\
&+ K \sum_{i=0}^{N_p-1} {A_e}^i \delta_{k+N_p-i-1} \\
&- K \sum_{i=0}^{N_p-2} {A_e}^i \delta_{k+N_p-i-2}
\end{aligned} \tag{6.23}
$$

Substituting eq. (6.19) into eq. (6.23), the latter equation can be rewritten as

$$
\begin{aligned}
\Delta G_{k+m} &= K(A_e - I) {A_e}^{m-1} x_{e,k} \\
&+ K \sum_{i=0}^{m-1} A_e^{m-i-1} B_e {L_i}^T \eta_k \\
&- K \sum_{i=0}^{m-2} A_e^{m-i-2} B_e {L_i}^T \eta_k \\
&+ K \sum_{i=0}^{m-1} {A_e}^i \delta_{k+m-i-1} \\
&- K \sum_{i=0}^{m-2} {A_e}^i \delta_{k+m-i-2}.
\end{aligned} \tag{6.24}
$$

within the prediction horizon. Now, the desired control should be calculated by minimizing the cost function

$$
\begin{aligned}
J = \sum_{m=1}^{N_p} \Big(\Delta G_{k+m} &+ \min\big(|G_k|, diag(\mathbf{K})\big)\mathrm{sgn}(G_k) \Big)^T \\
&\Big(\Delta G_{k+m} + \min\big(|G_k|, diag(\mathbf{K})\big)\mathrm{sgn}(G_k) \Big) \\
&+ {\eta_k}^T R \eta_k
\end{aligned} \tag{6.25}
$$

with respect to η_k and subject to the constraints described by eq. (5.20). Again, the control input increment Δu_k is calculated using eq. (6.19).

Notice that, if $R = 0$, the minimization of eq. (6.25) will lead to the predictive model of switching function dynamics defined by eq. (6.16), represented in the following form

$$\begin{aligned} G_{k+m+1} = G_{k+m} \quad &- \quad \min\left(|G_k|, diag(\mathbf{K})\right)\mathrm{sgn}(G_k) \\ &+ \quad K(\delta_{k+m} - \delta_{k+m-1}) \end{aligned} \tag{6.26}$$

for $m = \overline{2, N_p}$. If $\mathbf{K}$ is selected according to eq. (6.17), the sliding manifold will be reached in a finite time within the prediction horizon [4]. By choosing an input weight $R > 0$ of significant magnitude, the stability problem is solved in presence of the disturbance depending on the control input signal.

The both optimization problems, defined by eqs. (6.22) and (6.25), can be handled by a number of optimization routines [103]. The one used herein, which includes the Kuhn-Tucker conditions [105], together with Hildreth's algorithm [106], is described in detail in [107].

6.3 Experimental results

The modular servo system [100] is used for the demonstration of proposed control algorithms. The transfer function of the DC servo system is

$$G(s) = \frac{\theta(s)}{u(s)} = \frac{K_s}{s(T_s s + 1)} \tag{6.27}$$

where $K_s = 184.95$ rad/s, $T_s = 0.9$ s, and the system states are angular position $\theta = x_1$, and angular velocity $\omega = x_2$. It is assumed that the control signal is dimensionless scaled input voltage, $u(t) = v(t)/v_{\max}$ where $v_{\max} = 12$ V which satisfies $|u(t)| \leq 1$.

The discretization is done using Matlab function *c2d.m*, with the sampling time $T = 0.01s$, and the following augmented state-space model is obtained

$$A_e = \begin{bmatrix} 1 & 0.0099 & 0.0102 \\ 0 & 0.9890 & 2.0437 \\ 0 & 0 & 1 \end{bmatrix} \quad ; \quad B_e = \begin{bmatrix} 0.0102 \\ 2.0437 \\ 1 \end{bmatrix} ; C_e = \begin{bmatrix} 0 \\ 0 \\ 1 \end{bmatrix}^T .$$

The parameters for design of the Laguerre functions based PSMC described in Section 6.2 are: the prediction horizon $N_p = 30$, the number of Laguerre terms $N = 5$, Laguerre functions parameter $a = 0.15$, the switching function parameter

$$K = [-0.0358 \quad -0.0071 \quad 0]. \tag{6.28}$$

Notice that the proposed approach uses four times less parameters in comparison to traditional MPC [4] and, consequently, provides that the optimization problem is smaller.

The reference signal r is defined by

$$r = \begin{cases} 0 & \text{if Time} < 0.5s \\ 40 & \text{if } 0.5s \leq \text{Time} \leq 5s \\ 0 & \text{if Time} > 5s \end{cases} . \tag{6.29}$$

The constraints on the control signal and its increment are defined as

$$-1 \leq u_k \leq 1; \quad -0.2 \leq \Delta u_k \leq 0.2. \tag{6.30}$$

The first type of proposed PSMC based on equivalent control is applied to the DC servo system and two experiments are conducted in order to compare the performance of the system with and without the one-step-delayed estimator. The results are shown in Figs. 6.1 and 6.2. It can be seen that the steady state accuracy is better when the one-step-delayed estimator is used in the design of the proposed control law.

The control signals, Figs. 6.3 and 6.4, and the corresponding control increments, Figs. 6.5 and 6.6, respect the constraints defined by eq. (6.30) in both cases. One can notice that in the steady state, the control signal is not equal to zero. That happens because of the Coulomb friction and it is in the range of control signal from -0.15 to 0.15. From the previous set of experiments, it is concluded that the one-step-delayed disturbance estimator is needed to improve the system response accuracy.

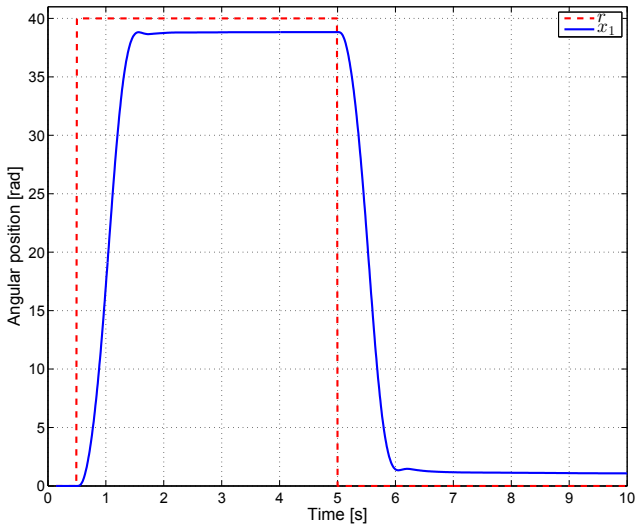

Figure 6.1: The angular position x_1 for PSMC based on equivalent control method (without the one-step-delayed estimator).

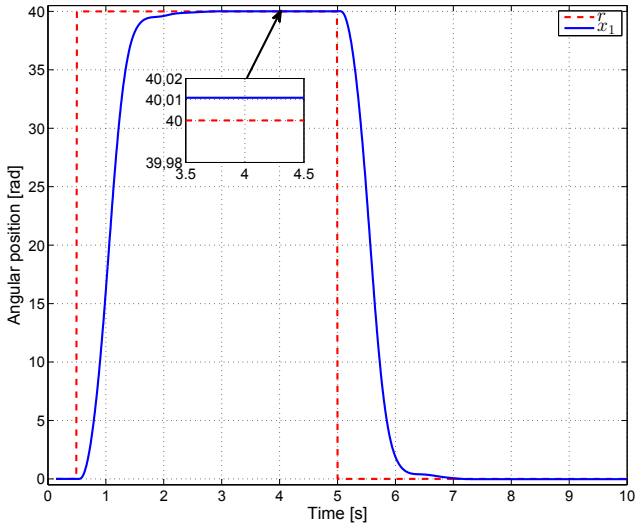

Figure 6.2: The angular position x_1 for PSMC based on equivalent control method (with the one-step-delayed estimator).

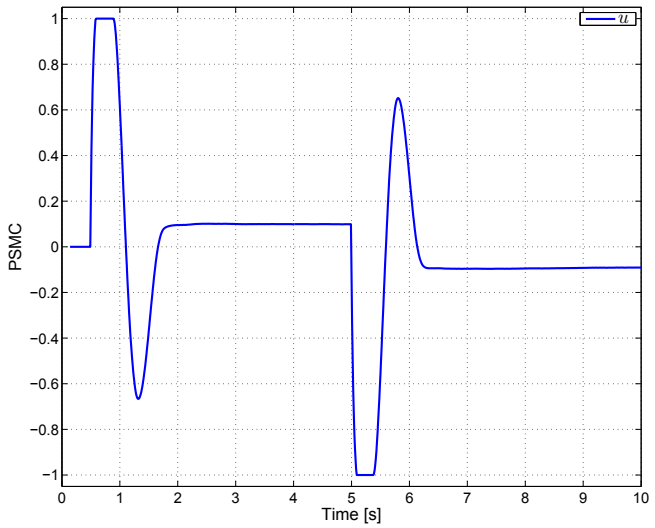

Figure 6.3: PSMC u based on equivalent control method (without the one-step-delayed estimator).

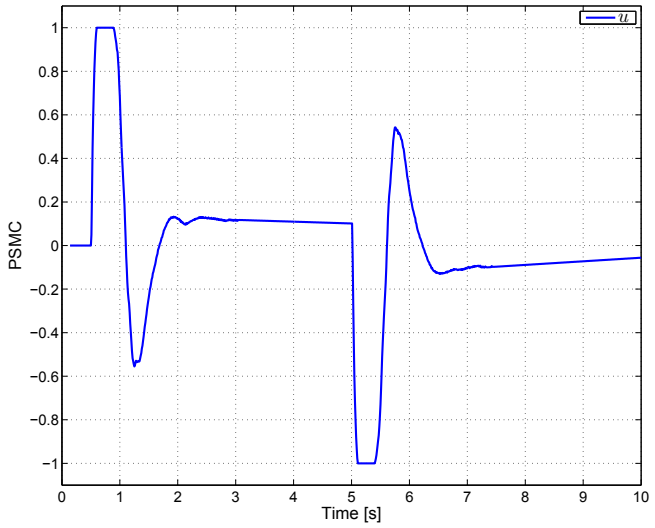

Figure 6.4: PSMC u based on equivalent control method (with the one-step-delayed estimator).

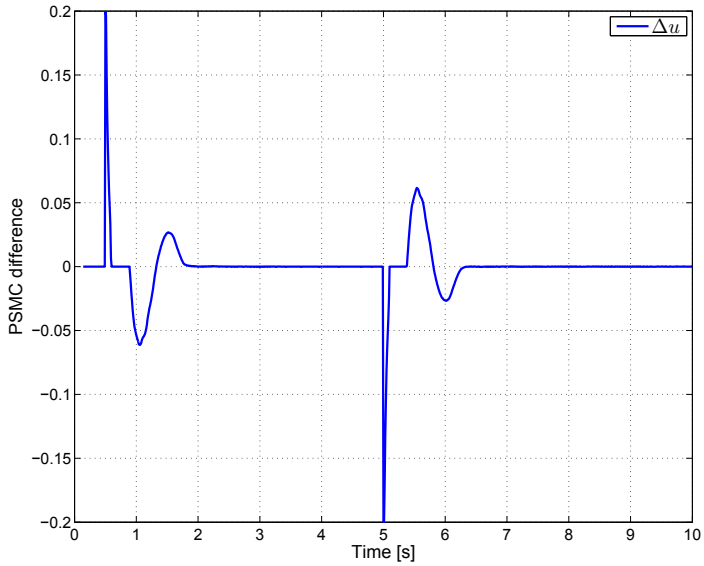

Figure 6.5: PSMC increment Δu based on equivalent control method (without the one-step-delayed estimator).

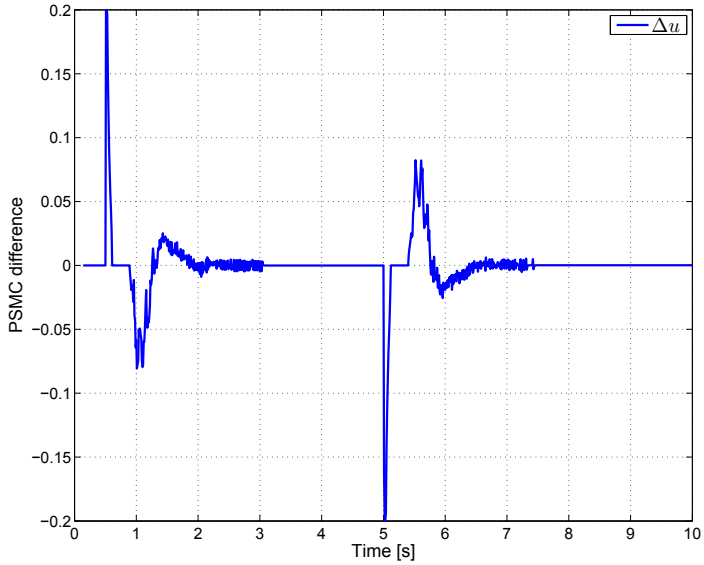

Figure 6.6: PSMC increment Δu based on equivalent control method (with the one-step-delayed estimator).

Then, the second type of PSMC, with the additional SMC term in the form of $\min\left(|G_k|, diag(\mathbf{K})\right)\text{sgn}(G_k)$ is implemented. In the first experiment, the second type of PSMC without the estimator is used to demonstrate the ability of additional control term to reject the disturbance as good as in the case when the PSMC based on the discrete-time equivalent control with the estimator is implemented. The additional control component parameter value was $\mathbf{K} = 0.1$. The system output response is depicted in Fig. 6.7. In the next experiment, the second type of PSMC is used with the estimator providing the zero steady-state error, which is presented in Fig. 6.8. The constraints, defined by eq. (6.30), are respected by the control signal and its increment, which is shown in Figs. 6.9 - 6.12, respectively.

In order to show the effectiveness of the proposed PSMC, two additional experiments are performed. It is demonstrated how the choice of the tuning parameter R affects the robustness of the closed loop. The PSMC is using a model where the value of B matrix is 40 % larger than the true value. Fig. 6.13 shows that the system is unstable with the tuning factor $R = 0.1$, while in Fig. 6.14 it is stable and has good performance when choosing $R = 10$. Next two figures illustrate system robustness when the additional SMC term is used. Stable system with the oscillations in the output response with $R = 0.001$ is presented in Fig. 6.15. In order to suppress the oscillations, tuning factor is chosen to be $R = 0.1$, which is demonstrated in Fig. 6.16.

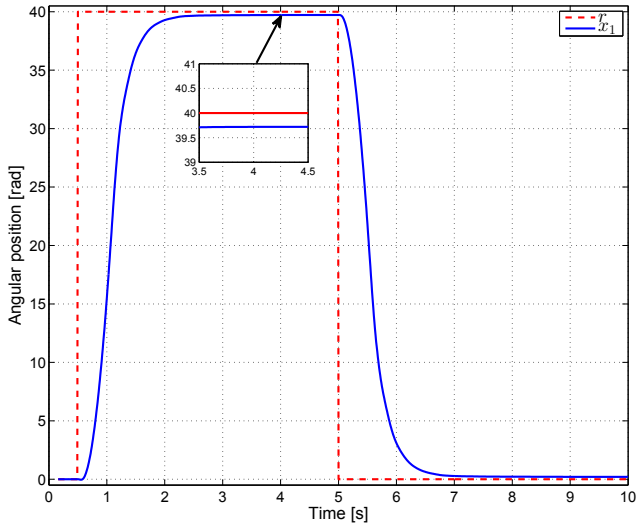

Figure 6.7: The angular position x_1 for PSMC with the additional SMC term ($\mathbf{K} = 0.1$, $R = 10$, without the one-step-delayed estimator).

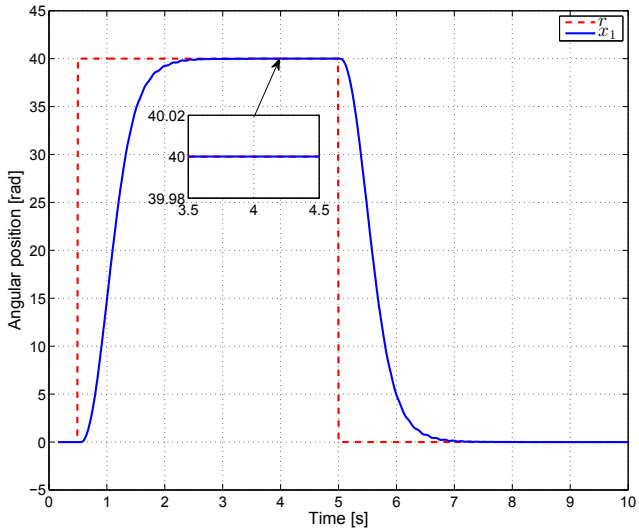

Figure 6.8: The angular position x_1 for PSMC with the additional SMC term ($\mathbf{K} = 0.1$, $R = 10$, with the one-step-delayed estimator).

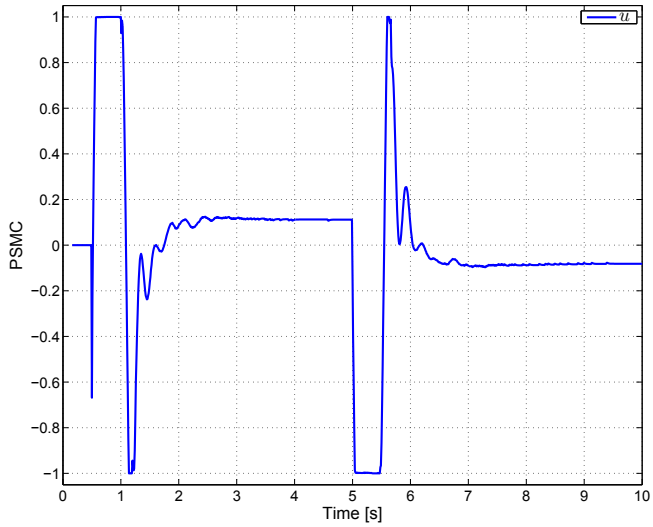

Figure 6.9: PSMC with the additional SMC term ($\mathbf{K} = 0.1$, $R = 10$, without the one-step-delayed estimator).

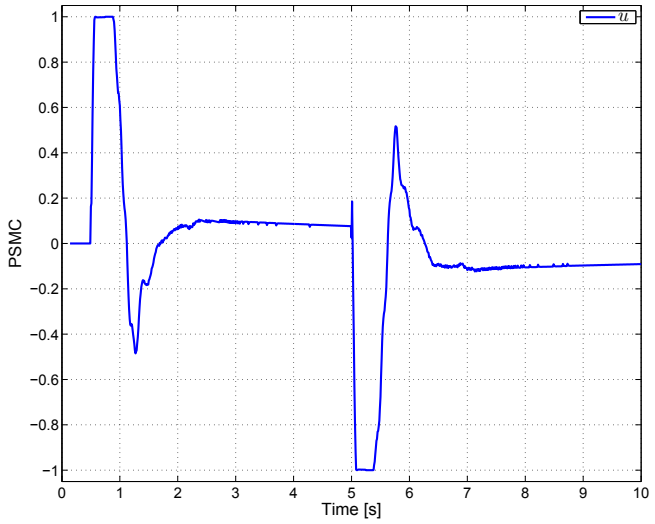

Figure 6.10: PSMC with the additional SMC term
($\mathbf{K} = 0.1$, $R = 10$, with the one-step-delayed estimator).

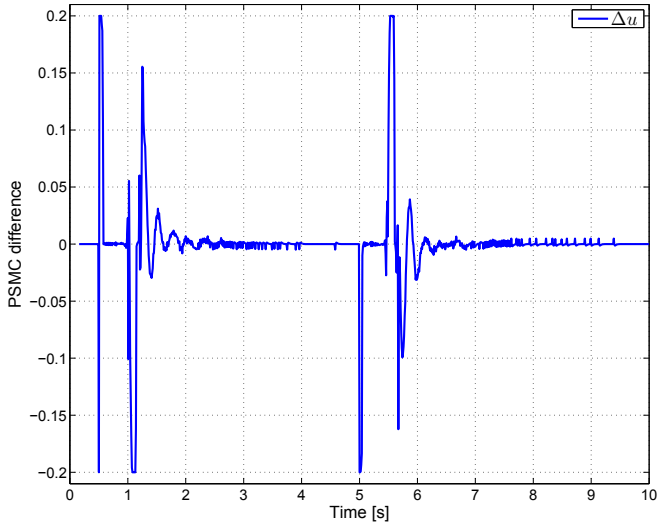

Figure 6.11: PSMC increment with the additional SMC term
($\mathbf{K} = 0.1$, $R = 10$, without the one-step-delayed estimator).

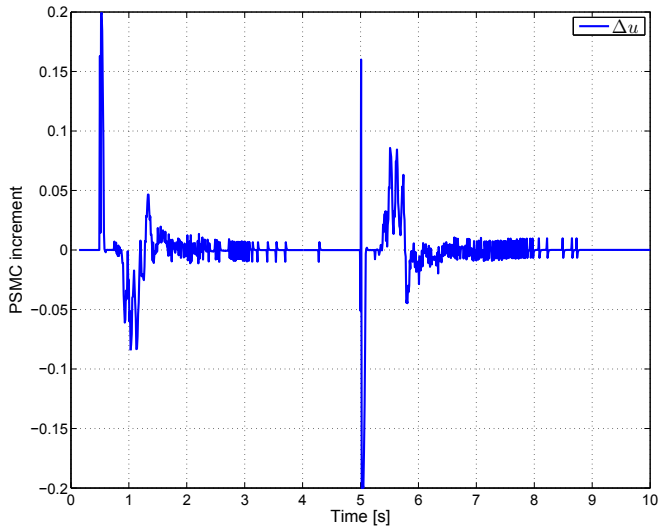

Figure 6.12: PSMC increment with the additional SMC term ($\mathbf{K} = 0.1$, $R = 10$, with the one-step-delayed estimator).

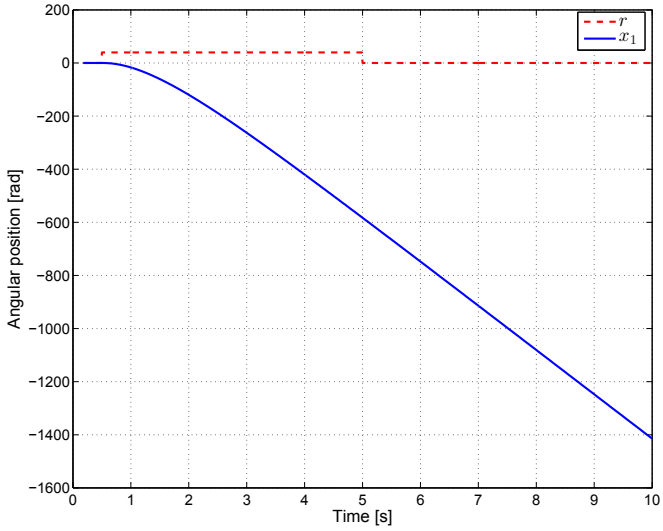

Figure 6.13: The angular position x_1 for PSMC based on equivalent control (perturbed system; $\mathbf{K} = 0.1$, $R = 0.1$, with the one-step-delayed estimator).

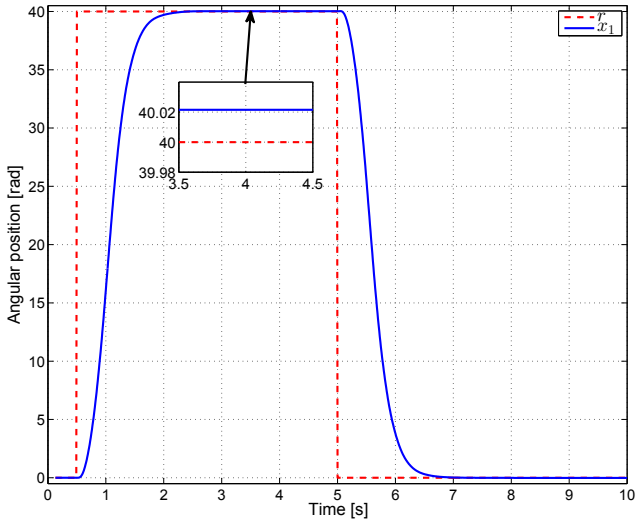

Figure 6.14: The angular position x_1 for PSMC with the additional SMC term ($\mathbf{K} = 0.1$, $R = 10$, with the one-step-delayed estimator).

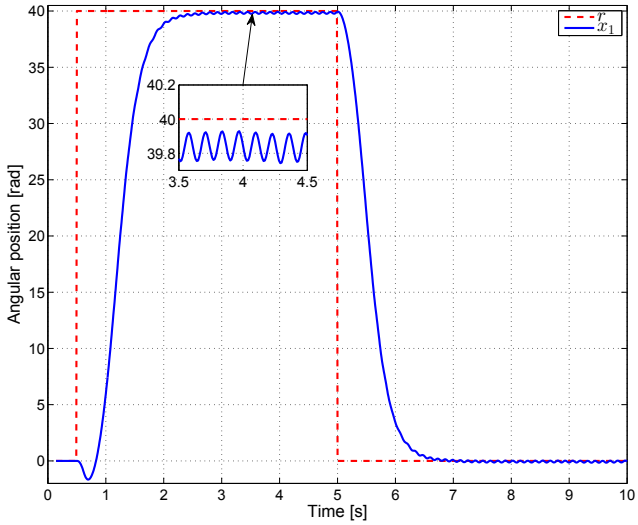

Figure 6.15: The angular position x_1 for PSMC with the additional SMC term (perturbed system; $\mathbf{K} = 0.1$, $R = 0.001$, with the one-step-delayed estimator).

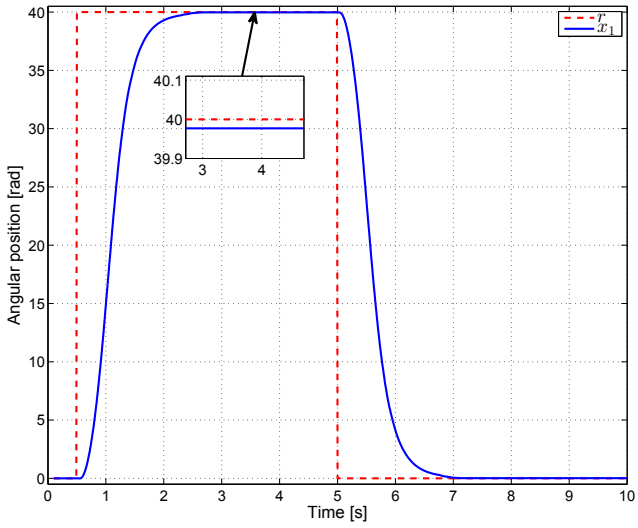

Figure 6.16: The angular position x_1 for PSMC with the additional SMC term ($\mathbf{K} = 0.1$, $R = 0.1$, with the one-step-delayed estimator).

6.4 Conclusion

In this chapter, an approach to design of Predictive Sliding Mode Control (PSMC) based on Laguerre functions has been studied. Two PSMC algorithms are presented [1]. The first one came from the discrete-time equivalent control method approach, which belongs to the class of deadbeat control laws and implies that the reaching law is not defined at all. The second one is based on the chattering free reaching law method resulting in the control signal with an additional Sliding Mode Control (SMC) component as proposed by [59]. In that way, the system dynamics under the reaching law is fully determined and the system robustness is improved. By using the Laguerre functions for PSMC, the online optimization problem is smaller and possibly can be solved faster compared to the traditional Model Predictive Control (MPC) approach. The constraints on control input signal and its increment are incorporated, which is impossible to achieve with traditional SMC. The stability problem of SMC, which may arise when the disturbance depends on the control input signal, is overcome by using a sufficiently large weight R. Improved system steady-state accuracy is achieved by introducing the one-step-delayed disturbance estimator in the proposed control algorithms, in order to reduce the effects of system nonlinearities and disturbances further. This combination of MPC and SMC is demonstrated by experimental results.

[1] All files for the controllers design can be found on http://automatika.elfak.ni.ac.rs/mspasic/

Chapter 7

Summary and future work

This chapter provides the summary inferred based on the work presented in this thesis. Additionally, Chapter 7 includes possible suggestions for future work for the presented control framework.

7.1 Conclusions

The work presented in this thesis is focused on the development of new control algorithms that provide the key properties of two different control methodologies. The reason for focusing on MPC and SMC was to obtain a robust controller that can be used in real-time, cope with defined constraints, and does not have prohibitive calculation requirements.

In the method presented in Chapter 3, an improved control system robustness is achieved using GPC in combination with SMC. GPC has been used as a replacement for the so-called equivalent control method within the traditional SMC approaches, which provides improved control system robustness.

TMPC with SMC as an auxiliary controller has been presented in Chapter 4. The original TMPC formulation has been used to emphasize the effect of SMC, as a low calculation demanding auxiliary controller, on the robustness properties of the controlled system. The procedure for calculation of constraints tightening is also given. Both SMC control laws, the traditional and chattering-free ones, are used in order to represent the proposed SMC control components.

Introducing the discrete-time Laguerre functions in the design of MPC was presented in Chapter 5. This chapter shows a way of implementation of the orthogonal-based functions in the design of MPC. That provides a smaller number of the MPC design parameters, which could affect the reduced computational burden when the large prediction horizon is needed.

Chapter 6 represents the PSMC approach that uses Laguerre functions in the de-

sign of the controller. In order to obtain improved system robustness and steady-state accuracy, the one-step delayed disturbance estimator has also been included, which additionally affects better system response and its robustness.

Simulation and real-time experimental results corroborate the theoretical background of all presented control algorithms.

7.2 Future work

The main drawback within SMC is a chattering phenomenon. In this thesis, so-called boundary layer control has been used for the reduction of a chattering. One idea for future improvements of presented algorithms can be realized by comparing these algorithms with the ones where the SMC component is of a higher order. Higher-order SMC is known as a method which is able to reduce the chattering effect while maintaining good stability properties. Another approach can be realized using integral sliding mode control (ISMC), which provides an "ideal" SMC and robustness of the controlled system since the initial time instant.

Orthogonal functions are widely used in the control systems and system identification area. The main advantage of introducing Laguerre functions for the design of the controller based on the orthogonal functions refers to the simplicity of the design procedure. Possible future work will be directed to employing some other orthogonal based functions in the design of MPC. The idea lies in opportunity for using complex poles, besides the real ones (as it is the case with Laguerre functions), in their structures. This approach will require a little more effort when it comes to programming, but it can allow more efficient tuning of the controller for obtaining the desired closed-loop system response.

Another direction for future work is to adapt the presented algorithms for its implementation on Arduino and programmable logic controller (PLC) platforms. This will make the used approaches available in an educational setting.

Appendix A

Proof of Theorem 4.2.1

The vector sequence $(g_k, g_{k+1}, \ldots, g_{k+i}, \ldots)$, denoted by (g_{k+i}), converges point-wise to the limit $g \in \mathbb{R}^{n_u}$ if each element of g_{k+i} converges to the corresponding element in g. In other words, (g_{k+i}) is convergent if $\lim g_{k+i} = g$, i.e. if for every real vector $\epsilon > \mathbf{0}$ there exists the natural number $N_u(\epsilon)$, such that

$$|g_{k+i} - g| < \epsilon, \quad \forall i > N_u(\epsilon) \tag{A.1}$$

(g_{k+i}) is the positive (negative) vector sequence if $g_{k+i} \geq \mathbf{0}$ $(g_{k+i} \leq \mathbf{0})$ for $i = 0, 1, 2, \ldots$. For multiple-input systems, it is probable that the elements of vector g_k have different signs, as they represent the switching functions of SMC inputs. After splitting the vector g_k onto two sub vectors g_k^+ and g_k^- with separated positive and negative elements of g_k, respectively, eq. (4.17) can be rewritten as

$$g_{k+i+1}^+ = g_{k+i}^+ - \Delta_u^+ \mathrm{sgn}(g_{k+i}^+) + (KE)^+ w_{k+i}^+ \tag{A.2}$$

$$g_{k+i+1}^- = g_{k+i}^- - \Delta_u^- \mathrm{sgn}(g_{k+i}^-) + (KE)^- w_{k+i}^- \tag{A.3}$$

where Δ_u^+ , Δ_u^- ,$(KE)^+$,$(KE)^-$, w_{k+i}^+ and w_{k+i}^- are diagonal matrices and sub vectors obtained from Δ_u , KE and w_{k+i} by extraction. Similarly, the theorem's condition given in eq. (4.18) can be expressed by

$$\Delta_u^+ \underline{1} > \Omega^+ > max|(KE)^+ w_k^+| \tag{A.4}$$

$$\Delta_u^- \underline{1} > \Omega^- > max|(KE)^- w_k^-| \tag{A.5}$$

and the domain G defined by eq. (4.19) as

$$G = G^+ \cup G^- \tag{A.6}$$

with

$$G^+ = \{g_{k+i}^+ : |g_{k+i}^+| < \Delta_u^+ \underline{1} + \Omega^+\} \tag{A.7}$$

$$G^- = \{g_{k+i}^- : |g_{k+i}^-| < \Delta_u^- \underline{1} + \Omega^-\} \tag{A.8}$$

It is obvious that (g^+_{k+i}) and (g^-_{k+i}), defined by eq. (A.2), are positive and negative sequences, respectively.

Let us prove now that (g^+_{k+i}) enters the domain G^+ in finite time for $k_0 \leq i \leq N$ and remains in that area. The proof is similar in the case of (g^-_{k+i}) with respect to G^-. If eq. (A.4) is true, then

$$\begin{aligned} g^+_{k+i+1} - g^+_{k+i} &= -\Delta^+_u \mathrm{sgn}(g^+_{k+i}) + (KE)^+ w^+_{k+i} \\ &< -\Delta^+_u \underline{1} + \Omega^+ < \mathbf{0} \end{aligned} \tag{A.9}$$

and $g^+_{k+i+1} < g^+_{k+i}$ so there exists a positive diagonal matrix

$$Q_{k+i} = diag\{q^1_{k+i} \quad q^2_{k+i} \quad \dots \quad q^{n^+_u}_{k+i}\}, \tag{A.10}$$

$$(0 < q^j_{k+i} < 1, j = 1, 2, \dots, n^+_u, n^+_u + n^-_u = n_u) \tag{A.11}$$

such that

$$g^+_{k+i+1} = Q_{k+i} g^+_{k+i}, \quad Q_{k+i} < I \tag{A.12}$$

where g^+_{k+i} and g^-_{k+i+p} $(p \in N)$ can be written as

$$g^+_{k+i} = \left(\prod_{j=k}^{k+i-1} Q_j \right) g^+_k \tag{A.13}$$

$$g^+_{k+i+p} = \left(\prod_{j=k}^{k+i+p-1} Q_j \right) g^+_k \tag{A.14}$$

giving the following inequality $(\epsilon > \mathbf{0})$

$$\begin{aligned} &|g^+_{k+i+p} - g^+_{k+i}| \\ &= \left| \left(\prod_{j=k}^{k+i-1} Q_j \right) \left(\left(\prod_{l=k+i}^{k+i+p-1} Q_l \right) - I \right) g^+_k \right| < \epsilon \end{aligned} \tag{A.15}$$

According to Cauchy's theorem, the convergence of vector sequence (g_{k+i}), satisfying eq. (A.15), is proved. Its convergence domain is

$$\overline{G}^+ = \{g^+_{k+i} : |g^+_{k+i}| > \Delta^+_u \underline{1} + \Omega^+\} \tag{A.16}$$

directly satisfying eq. (A.12).

Let us now show that system trajectory enters the domain G^+ in finite time. The sequence (g^+_{k+i}) converges inside domain $\overline{G}^+$, so it is limited and $\lim_{i \to \infty} g^+_{k+i} = g^+_\infty$. Assume that $g^+_k > \Delta^+_u \underline{1} + \Omega^+$. According to eq. (A.2)

$$g^+_{k+i} = g^+_k - \sum_{j=0}^{k+i-1} (\Delta^+_u \underline{1} - (KE)^+ w^+_{k+j}). \tag{A.17}$$

Suppose that g^+_{k+i} never enters the domain G^+. For $i \to \infty$, we obtain

$$\sum_{j=0}^{\infty}(\Delta^+_u \underline{1} - (KE)^+ w^+_{k+j}) < g^+_k - \Delta^+_u \underline{1} - \Omega^+. \tag{A.18}$$

Equation (A.18) implies that the vector series

$$\sum_{j=0}^{\infty}(\Delta^+_u \underline{1} - (KE)^+ w^+_{k+j})$$

is convergent, and its general element $\Delta^+_u \underline{1} - (KE)^+ w^+_{k+j}$ converges to zero as $j \to \infty$, i.e.

$$\Delta^+_u \underline{1} = \lim_{j\to\infty}\left((KE)^+ w^+_{k+j}\right) \tag{A.19}$$

that contradicts eq. (A.4), and the initial assumption that g^+_{k+i} never enters the domain G^+ is false. Moreover, g^+_{k+i} enters the domain G^+ at time instant k_0 which is bounded by the maximal element of vector

$$\overline{k_0} = int\left(\left((\Delta^+_u \underline{1} - \Omega^+)I\right)^{-1}\left(|g^+_k| - \Delta^+_u \underline{1} - \Omega^+\right)\right) + \underline{1} \tag{A.20}$$

It is obvious that the length of the prediction horizon N should be greater than k_0 and selected in accordance with eq. (A.20).

We will now show that for every $k_0 < i < N$, g^+_{k+i} remains in the domain G^+. Let $s_{k+k_0} \in G^+_+ = \{g^+_{k+i} : 0 < g^+_{k+i} < \Delta^+_u \underline{1} + \Omega^+\}$. Then, according to eq. (A.2), we have

$$\begin{aligned} -\Delta^+_u \underline{1} - \Omega^+ &\underset{(A.4)}{<} -\Delta^+_u \underline{1} + (KE)^+ w^+_{k+k_0} \\ &\underset{(A.4)}{<} g^+_{k+k_0} - \Delta^+_u \underline{1} + (KE)^+ w^+_{k+k_0} \\ &= g^+_{k+k_0+1} \underset{(A.4)}{<} 2\Omega^+ < \Delta^+_u \underline{1} + \Omega^+ \end{aligned} \tag{A.21}$$

and thus g^+_{k+i} does not leave the domain G^+. This is also true when $g^+_{k+k_0} \in G^+_- = \{g^+_{k+i} : -\Delta^+_u \underline{1} - \Omega^+ < g^+_{k+i} < 0\}$ since

$$\begin{aligned} -\Delta^+_u \underline{1} - \Omega^+ &\underset{(A.4)}{<} -2\Omega^+ \\ &\underset{(A.4)}{<} -\Omega^+ + (KE)^+ w^+_{k+k_0} \\ &\underset{(A.4)}{<} -\Delta^+_u \underline{1} - \Omega^+ + \Delta^+_u \underline{1} \\ &+ (KE)^+ w^+_{k+k_0} \\ &\underset{(A.4)}{<} g^+_{k+k_0+1} = g^+_{k+k_0} + \Delta^+_u \underline{1} \\ &+ (KE)^+ w^+_{k+k_0} \\ &\underset{(A.4)}{<} \Delta^+_u \underline{1} + \Omega^+ \end{aligned} \tag{A.22}$$

The case $g^+_{k+k_0+1} < 0$ and $g^+_{k+k_0+1} \notin G^+$ for g^+_k, $g^+_{k+k_0} > \Delta^+_u \underline{1} + \Omega^+$ is not possible since

$$\begin{aligned} g^+_{k+k_0+1} &= g^+_{k+k_0} - \Delta^+_u \underline{1} \\ &+ (KE)^+ w^+_{k+k_0} \\ &> \Omega^+ + (KE)^+ w^+_{k+k_0} > 0. \end{aligned} \tag{A.23}$$

Similarly, the case $g^+_{k+k_0+1} > 0$ and $g^+_{k+k_0+1} \notin G^+$ for g^+_k, $g^+_{k+k_0} < -\Delta^+_u \underline{1} - \Omega^+$ cannot happen as

$$\begin{aligned} g^+_{k+k_0+1} &= g^+_{k+k_0} + \Delta^+_u \underline{1} \\ &+ (KE)^+ w^+_{k+k_0} \\ &< -\Omega^+ + (KE)^+ w^+_{k+k_0} < 0. \end{aligned} \tag{A.24}$$

Therefore, we have proven that $g^+_{k+k_0+1} \in G^+$ and, by induction, the latter can be generalized to

$$g^+_{k+k_0+m} \in G^+, \tag{A.25}$$

for every $m > 0$. The sign of g_k may change at each time step, causing the chattering in that way, but g_k will stay in G^+. Having demonstrated that eq. (A.25) is satisfied if eq. (A.4) is valid, the proof ends.

Appendix B

Proof of Theorem 4.2.2

Assume that $g_k \notin G$. Then, eq. (4.22) becomes eq. (5.29) and the proof is similar to the one discussed in Appendix A. This means that $g_{k+k_0} \in G$ where k_0 is determined by eq. (A.20). Let g_k^j be the j^{th} element of g_k and assume that corresponding element $(KEw_{k+k_0})^j < 0$. Then

$$\begin{aligned} g_{k+k_0+1}^j &= g_{k+k_0}^j - \delta_u^j - |(KEw_{k+k_0})^j| \\ &< \Omega^j - |(KEw_{k+k_0})^j| \\ &< \delta_u^j - |(KEw_{k+k_0})^j| \\ &< \delta_u^j \end{aligned} \tag{B.1}$$

where δ_u^j and Ω^j are the j^{th} elements in the diagonal of Δ_u and in vector Ω, respectively . Then, from eqs. (B.1) and (4.22) we have

$$g_{k+k_0+1}^j = (KEw_{k+k_0})^j \in G^j \tag{B.2}$$

If $(KEw_{k+k_0})^j > 0$, g_{k+i}^j will continue to decrease and, after k_1 time instants

$$k_1 = int\big((\delta_u^j + \Omega^j)^{-1}(\delta_u^j - \Omega^j)\big) + 1 \tag{B.3}$$

$g_{k+k_0+k_1}^j \in \{g_{k+i}^j : -\delta_u^j - \Omega^j < g_{k+i}^j < 0\}$ and

$$\begin{aligned} g_{k+k_0+k_1+1}^j &= g_{k+k_0+k_1}^j + \delta_u^j \\ &+ |(KEw_{k+k_0+k_1})^j| \\ &> -\Omega^j + |(KEw_{k+k_0+k_1})^j| \\ &> -\delta_u^j + |(KEw_{k+k_0+k_1})^j| \\ &> -\delta_u^j \end{aligned} \tag{B.4}$$

Meanwhile, if $KEw_i < 0$ for some $i > k + k_0$ then eqs. (B.1) and (B.2) stand. It is implied by eqs. (B.4) and (4.22) that, from $i = k_0 + k_1$

$$g_{k+k_0+k_1+1}^j = (KEw_{k+k_0+k_1})^j \in G^j \tag{B.5}$$

From eqs. (B.2) and (B.5) we have that once g_k enters G, it will stay in it, i.e.

$$g_{k+i+1} = KEw_{k+i} \in G \tag{B.6}$$

and, therefore, there is no chattering in sliding mode.

References

[1] J. B. Rawlings and D. Q. Mayne, *Model Predictive Control: Theory and Design*. Nob Hill Publishing, Madison, Wisconsin, USA, 2009.

[2] D. Mitić, "Digital variable structure control systems based on input-output models (in Serbian)," Ph.D. dissertation, University of Nis, Faculty of Electronic Engineering, 2006.

[3] D. Mitić, M. Spasić, M. Hovd, and D. Antić, "An approach to design of sliding mode based generalized predictive control," in *2013 IEEE 8th International Symposium on Applied Computational Intelligence and Informatics (SACI)*, May 2013, pp. 347–351.

[4] M. Spasić, M. Hovd, D. Mitić, and D. Antić, "Tube model predictive control with an auxiliary sliding mode controller," *Modeling, Identification and Control*, vol. 37, pp. 181–193, 2016.

[5] M. Spasić, D. Mitić, M. Hovd, and D. Antić, "Tube model predictive control based on laguerre functions with an auxiliary sliding mode controller," in *2017 IEEE 15th International Symposium on Intelligent Systems and Informatics (SISY)*, Sept 2017, pp. 000 243–000 248.

[6] M. Spasić, D. Mitić, M. Hovd, and D. Antić, "Predictive sliding mode control based on laguerre functions," *Journal of Control Engineering and Applied Informatics*, vol. 21, no. 1, pp. 12–20, March 2019.

[7] R. E. Kalman, "On the general theory of control systems," in *Proceedings of the First International Congress on Automatic Control*, 1960, pp. 481–493.

[8] R. E. Kalman, "A new approach to linear filtering and prediction problems," *Transactions of ASME, Journal of Basic Engineering*, vol. 87, no. 1, pp. 35–45, March 1960.

[9] H. Kwakernaak and R. Sivan, *Linear Optimal Control Systems*. Wiley, 1972.

[10] J. Richalet, A. Rault, J. Testud, and J. Papon, "Model predictive heuristic control: Applications to industrial processes," *Automatica*, vol. 14, no. 5, pp. 413 – 428, 1978. [Online]. Available: http://www.sciencedirect.com/science/article/pii/0005109878900018

[11] C. R. Cutler and B. L. Ramaker, "Dynamic matrix control??a computer control algorithm," *Joint Automatic Control Conference*, vol. 17, p. 72, 1980.

[12] P. Lunström, J. Lee, M. Morari, , and S. Skogestad, "Limitations of dynamic matrix control," *Comp. Chem. Engng.*, vol. 4, no. 19, pp. 409–421, 1995.

[13] R. Shridhar and D. J. Cooper, "A novel tuning strategy for multivariable model predictive control," *ISA Transactions*, vol. 36, no. 4, pp. 273 – 280, 1997. [Online]. Available: http://www.sciencedirect.com/science/article/pii/S0019057897000360

[14] J. B. Rawlings and K. R. Muske, "The stability of constrained receding horizon control," *IEEE Transactions on Automatic Control*, vol. 38, no. 10, pp. 1512–1516, Oct 1993.

[15] A. Al-Ghazzawi, E. Ali, A. Nouh, and E. Zafiriou, "On-line tuning strategy for model predictive controllers," *Journal of Process Control*, vol. 11, no. 3, pp. 265 – 284, 2001. [Online]. Available: http://www.sciencedirect.com/science/article/pii/S0959152400000330

[16] C. E. Garcia and A. Morshedi, "Quadratic programming solution of dynamic matrix control (qdmc)," *Chemical Engineering Communications*, vol. 46, no. 1-3, pp. 73–87, 1986. [Online]. Available: https://doi.org/10.1080/00986448608911397

[17] K. J. Astrom, *Introduction to stochastic control theory*. Academic Press, USA, 1970.

[18] D. Clarke, C. Mohtadi, and P. Tuffs, "Generalized predictive control—part i. the basic algorithm," *Automatica*, vol. 23, no. 2, pp. 137 – 148, 1987. [Online]. Available: http://www.sciencedirect.com/science/article/pii/0005109887900872

[19] D. Clarke, C. Mohtadi, and P. Tuffs, "Generalized predictive control—part ii extensions and interpretations," *Automatica*, vol. 23, no. 2, pp. 149 – 160, 1987. [Online]. Available: http://www.sciencedirect.com/science/article/pii/0005109887900884

[20] R. Bitmead, M. Gevers, and V. Wertz, *Adaptive Optimal Control: The Thinking Man's GPC*, ser. Prentice Hall Information and System Sciences Series. Prentice

Hall, 1990, no. p. 3. [Online]. Available: https://books.google.rs/books?id=SZ4eAQAAIAAJ

[21] K. R. Muske and J. B. Rawlings, "Model predictive control with linear models," *AIChE Journal*, vol. 39, no. 2, pp. 262–287, 1993.

[22] D. Mayne, J. Rawlings, C. Rao, and P. Scokaert, "Constrained model predictive control: Stability and optimality," *Automatica*, vol. 36, no. 6, pp. 789 – 814, 2000. [Online]. Available: http://www.sciencedirect.com/science/article/pii/S0005109899002149

[23] D. Mayne, M. Seron, and S. Raković, "Robust model predictive control of constrained linear systems with bounded disturbances," *Automatica*, vol. 41, no. 2, pp. 219 – 224, 2005. [Online]. Available: http://www.sciencedirect.com/science/article/pii/S0005109804002870

[24] S. V. Raković, B. Kouvaritakis, R. Findeisen, and M. Cannon, "Homothetic tube model predictive control," *Automatica*, vol. 48, no. 8, pp. 1631 – 1638, 2012. [Online]. Available: http://www.sciencedirect.com/science/article/pii/S0005109812001768

[25] S. V. Raković, B. Kouvaritakis, M. Cannon, C. Panos, and R. Findeisen, "Parameterized tube model predictive control," *IEEE Transactions on Automatic Control*, vol. 57, no. 11, pp. 2746–2761, Nov 2012.

[26] S. V. Raković, B. Kouvaritakis, and M. Cannon, "Equi-normalization and exact scaling dynamics in homothetic tube model predictive control," *Systems & Control Letters*, vol. 62, no. 2, pp. 209 – 217, 2013. [Online]. Available: http://www.sciencedirect.com/science/article/pii/S0167691112002344

[27] S. V. Raković, W. S. Levine, and B. Açıkmeşe, "Elastic tube model predictive control," in *2016 American Control Conference (ACC)*, July 2016, pp. 3594–3599.

[28] L. Wang, "Discrete time model predictive control design using laguerre functions," in *Proceedings of the 2001 American Control Conference. (Cat. No.01CH37148)*, vol. 3, 2001, pp. 2430–2435.

[29] M. Chen, A. Zhang, and K. T. Chong, "A novel controller design for three-phase voltage source inverter," *International Journal of Control, Automation and Systems*, vol. 16, no. 5, pp. 2136–2145, Oct 2018. [Online]. Available: https://doi.org/10.1007/s12555-017-0651-8

[30] A. Zhang, I. G. Ramirez-Alpizar, K. G. Esclasse, O. Stasse, and K. Harada, "Humanoid walking pattern generation based on model predictive control approximated with basis functions," *Advanced Robotics*, vol. 33, no. 9, pp. 454–468, 2019. [Online]. Available: https://doi.org/10.1080/01691864.2019.1594366

[31] X. Qian, Y. Yin, X. Zhang, X. Sun, and H. Shen, "Model predictive controller using laguerre functions for dynamic positioning system," in *2016 35th Chinese Control Conference (CCC)*, July 2016, pp. 4436–4441.

[32] D. Clarke and C. Mohtadi, "Properties of generalized predictive control," *Automatica*, vol. 25, no. 6, pp. 859 – 875, 1989. [Online]. Available: http://www.sciencedirect.com/science/article/pii/0005109889900538

[33] P. E. Wellstead and M. B. Zarrop, *Self-Tuning Systems: Control and Signal Processing*, 1st ed. New York, NY, USA: John Wiley & Sons, Inc., 1991.

[34] T. Barry and L. Wang, "A model-free predictive controller with laguerre polynomials," in *2004 5th Asian Control Conference (IEEE Cat. No.04EX904)*, vol. 1, July 2004, pp. 177–184 Vol.1.

[35] E. G. Gilbert and K. T. Tan, "Linear systems with state and control constraints: the theory and application of maximal output admissible sets," *IEEE Transactions on Automatic Control*, vol. 36, no. 9, pp. 1008–1020, Sep. 1991.

[36] S. V. Raković, E. C. Kerrigan, K. I. Kouramas, and D. Q. Mayne, "Invariant approximations of the minimal robustly positively invariant sets," *IEEE Transactions on Automatic Control*, pp. 406 – 410, 2005.

[37] I. Kolmanovsky and E. G. Gilbert, "Theory and computation of disturbance invariant sets for discrete-time linear systems," *Mathematical Problems in Engineering*, vol. 4, no. 4, pp. 317 – 367, 1998.

[38] D. Q. Mayne and W. Langson, "Robustifying model predictive control of constrained linear systems," *Electronics Letters*, vol. 37, no. 23, pp. 1422–1423, Nov 2001.

[39] L. Chisci, J. Rossiter, and G. Zappa, "Systems with persistent disturbances: predictive control with restricted constraints," *Automatica*, vol. 37, no. 7, pp. 1019 – 1028, 2001. [Online]. Available: http://www.sciencedirect.com/science/article/pii/S0005109801000516

[40] S. V. Emelyanov, *Variable Structure Control Systems*. Moscow: Nauka (in Russian), 1967.

[41] Č. Milosavljevic, "On one class of discrete variable structure systems," in *Proceedings of the IASTED Int. Symposium on Modeling, Identification and Control*, 1984, pp. 56–60.

[42] Y. Dote and R. G. Hoft, "Microprocessor based sliding mode controller for dc motor drives," *IEEE IAS Conference Record*, pp. 641–645, 1980.

[43] Y. Dote, T. Manabe, and S. Murakami, "Microprocessor-based force control for manipulator using variable structure with sliding mode," *IFAC Proceedings Volumes*, vol. 16, no. 16, pp. 145 – 149, 1983, 3rd IFAC Symposium on Control in Power Electronics and Electrical Drives, Lausanne, Switzerland, 12-14 September, 1983. [Online]. Available: http://www.sciencedirect.com/science/article/pii/S1474667017618615

[44] S. C. Lin and S. J. Tsai, "A microprocessor-based incremental servo system with variable structure," *IEEE Transactions on Industrial Electronics*, vol. IE-31, no. 4, pp. 313–316, Nov 1984.

[45] Č. Milosavljević, "General conditions for the existence of a quasisliding mode on the switching hyperplane in discrete variable structure systems," *Automation and Remote Control*, vol. 46, no. 3, pp. 307–314, January 1985.

[46] R. B. Potts and X. Yu, "Discrete variable structure system with pseudo-sliding mode," *The Journal of the Australian Mathematical Society. Series B. Applied Mathematics*, vol. 32, no. 4, p. 365–376, 1991.

[47] R. Potts and X.-H. Yu, "Difference equation modelling of a variable structure system," *Computers & Mathematics with Applications*, vol. 28, no. 1, pp. 281 – 289, 1994. [Online]. Available: http://www.sciencedirect.com/science/article/pii/0898122194001162

[48] X. Yu and R. B. Potts, "Computer-controlled variable-structure systems," *The Journal of the Australian Mathematical Society. Series B. Applied Mathematics*, vol. 34, no. 1, p. 1–17, 1992.

[49] Č. Milosavljević, "Neki problemi diskretne realizacije zakona upravljanja sistema sa promenljivom strukturom [in serbian]," Ph.D. dissertation, University of Sarajevo, Faculty of Electrical Engineering, Yugoslavia, 1982.

[50] S. Sarpturk, Y. Istefanopulos, and O. Kaynak, "On the stability of discrete-time sliding mode control systems," *IEEE Transactions on Automatic Control*, vol. 32, no. 10, pp. 930–932, Oct 1987.

[51] U. Kotta, S. Z. Sarpturk, and Y. Istefanopulos, "Comments on "on the stability of discrete-time sliding mode control systems" [with reply]," *IEEE Transactions on Automatic Control*, vol. 34, no. 9, pp. 1021–1022, Sept 1989.

[52] H. SIRA-RAMIREZ, "Non-linear discrete variable structure systems in quasi-sliding mode," *International Journal of Control*, vol. 54, no. 5, pp. 1171–1187, 1991. [Online]. Available: https://doi.org/10.1080/00207179108934203

[53] S. Drakunov and V. Utkin, "On discrete-time sliding modes," *IFAC Proceedings Volumes*, vol. 22, no. 3, pp. 273 – 278, 1989, nonlinear Control Systems Design, Capri, Italy, 14-16 June 1989. [Online]. Available: http://www.sciencedirect.com/science/article/pii/S1474667017536472

[54] S. V. DRAKUNOV and V. I. UTKIN, "Sliding mode control in dynamic systems," *International Journal of Control*, vol. 55, no. 4, pp. 1029–1037, 1992. [Online]. Available: https://doi.org/10.1080/00207179208934270

[55] K. Furuta, "Sliding mode control of a discrete system," *Systems & Control Letters*, vol. 14, no. 2, pp. 145–152, February 1990.

[56] W. Gao, Y. Wang, and A. Homaifa, "Discrete-time variable structure control systems," *IEEE Transactions on Industrial Electronics*, vol. 42, no. 2, pp. 117–122, Apr 1995.

[57] G. Bartolini, A. Ferrara, and V. Utkin, "Adaptive sliding mode control in discrete-time systems," *Automatica*, vol. 31, no. 5, pp. 769 – 773, 1995. [Online]. Available: http://www.sciencedirect.com/science/article/pii/000510989400154B

[58] G. Golo and Č. Milosavljević, "Two-phase triangular wave oscillator based on discrete-time sliding mode control," *Electronics Letters*, vol. 33, no. 22, pp. 1838–1839, Oct 1997.

[59] G. Golo and Čedomir Milosavljević, "Robust discrete-time chattering free sliding mode control," *Systems & Control Letters*, vol. 41, no. 1, pp. 19–28, September 2000.

[60] A. Šabanović, K. Jezernik, and K. Wada, "Chattering-free sliding modes in robotic manipulators control," *Robotica*, vol. 14, no. 1, p. 17–29, 1996.

[61] G. Bartolini, A. Pisano, and E. Usai, *DIGITAL SLIDING MODE CONTROL WITH $O(T^3)$ ACCURACY*, 2000, pp. 103–112. [Online]. Available: https://www.worldscientific.com/doi/abs/10.1142/9789812792082_0009

[62] G. Bartolini, A. Pisano, and E. Usai, "Digital second-order sliding mode control for uncertain nonlinear systems," *Automatica*, vol. 37, no. 9, pp. 1371 – 1377, 2001. [Online]. Available: http://www.sciencedirect.com/science/article/pii/S0005109801000851

[63] W.-C. Su, S. V. Drakunov, and Ü. Özgüner, *Implementation of variable structure control for sampled-data systems*. Berlin, Heidelberg: Springer Berlin Heidelberg, 1996, pp. 87–106. [Online]. Available: http://dx.doi.org/10.1007/BFb0027562

[64] W.-C. Su, S. V. Drakunov, and U. Ozguner, "An o(t2) boundary layer in sliding mode for sampled-data systems," *IEEE Transactions on Automatic Control*, vol. 45, no. 3, pp. 482–485, Mar 2000.

[65] K. D. Young, V. I. Utkin, and U. Ozguner, "A control engineer's guide to sliding mode control," *IEEE Transactions on Control Systems Technology*, vol. 7, no. 3, pp. 328–342, May 1999.

[66] J. Y. Hung, W. Gao, and J. C. Hung, "Variable structure control: a survey," *IEEE Transactions on Industrial Electronics*, vol. 40, no. 1, pp. 2–22, Feb 1993.

[67] O. Kaynak, K. Erbatur, and M. Ertugnrl, "The fusion of computationally intelligent methodologies and sliding-mode control-a survey," *IEEE Transactions on Industrial Electronics*, vol. 48, no. 1, pp. 4–17, Feb 2001.

[68] X. Yu and O. Kaynak, "Sliding-mode control with soft computing: A survey," *IEEE Transactions on Industrial Electronics*, vol. 56, no. 9, pp. 3275–3285, Sept 2009.

[69] A. Pisano and E. Usai, "Sliding mode control: A survey with applications in math," *Mathematics and Computers in Simulation*, vol. 81, no. 5, pp. 954 – 979, 2011. [Online]. Available: http://www.sciencedirect.com/science/article/pii/S0378475410003095

[70] P. Latosiński, "Sliding mode control based on the reaching law approach - a brief survey," in *2017 22nd International Conference on Methods and Models in Automation and Robotics (MMAR)*, Aug 2017, pp. 519–524.

[71] A. Bartoszewicz and J. Żuk, "Sliding mode control — basic concepts and current trends," in *2010 IEEE International Symposium on Industrial Electronics*, July 2010, pp. 3772–3777.

[72] B. Drazenovic, "The invariance conditions in variable structure systems," *Automatica*, vol. 5, no. 3, pp. 287 – 295, 1969. [Online]. Available: http://www.sciencedirect.com/science/article/pii/0005109869900715

[73] V. I. Utkin, *Sliding Modes and Their Applications in Variable Structure Systems*. Moscow, USSR: MIR, 1978.

[74] W. Gao and J. C. Hung, "Variable structure control of nonlinear systems: a new approach," *IEEE Transactions on Industrial Electronics*, vol. 40, no. 1, pp. 45–55, Feb 1993.

[75] J.-J. E. SLOTINE, "Sliding controller design for non-linear systems," *International Journal of Control*, vol. 40, no. 2, pp. 421–434, 1984. [Online]. Available: https://doi.org/10.1080/00207178408933284

[76] J. . Xu, H. Hashimoto, J. . E. Slotine, Y. Arai, and F. Harashima, "Implementation of vss control to robotic manipulators-smoothing modification," *IEEE Transactions on Industrial Electronics*, vol. 36, no. 3, pp. 321–329, Aug 1989.

[77] P. Kachroo and M. Tomizuka, "Chattering reduction and error convergence in the sliding-mode control of a class of nonlinear systems," *IEEE Transactions on Automatic Control*, vol. 41, no. 7, pp. 1063–1068, July 1996.

[78] K.-K. Shyu, Y.-W. Tsai, and C.-F. Yung, "A modified variable structure controller," *Automatica*, vol. 28, no. 6, pp. 1209 – 1213, 1992. [Online]. Available: http://www.sciencedirect.com/science/article/pii/000510989290062K

[79] J.-X. XU, T. H. LEE, M. WANG, and X.-H. YU, "Design of variable structure controllers with continuous switching control," *International Journal of Control*, vol. 65, no. 3, pp. 409–431, 1996. [Online]. Available: https://doi.org/10.1080/00207179608921704

[80] A. Levant, "Sliding order and sliding accuracy in sliding mode control," *International Journal of Control*, vol. 58, no. 6, pp. 1247–1263, 1993. [Online]. Available: https://doi.org/10.1080/00207179308923053

[81] G. Bartolini, A. Ferrara, and E. Usai, "Chattering avoidance by second-order sliding mode control," *IEEE Transactions on Automatic Control*, vol. 43, no. 2, pp. 241–246, Feb 1998.

[82] T.-L. Chen and Y.-C. Wu, "An optimal variable structure control with integral compensation for electrohydraulic position servo control systems," *IEEE Transactions on Industrial Electronics*, vol. 39, no. 5, pp. 460–463, Oct 1992.

[83] R. Palm, "Robust control by fuzzy sliding mode," *Automatica*, vol. 30, no. 9, pp. 1429 – 1437, 1994. [Online]. Available: http://www.sciencedirect.com/science/article/pii/0005109894900086

[84] C. Batur and V. Kasparian, "Model based fuzzy control," *Mathematical and Computer Modelling*, vol. 15, no. 12, pp. 3 – 14, 1991. [Online]. Available: http://www.sciencedirect.com/science/article/pii/0895717791900378

[85] W.-C. Su, S. Drakunov, and U. Ozgüner, "Sliding mode control in discrete time linear systems," *{IFAC} Proceedings Volumes*, vol. 26, no. 2, Part 2, pp. 267 – 270, 1993, 12th Triennal Wold Congress of the International Federation of Automatic control. Volume 2 Robust Control, Design and Software, Sydney, Australia, 18-23 July. [Online]. Available: http://www.sciencedirect.com/science/article/pii/S1474667017489415

[86] A. Bartoszewicz, "Discrete-time quasi-sliding-mode control strategies," *IEEE Transactions on Industrial Electronics*, vol. 45, no. 4, pp. 633–637, Aug 1998.

[87] J.-X. Xu, F. Zheng, and T. H. Lee, *On sampled data variable structure control systems*. London: Springer London, 1999, pp. 69–92. [Online]. Available: https://doi.org/10.1007/BFb0109971

[88] D. Mitić and v. Milosavljevic, "Sliding mode-based minimum variance and generalized minimum variance controls with o(t2) and o(t3) accuracy," *Electrical Engineering*, vol. 86, no. 4, pp. 229–237, Jul 2004. [Online]. Available: https://doi.org/10.1007/s00202-003-0198-y

[89] M. L. Corradini and G. Orlando, "A vsc algorithm based on generalized predictive control," *Automatica*, vol. 33, no. 5, pp. 927–932, May 1997.

[90] W. García-Gabín and E. F. Camacho, "Sliding mode model based predictive control for non minimum phase systems," in *2003 European Control Conference (ECC)*, Sept 2003, pp. 904–909.

[91] W. García-Gabín, D. Zambrano, and E. Camacho, "Sliding mode predictive control for chemical process with time delay," *IFAC Proceedings Volumes*, vol. 38, no. 1, pp. 627 – 632, 2005, 16th IFAC World Congress. [Online]. Available: http://www.sciencedirect.com/science/article/pii/S147466701637690X

[92] W. Garcia-Gabin, D. Zambrano, and E. F. Camacho, "Sliding mode predictive control of a solar air conditioning plant," *Control Engineering Practice*, vol. 17, no. 6, pp. 652–663, June 2009.

[93] V. A. Neelakantan, "Modeling, design, testing and control of a two-stage actuation mechanism using piezoelectric actuators for automotive applications," Ph.D. dissertation, Ohio State University, Department of Mechanical Engineering, 2005.

[94] G. P. Incremona, A. Ferrara, and L. Magni, "Hierarchical model predictive/sliding mode control of nonlinear constrained uncertain systems," in *Proceedings of 5th IFAC Conference on Nonlinear Model Predictive Control*, 2015, pp. 102–109.

[95] S. E. Benattia, S. Tebbani, and D. Dumur, "Hierarchical control strategy based on robust mpc and integral sliding mode - application to a continuous photobioreactor," in *Proceedings of 5th IFAC Conference on Nonlinear Model Predictive Control*, 2015, pp. 212–217.

[96] M. Rubagotti, A. Estrada, F. Castanos, A. Ferrara, and L. Fridman, "Integral sliding mode control for nonlinear systems with matched and unmatched perturbations," *IEEE Transactions on Automatic Control*, vol. 56, no. 11, pp. 2699–2704, Nov 2011.

[97] M. Rubagotti, D. M. Raimondo, A. Ferrara, and L. Magni, "Robust model predictive control with integral sliding mode in continuous-time sampled-data nonlinear systems," *IEEE Transactions on Automatic Control*, vol. 56, no. 3, pp. 556–570, March 2011.

[98] Č. Milosavljević, "Discrete-time vss," in *Variable Structure Systems: from Principles to Implementation*, A. Sabanović, L. Fridman, and S. Spurgeon, Eds. London: The Institution of Engineering and Technology, 2004, ch. 5, pp. 99–128.

[99] F. J. Doyle, B. A. Ogunnaike, and R. K. Pearson, "Nonlinear model-based control using second-order volterra models," *Automatica*, vol. 31, no. 5, pp. 697 – 714, 1995. [Online]. Available: http://www.sciencedirect.com/science/article/pii/000510989400150H

[100] Inteco, *Modular Servo System - Manual*, Inteco, 2011.

[101] D. Mignone, "The really big collection of logic propositions and linear inequalities," Tech. Rep., 2001. [Online]. Available: http://control.ee.ethz.ch/index.cgi?action=details;id=377;page=publications

[102] A. Bemporad and M. Morari, "Control of systems integrating logic, dynamics, and constraints," *Automatica*, vol. 35, no. 3, pp. 407 – 427, 1999.

[103] S. Boyd and L. Vandenberghe, *Convex Optimization*. Cambridge University Press, 2004.

[104] D. Mitić, S. Perić, D. Antić, Z. Jovanović, M. Milojković, and S. Nikolić, "Digital sliding mode control of anti-lock braking system," *Advances in Electrical and Computer Engineering*, vol. 13, no. 1, pp. 33 – 40, 2013.

[105] D. G. Luenberger, *Linear and Nonlinear Programming*. Springer US, USA, 2003.

[106] C. Hildreth, "A quadratic programming procedure," *Naval Research Logistics Quarterly*, vol. 4, no. 1, pp. 79–85, 1957.

[107] L. Wang, *Model Predictive Control System Design and Implementation Using MATLAB*. London, UK: Springer, 2009.

ISBN 978-82-326-4262-5 (printed version)
ISBN 978-82-326-4263-2 (electronic version)
ISSN 1503-8181

NTNU
Norwegian University of
Science and Technology

Doctoral Thesis
Miodrag Spasić

Doctoral theses at NTNU, 2019:333

Miodrag Spasić

Model Predictive Control based on Sliding Mode Control

NTNU
Norwegian University of
Science and Technology
Faculty of Information Technology
and Electrical Engineering
Department of Engineering Cybernetics

Doctoral theses at NTNU, 2019:333
NTNU

NTNU
Norwegian University of
Science and Technology